

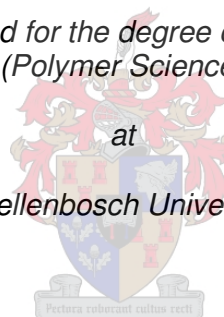
***The use of chromium/bis(diphenylphosphino)amine catalysts
in tandem ethylene copolymerization processes***

By Aletta du Toit

*Dissertation presented for the degree of Doctor of Philosophy
(Polymer Science)*

at

Stellenbosch University



Promotor: Prof AJ van Reenen

March 2012

By submitting this dissertation electronically, I declare that the entirety of the work contained therein is my own, original work, that I am the sole author thereof (save to the extent explicitly otherwise stated), that reproduction and publication thereof by Stellenbosch University will not infringe any third party rights and that I have not previously in its entirety or in part submitted it for obtaining any qualifications.

Date: 28 February 2012

Abstract

The possibility of utilizing the chromium/bis(diphenylphosphino)amine (PNP) type of catalysts in ethylene polymerization processes was investigated. These processes include the production of linear low density polyethylene (LLDPE), the production of polyethylene waxes and the synthesis of special comonomers for ethylene copolymerization.

The chromium/ $\text{Ph}_2\text{PN}\{\text{CH}(\text{CH}_3)_2\}\text{PPh}_2$ tetramerization system was used in combination with a polymerization catalyst to yield ethylene copolymers with controlled branching. Copolymers with bimodal chemical composition distributions were obtained in these tandem reactions. This chromium/PNP-type tetramerization catalyst and metallocene polymerization catalysts are not completely compatible in tandem catalytic systems due to different optimum temperatures for their effective functioning. The oligomerization to polymerization catalyst ratios, the catalyst to cocatalyst ratios and the temperature profile are all factors influencing the amount of α -olefins formed and therefore the type of copolymer produced. The activity of the polymerization catalyst decreases in the presence of the oligomerization catalyst, indicating that the two catalysts interfere chemically. The main difference between copolymers produced in conventional or tandem fashion is the presence of a small amount of low molecular weight material produced by the oligomerization catalyst and also the presence of a highly crystalline component. The latter component results from the initial low concentration of α -olefins in the first conversion, but such a component is also independently produced by the oligomerization catalyst.

LLDPE with butyl branches is obtained when a selective trimerization catalyst is used in combination with a polymerization catalyst. The chromium/ $(o\text{-OMeC}_6\text{H}_4)_2\text{PN}(\text{CH}_3)\text{P}(o\text{-OMeC}_6\text{H}_4)_2$ trimerization system is more suitable than the chromium/ $\text{Ph}_2\text{PN}\{\text{CH}(\text{CH}_3)_2\}\text{PPh}_2$ tetramerization system for use in tandem reactions with a metallocene catalyst due to its high activity and selectivity at higher temperatures. The chemical composition distribution varies with an increase in reaction time due to the increasing amount of 1-hexene produced. Comparison of CRYSTAF traces of tandem copolymers with conventional copolymers show that the tandem copolymers have a broader chemical composition distribution. Addition of 1-hexene during the course of a conventional copolymerization reaction produces copolymers with similar chemical composition distributions to that of the tandem

copolymers. Later addition of the polymerization catalyst to the oligomerization reaction mixture results in copolymers with higher comonomer content, similar to conventional copolymers.

Chromium/ $(o\text{-EtC}_6\text{H}_4)_2\text{PN}(\text{CH}_3)\text{P}(o\text{-EtC}_6\text{H}_4)_2$ is not suitable for LLDPE production in tandem reactions, since it is selective to higher oligomers or polyethylene waxes at higher temperatures. Variation of the MAO cocatalyst and hydrogen concentrations significantly influences the yield, viscosity and crystallization behaviour of the wax-like products. Low MAO concentrations resulted in multiple melting peaks, while higher concentrations display single melting peaks and lower viscosity values.

Ethylene co-oligomerization reactions with styrene or *p*-methylstyrene using the chromium/PNP-type oligomerization technology produce various phenyl-hexene and phenyl-octene isomers either through cotrimerization or cotetramerization. The known ethylene trimerization catalysts show cotrimerization behaviour, while the catalysts with known selectivity for ethylene tetramerization also yield cotetramerization products. Chromium complexes that contain the more bulky ligands display lower selectivity towards co-oligomerization and greater preference for ethylene homotrimerization.

These co-oligomerization products can be incorporated into a polyethylene chain by copolymerization in a simultaneous or sequential tandem reaction. The combined co-oligomerization-polymerization reactions yield copolymers with lower crystallinity than obtained from the conventional ethylene-styrene copolymerization reaction due to higher comonomer incorporation. The polymer yields are higher in the co-oligomerization-copolymerization reactions. The ability of the different co-oligomerization products to incorporate into the polyethylene chain was established: unreacted styrene and the more bulky isomers, 3-phenyl-1-hexene and 3-phenyl-1-octene, are not incorporated readily, while branches resulting from 4-phenyl-1-hexene, 4-phenyl-1-octene, 5-phenyl-1-octene and 6-phenyl-1-octene are detected in the NMR spectrum.

Opsomming

Die moontlikheid om die chroom/bis-(difenielfosfino)amien (PNP) tipe katalisatore in etileen-polimerisasie reaksies te gebruik is ondersoek. Hierdie prosesse sluit die produksie van lineêre lae digtheid poliëtileen (LLDPE), die produksie van poliëtileenwasse en die sintese van spesiale komonomere vir etileenkopolimerisasie in.

Die chroom/ $\text{Ph}_2\text{PN}\{\text{CH}(\text{CH}_3)_2\}\text{PPh}_2$ tetramerisasie-sisteem is gebruik in kombinasie met 'n polimerisasiekatalisator om etileenkopolimere met gekontroleerde vertakkings te vorm. Kopolimere met 'n bimodale chemiese samestellingsverspreiding word verkry in hierdie tandemreaksies. Hierdie chroom/PNP-tipe tetramerisasiekatalisator en die metalloseenkatalisators is nie heeltemal verenigbaar in die tandemsisteem nie weens verskille in hul optimum reaksietemperature vir effektiewe funksionering. Die oligomerisasie tot polimerisasiekatalisatorverhouding, die katalisator tot kokatalisatorverhouding en die temperatuurprofiel is almal faktore wat die gevormde hoeveelheid α -olefiene beïnvloed, en dus die tipe kopolimeer wat gevorm word. Die aktiwiteit van die polimerisasiekatalisator verminder in die teenwoordigheid van die oligomerisasiekatalisator, wat aandui dat die twee katalisatore chemies met mekaar inmeng. Die duidelikste verskil tussen die kopolimere wat geproduseer word op die konvensionele of die tandem manier is die teenwoordigheid van 'n klein hoeveelheid lae molekulere massa materiaal wat gevorm word deur die oligomerisasiekatalisator, asook 'n komponent met baie hoë kristalliniteit. Die laasgenoemde komponent ontstaan weens die aanvanklike lae konsentrasie van die α -olefiene in die eerste omsetting, maar so 'n komponent word ook onafhanklik gevorm deur die oligomerisasiekatalisator.

LLDPE met butiel-vertakkings word verkry wanneer 'n selektiewe trimerisasiekatalisator in kombinasie met 'n polimerisasiekatalisator gebruik word. Die chroom/ $(o\text{-OMeC}_6\text{H}_4)_2\text{PN}(\text{CH}_3)\text{P}(o\text{-OMeC}_6\text{H}_4)_2$ trimerisasiesisteem is meer geskik as die chroom/ $\text{Ph}_2\text{PN}\{\text{CH}(\text{CH}_3)_2\}\text{PPh}_2$ tetramerisasiesisteem vir gebruik in tandem met 'n metalloseenkatalisator weens die katalisator se hoë aktiwiteit en selektiwiteit vir 1-hekseen by hoër reaksietemperature. Die chemiese samestellingsverspreiding verander soos die reaksietyd toeneem weens die toenemende hoeveelheid 1-hekseen wat gevorm word. Vergelyking van die CRYSTAF-diagram van die tandemkopolimere met konvensionele kopolimere toon

dat die tandemkopolimere 'n wyer chemiese samestellingsverspreiding het. Geleidelike byvoeging van 1-hekseen gedurende die loop van 'n konvensionele reaksie, vorm kopolimere met 'n soortgelyke chemiese samestellingsverspreiding as die tandemkopolimere. Latere byvoeging van die polimerisasiekatalisator lei tot die vorming van kopolimere met 'n hoër komonomeerinhoud, soortgelyk aan die konvensionele kopolimere.

Chroom/ $(o\text{-EtC}_6\text{H}_4)_2\text{PN}(\text{CH}_3)\text{P}(o\text{-EtC}_6\text{H}_4)_2$ is nie geskik om LLDPE in tandemreaksies te vorm nie, aangesien dit selektief is vir hoër oligomere of poliëtileenwasse by hoër reaksietemperature. Variasie van die MAO-kokatalisator en die waterstofkonsentrasies beïnvloed die hoeveelheid produk wat gevorm word, asook die viskositeit en kristallasiegedrag daarvan. Lae MAO konsentrasies lei tot meer as een smeltpiek, terwyl hoër konsentrasies 'n enkelpiek vertoon. Die viskositeit van die produkmengsel is ook laer.

Die gebruik van die chroom/PNP-tipe oligomerisatietegnologie in etileenko-oligomerisasiereaksies met stireen, lei tot die vorming van verskeie feniel-hekseen- en feniel-okteenisomere deur of kotrimerisasie, of kotetramerisasie. Katalisatore met bekende etileentriemerisasieligande vertoon kotrimerisatiegedrag terwyl die ligande wat bekend is vir selektiwiteit in etileentetramerisasie, kotetramerisatieprodukte vorm. Die chroomkomplekse met die meer bonkige ligande het laer selektiwiteit vir ko-oligomerisasie en vertoon 'n groter voorkeur vir etileenhomo-trimerisasie.

Die ko-oligomerisasieprodukte kan in 'n poliëtileenketting ingebou word deur kopolimerisasie in 'n gelyktydige of opeenvolgende tandemreaksie. Die gekombineerde ko-oligomerisasie-polimerisatie reaksie vorm kopolimere van 'n laer kristalliniteit as wat gevind word met die konvensionele etileen-stireen kopolimerisasie reaksie weens hoër komonomeerinkorporasie. Meer polimeer word gevorm in die ko-oligomerisasie-kopolimerisasie reaksie. Die vermoë van die verskillende ko-oligomerisasieprodukte om in die poliëtileenketting ingesluit te word is bepaal. Ongereageerde stireen en die meer bonkige isomere, 3-feniel-1-hekseen en 3-feniel-1-okteen, word nie maklik ingevoeg nie. Vertakkings as gevolg van die inkorporasie van 4-feniel-1-hekseen, 4-feniel-1-okteen, 5-feniel-1-okteen and 6-feniel-1-okteen kan waargeneem word in die KMR spektrum.

Table of contents

1	Introduction and objectives	1
	1.1 Background	1
	1.2 Motivation for this study	1
	1.3 Objectives of the study	2
	1.4 Layout of this dissertation	3
	1.5 References	4
2	Literature Background	5
	2.1 Introduction	5
	2.2 Industrial ethylene oligomerization	5
	2.3 Homogeneous ethylene oligomerization catalysts and oligomerization mechanism	7
	2.4 Co-oligomerization	13
	2.5 Combined oligomerization-copolymerization (tandem catalysis)	18
	2.6 Homogeneous chromium catalysts selective to higher oligomers or polymers	22
	2.7 References	26
3	Tetramerization tandem catalysis	31
	3.1 Introduction	31
	3.2 Experimental	32
	3.3 Results and discussion	35
	3.3.1 The effect of temperature	35
	3.3.2 The effect of a temperature gradient	43
	3.3.3 The effect of catalyst and cocatalyst ratios	44
	3.3.4 Chemical compatibility	48
	3.3.5 Comparative study of tandem copolymers with commercial 1-octene copolymers	53
	3.3.6 Fractionation of tandem copolymers by prep-TREF	63
	3.4 Conclusions	66
	3.5 References	67

4	Trimerization tandem catalysis	69
	4.1 Introduction	69
	4.2 Experimental	70
	4.3 Results and Discussion	74
	4.3.1 The effect of the PNP-type ligand on 1-hexene copolymerization	74
	4.3.2 The effect of reaction time	75
	4.3.3 Comparative study of tandem copolymers with conventional 1-hexene copolymers	78
	4.4 Wax formation with the trimerization catalyst, (o- EtC ₆ H ₄) ₂ PN(CH ₃)P(o-EtC ₆ H ₄) ₂ /CrCl ₃ /MAO, at high temperatures	83
	4.4.1 The effect of MAO concentration	83
	4.4.2 The effect of hydrogen concentration	85
	4.5 Conclusions	88
	4.6 References	90
5	Tandem ethylene-styrene co-oligomerization-copolymerization	92
	5.1 Introduction	92
	5.2 Experimental	93
	5.3 Results and discussion	95
	5.3.1 Co-oligomerization	95
	5.3.2 Copolymerization	106
	5.4 Conclusions	123
	5.5 References	124
6	Summary and general conclusion	126

List of Figures

Figure 2.1:	Nickel complex employed in the SHOP process	8
Figure 2.2:	Examples of general structures for oligomerization catalysts producing Schulz-Flory distributions of α -olefins	9
Figure 2.3:	Examples of highly active and selective trimerization ligands and a catalyst precursor	12
Figure 3.1:	Structure of the selective tetramerization ligand $\text{Ph}_2\text{PN}\{\text{CH}(\text{CH}_3)_2\}\text{PPh}_2$	31
Figure 3.2:	Structure of $\text{Ph}_2\text{C}(\text{Cp})(9\text{-Flu})\text{ZrCl}_2$	35
Figure 3.3:	Effect of temperature on the main product distribution of tandem reactions	37
Figure 3.4:	CRYSTAF traces of tandem copolymers produced at (a) 40 °C; (b) 60 °C; (c) 80 °C; (d) 100 °C	38
Figure 3.5:	CRYSTAF traces of conventional copolymers produced at (a) 40 °C; (b) 60 °C; (c) 80 °C; (d) 100 °C	40
Figure 3.6:	CRYSTAF traces of polymers obtained from oligomerization reactions at different temperatures	41
Figure 3.7:	CRYSTAF traces of fractions obtained from a tandem copolymerization reaction when sampling at different temperature intervals	43
Figure 3.8:	Structure of $\text{EtIn}_2\text{ZrCl}_2$	44
Figure 3.9:	CRYSTAF traces of tandem copolymers prepared at varying co-catalyst to oligomerization catalyst ratios	46
Figure 3.10:	CRYSTAF traces of tandem copolymers prepared using $\text{EtIn}_2\text{ZrCl}_2$ at varying tetramerization catalyst to polymerization catalyst ratios	47
Figure 3.11:	Effect of $\text{Cr}(\text{acac})_3:\text{Ph}_2\text{C}(\text{Cp})(9\text{-Flu})\text{ZrCl}_2$ on polymerization activity at constant comonomer concentration	49
Figure 3.12:	CRYSTAF traces showing the effect of $\text{Cr}(\text{acac})_3:\text{Ph}_2\text{C}(\text{Cp})(9\text{-Flu})\text{ZrCl}_2$ on chemical composition distribution at constant comonomer concentration	50
Figure 3.13:	Effect of varying the PNP-type ligand to polymerization catalyst ratio at 100 °C on copolymer properties	51
Figure 3.14:	Effect of varying the $\text{Cr}(\text{acac})_3$ to polymerization catalyst ratio at 100 °C on copolymer properties	52
Figure 3.15:	^{13}C NMR spectrum of a copolymer with 4 mol% comonomers	55

Figure 3.16:	^{13}C NMR spectrum of a copolymer with 6 mol% comonomers	55
Figure 3.17:	^{13}C NMR spectrum of a copolymer (6 mol% comonomer) prepared by the conventional way of adding 1-octene	56
Figure 3.18:	^{13}C NMR spectrum of a commercial 1-octene copolymer with 6 mol% 1-octene	57
Figure 3.19:	CRYSTAF traces of tandem copolymers of varying comonomer content	57
Figure 3.20:	Comparison of a commercial copolymer (6 mol% 1-octene) with a tandem copolymer with similar comonomer content	58
Figure 3.21:	Comparison of commercial copolymer (4 mol% 1-octene) with a tandem copolymer with similar comonomer content	58
Figure 3.22:	(a) Polymer obtained from tandem reaction at 40 °C; (b) Solid obtained from oligomerization reaction at 40 °C for 1 hour followed by heating above 100 °C	59
Figure 3.23:	Melting and crystallization maximum peak maximum temperatures as function of the comonomer content	60
Figure 3.24:	Comparison of the temperature dependent weight fraction crystallinity curves of tandem and commercial copolymers	61
Figure 3.25:	Effect of comonomer content on modulus of the copolymers	62
Figure 3.26:	Effect of comonomer content on tensile strength at break of the copolymers	63
Figure 3.27:	Distribution of fractions obtained from the prep-TREF analysis of a tandem copolymer	64
Figure 3.28:	Comparison of the chemical composition distributions in different TREF-fractions of a tandem copolymer	64
Figure 4.1:	Structures of trimerization ligands	69
Figure 4.2:	Effect of the substituents on PNP-type ligand and ligand: $\text{EtIn}_2\text{ZrCl}_2$ molar ratio on the polymer yield	75
Figure 4.3:	Effect of reaction time on the tandem copolymerization reactions	76
Figure 4.4:	CRYSTAF trace showing the effect of reaction time on the chemical composition distribution of the tandem copolymers	77
Figure 4.5:	Comparison of CRYSTAF traces of tandem (P1) and conventional copolymers (P3 and P4)	79
Figure 4.6:	CRYSTAF comparison of tandem copolymers and the copolymer obtained by feeding 1-hexene during a copolymerization reaction	80
Figure 4.7:	CRYSTAF traces of tandem copolymers with delayed addition of the polymerization catalyst and a conventional copolymer	82

Figure 4.8:	DSC curves of waxes prepared using different MAO ratios	85
Figure 4.9:	Comparison of CRYSTAF traces at changing hydrogen concentrations	87
Figure 5.1:	PNP-type ligands employed in ethylene-styrene co-oligomerization screening experiments	97
Figure 5.2:	A typical gas chromatogram showing the distribution of co-oligomerization products (ligand 3) in the ethylene-styrene co-oligomerization reaction	99
Figure 5.3:	<i>Rac</i> -ethylenebis(indenyl)zirconiumdichloride (EtIn ₂ ZrCl ₂)	106
Figure 5.4:	Comparison of CRYSTAF traces of Polymers 1 and 2	108
Figure 5.5:	CRYSTAF traces of Polymers 3, 4 and 5	119
Figure 5.6:	The aromatic region in the ¹³ C NMR spectrum of Polymer 3	110
Figure 5.7:	The aliphatic region in the ¹³ C NMR spectrum of Polymer 3	110
Figure 5.8:	Aliphatic region in the ¹³ C NMR spectrum of an ethylene-p-methylstyrene copolymer prepared at higher temperature than Polymer 5	111
Figure 5.9:	CRYSTAF trace of hexane soluble fraction from Polymer 3 compared to Polymer 3	113
Figure 5.10:	¹³ C APT NMR spectrum of the hexane extracted fraction from Polymer 3	114
Figure 5.11:	¹³ C APT NMR spectrum of the hexane soluble fraction from Polymer 3	115

Scheme 2.1: Ziegler ethylene oligomerization	6
Scheme 2.2: Cossee-Arlman mechanism.....	7
Scheme 2.3: Proposed pathway for selective ethylene dimerization.....	10
Scheme 2.4: Proposed mechanism for selective trimerization of ethylene	10
Scheme 2.5: Possible routes to cotrimerization products (continued on next page)....	15
Scheme 2.6: Proposed route for formation of 3-ethyl-1-phenyl-1-hexene during styrene-ethylene-co-oligomerization	17
Scheme 3.1: Numbering scheme⁴ for carbons in the copolymer framework	33
Scheme 4.1: Numbering scheme for carbons in the copolymer framework.....	72
Scheme 4.2: Proposed mechanism for methyl branching	88
Scheme 5.1: Possible routes to ethylene-styrene cotetramerization products (continued on next page)	102
Scheme 5.2: Numbering scheme for carbons in an ethylene-<i>p</i>-methylstyrene- copolymer	111
Scheme 5.3: Numbering scheme for 6-phenyl-1-hexene carbons in copolymer framework	116
Scheme 5.4: Numbering scheme for carbons in the copolymer frameworks resulting from the incorporation of the co-oligomerization products	117
Scheme 5.5: Possible routes to the observed co-oligomerization products.....	122

List of Schemes

Scheme 2.1: Ziegler ethylene oligomerization	6
Scheme 2.2: Cossee-Arlman mechanism	7
Scheme 2.3: Proposed pathway for selective ethylene dimerization	10
Scheme 2.4: Proposed mechanism for selective trimerization of ethylene	10
Scheme 2.5: Possible routes to cotrimerization products	15
Scheme 2.6: Proposed route for formation of 3-ethyl-1-phenyl-1-hexene during styrene-ethylene-co-oligomerization	17
Scheme 3.1: Numbering scheme for carbons in the copolymer framework	33
Scheme 4.1: Numbering scheme for carbons in the copolymer framework	72
Scheme 4.2: Proposed mechanism for methyl branching	88
Scheme 5.1: Possible routes to ethylene-styrene cotetramerization products	102
Scheme 5.2: Numbering scheme for carbons in an ethylene- <i>p</i> -methylstyrene- copolymer	111
Scheme 5.3: Numbering scheme for 6-phenyl-1-hexene carbons in copolymer framework	116
Scheme 5.4: Numbering scheme for carbons in the copolymer frameworks resulting from the incorporation of the co-oligomerization products	117
Scheme 5.5: Possible routes to the observed co-oligomerization products	122

List of Tables

Table 2.1:	Effect of ligand structure on wax synthesized at 120 °C	24
Table 2.2:	Effect of the reaction temperature and pressure on wax synthesis using chromium/PNP-type catalysts	25
Table 3.1:	Effect of temperature on solid formation in the tandem and oligomerization reactions	37
Table 3.2 :	GPC results from tandem copolymerization, oligomerization and conventional copolymerization	42
Table 3.3:	Effect of catalyst and cocatalyst ratios on tandem reactions with the metallocene $\text{EtIn}_2\text{ZrCl}_2$	45
Table 3.4:	Effect of catalyst and cocatalyst ratios on tandem reactions with the metallocene $\text{Ph}_2\text{C}(\text{Cp})(9\text{-Flu})\text{ZrCl}_2$	47
Table 3.5:	Effect of $\text{Cr}(\text{acac})_3:\text{Ph}_2\text{C}(\text{Cp})(9\text{-Flu})\text{ZrCl}_2$ on copolymer properties at constant comonomer concentration	49
Table 3.6:	Effect of varying the PNP-type ligand to polymerization catalyst ratio at 100 °C on copolymer properties	52
Table 3.7:	Effect of varying the $\text{Cr}(\text{acac})_3$ to polymerization catalyst ratio at 100 °C on copolymer properties	52
Table 3.8:	Comparison of molecular weight distributions and MFI	60
Table 3.9:	Comparison of tensile properties of tandem and commercial copolymers	62
Table 3.10:	DSC data of prep-TREF fractions of a tandem copolymer	65
Table 3.11:	GPC data of prep-TREF fractions of a tandem copolymer	66
Table 4.1:	Thermal properties of tandem copolymers obtained after 5, 10 and 15 minutes	76
Table 4.2:	Variation in tandem copolymer molecular weights with an increase reaction time	77
Table 4.3:	Comparison of thermal properties of the copolymers	79
Table 4.4:	Molecular weight data of the different copolymers	80
Table 4.5:	Tensile properties of tandem and conventional copolymers	81
Table 4.6:	Molecular weight data of copolymers	82
Table 4.7:	Effect of MAO concentration on wax yield and characteristics	84
Table 4.8:	Effect of H_2 on the wax yield and properties	86

Table 4.9:	Molecular weight data of waxes synthesized at varying H ₂ concentrations	87
Table 5.1:	Effect of ethylene pressure and styrene concentration on ethylene-styrene co-oligomerization	96
Table 5.2:	The effect of ligand on ethylene-styrene co-oligomerization	98
Table 5.3:	Identification of peaks from GC-MS analysis for the co-oligomerization products (ligand 3)	100
Table 5.4:	Selectivity in the co-oligomerization fraction	101
Table 5.5:	Comparison of the selectivity in the co-oligomerization fraction of ethylene-styrene and ethylene- <i>p</i> -methylstyrene co-oligomerization reactions	105
Table 5.6:	Effect of the reaction temperature on the ethylene-styrene co-oligomerization	105
Table 5.7:	Copolymers from tandem and sequential co-oligomerization-copolymerization reactions	107
Table 5.8:	Assignment of the ¹³ C NMR resonances in ethylene-styrene-copolymers	112
Table 5.9:	Values of the terms used in the calculation of the chemical shifts	115
Table 5.10:	Peak assignments for carbons in a 4-phenylbutyl branched polyethylene	116
Table 5.11:	Calculated chemical shifts for ethylene copolymers containing phenyl-hexene isomers	118
Table 5.12:	Calculated chemical shifts for ethylene copolymers containing phenyl-octene isomers	118
Table 5.13:	Proposed assignments of the ¹³ C NMR resonances in the (<i>p</i> -methyl)styrene co-oligomerization-co-polymerization products	121

List of Abbreviations

Δh_m	Enthalpy of melting
Δh_c	Enthalpy of crystallization
^{13}C NMR	Carbon thirteen nuclear magnetic resonance
APT	Attached proton test
BHT	2,6-di-tert-butyl-4-methylphenol
C_7/C_8	heptane/octane
cp	crystallization peak maximum temperature
[Cr]	Chromium complex
$\text{Cr}(\text{acac})_3$	chromium(III)acetylacetonato
CRYSTAF	Crystallization analysis fractionation
DSC	Differential scanning calorimetry
ESL	Ethylene sequence length
$\text{EtIn}_2\text{ZrCl}_2$	<i>rac</i> -ethylenebis(indenyl)zirconiumdichloride
GC	Gas chromatography
GPC	Gel permeation chromatography
LLDPE	Linear low density polyethylene
MAO	Methyl aluminoxane
MFI	Melt flow index
$\langle M_n \rangle$	Number average molecular weight
$\langle M_w \rangle$	Peak molecular weight
M_p	Weight average molecular weight
mp	melting peak maximum temperature
PE	polyethylene
PI	Polydispersity index

$\text{Ph}_2\text{C}(\text{Cp})(9\text{-Flu})\text{ZrCl}_2$	diphenylmethylidene(cyclopentadienyl)(9-fluorenyl)zirconiumdichloride
Ph	Phenyl
PNP-type	bis(diphenylphosphino)amine-type
Prep-TREF	preparative temperature rising elution fractionation
SNS	bis(2-dodecylsulfanyl-ethyl)amine
TCB	Trichlorobenzene
TCE	Tetrachloroethylene
THF	Tetrahydrofuran
SHOP	Shell higher olefin process
$w_c(T)$	temperature dependent crystallinity fraction

1 Introduction and objectives

1.1 Background

Metal complexes with the bis-(diphenylphosphino)amine (PNP) type of ligands have been investigated as catalysts in various homogeneously catalyzed processes at Sasol Technology since 2003. Selective ethylene tetramerization was the most remarkable discovery resulting from these studies.¹

This thesis describes the use of the chromium/PNP-type oligomerization catalysts in ethylene polymerization processes. These processes include the production of linear low density polyethylene (LLDPE), polyethylene waxes and the synthesis of special comonomers for ethylene copolymerization. It covers the fields of homogeneously catalyzed ethylene homo- and co-oligomerization, ethylene homo- and copolymerization as well as polyolefin characterization.

1.2 Motivation for this study

LLDPE is conventionally prepared by the copolymerization of ethylene with longer chain linear α -olefins, i.e. 1-butene, 1-hexene or 1-octene. These α -olefin comonomers can be obtained from an ethylene oligomerization process. Many of the current commercial ethylene oligomerization processes produce a distribution of olefins. After isolation and purification steps some of these α -olefins, mostly 1-hexene and 1-octene, are consumed in the manufacturing of LLDPE. A possible way to reduce the cost of LLDPE is to produce these specific comonomers *in situ* from ethylene by selective oligomerization and copolymerization of the resulting product with ethylene, without any purification steps, using a polymerization catalyst. This combined process of producing α -olefins from ethylene and copolymerization thereof can occur simultaneously or sequentially. In literature it is referred to as tandem catalysis or *in situ* copolymerization.² The first part of the study investigates how to

1. Introduction and objectives

obtain LLDPE via such a tandem process using the selective chromium/PNP-type of oligomerization catalysts.

It is known that some of the chromium/PNP-type catalysts produce low molecular weight polyethylene under specific reaction conditions.³ This study also investigates the synthesis and properties of these waxlike materials more closely.

The last part of the study investigates the use of the chromium/PNP-type oligomerization catalysts to synthesize special comonomers through the co-oligomerization of ethylene and *p*-methylstyrene. The synthesis of well-defined functional copolymers through the metal catalyzed copolymerization of ethylene is a quest in the scientific literature.⁴ In general, it is difficult to copolymerize functional monomers, because the functional groups interact too strongly with the titanium or zirconium catalyst centre. A way to eliminate this is to use a comonomer, such as *p*-methylstyrene, which can be functionalized in a post-polymerization step. *p*-Methylstyrene can be functionalized after the polymerization reaction at the activated methyl group. The copolymerization reaction is not very effective due to the bulky nature of the monomer and interaction of the phenyl group with the catalyst centre. When the phenyl group is spaced further away from the double bond of the vinyl monomer it should insert more readily. Co-oligomers obtained from the selective co-oligomerization of ethylene and styrene could most probably be suitable for such an approach.

1.3 Objectives of the study

The main objective of this project was to investigate the possibility of utilizing the PNP-type ligands in various ethylene polymerization processes.

The first goal was to use the chromium/PNP-type of oligomerization systems in combination with a suitable polymerization catalyst to afford ethylene copolymers with controlled branching. The aim was to understand the factors of importance when using multiple catalysts in one reactor to produce LLDPE from a single monomer feed. It was necessary to investigate variables like oligomerization catalyst to polymerization catalyst ratios, the ratios of these catalysts to the cocatalyst as well as reaction variables, i.e reaction temperatures and reaction times, on the type and amount of product produced. A part of the study was designed to determine and compare the properties and microstructures of the resulting tandem

1. Introduction and objectives

copolymers with copolymers obtained from the conventional process of adding a comonomer to the reactor. The synthesis of polyethylene waxes using a specific chromium/PNP-type of catalysts was also to be studied.

The second goal was to utilize the chromium/PNP-type oligomerization technology in ethylene co-oligomerization reactions with styrene. The effects of reaction conditions and ligand structure on selectivity and activity of the reaction were to be studied. The possibility of including these co-oligomerization products in a polyethylene chain by copolymerization in a tandem or sequential manner was also to be investigated.

The questions to be addressed here were:

- what the microstructure of these copolymers would be,
- which co-oligomers would incorporate easier, and
- how the co-oligomers would influence the activity of the reaction.

1.4 Layout of this dissertation

Chapter 2 gives a broad overview of preceding studies relevant to the topics covered in this dissertation. The subsequent chapters first discuss earlier research on the chosen theme, followed by results obtained in the current study.

In Chapter 3 the production of LLDPE using a selective chromium/PNP-type tetramerization catalyst in combination with a polymerization catalyst is discussed. In Chapter 4 the focus is on the production of LLDPE when a selective chromium/PNP-type trimerization catalyst is employed in combination with a polymerization catalyst. The synthesis of polyethylene waxes using a temperature-switchable chromium/PNP-type trimerization catalyst is also reported in this chapter.

In Chapter 5 the co-oligomerization of styrene and ethylene is described using different chromium/PNP-type catalysts. Copolymerization of the formed co-oligomerization products is also described.

1.5 References

1. Bollman, A., Blann, K., Dixon, J. T., Hess, F. M., Killian, E., Maumela, H., McGuinness, D. S., Morgan, D. H., Neveling, A., Otto, S., Overett, M., Slawin, A. M. Z., Wasserscheid, P., Kuhlmann, S., *Journal of the American Chemical Society*, 2004, 126, 14712
2. Wasilke, J., Obrey, S. J., Baker, T., Bazan, G. C., *Chemical Reviews*, 2005, 105, 1001
3. Blann, K., De Wet-Roos, D., Joubert, D. J., Killian, E., Dixon, J. T., Phelembe, N. J., Du Toit, A., US Patent 7285607 to Sasol Technology, 2007
4. Chung, T. C. in *Functionalization of Polyolefins*, Academic Press, San Diego, CA, 2002; Boen, N. K., Hillmyer, M. A., *Chemical Society Reviews*, 2005, 34, 267–275; Boffa, L. S., Novak, B. M., *Chemical Reviews*, 2000, 1479, Aaltonen, P., Lijfgren, B., *Macromolecules*, 1995, 28, 5353

2 Literature Background

2.1 Introduction

The objective of this study is to illustrate the use of chromium bis(diphenylphosphino)amine (PNP) type of oligomerization catalysts in the synthesis of ethylene based oligomers and *in situ* copolymers. Subsequently, this chapter gives an overview of homogeneous, transition metal catalyzed ethylene oligomerization (with the focus on PNP-type ligand systems), co-oligomerization and ethylene copolymerization.

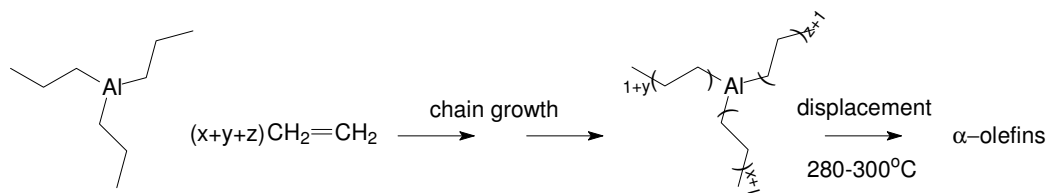
2.2 Industrial ethylene oligomerization

Linear α -olefins are generally obtained from ethylene oligomerization or are extracted from the product mixture of the Fischer-Tropsch process.¹ Most of the industrial ethylene oligomerization processes currently in use produce a broad distribution of olefins.² Examples of these processes include the Ziegler Process and the Shell Higher Olefin Process. The distributions of α -olefins obtained from such oligomerization processes are not necessarily in a desired carbon number range and additional steps are required to manipulate the product distribution in order to match market demand.

The Alfen, Gulf Oil and Ethyl processes are variations of the Ziegler Process and are based on an alkylaluminum compound.³ The production of α -olefins was initially realized by a stoichiometric process where the chain growth on aluminum was followed by liberation of the product in a separate reactor at higher temperatures through displacement with ethylene (Scheme 2.1). However, in a process where the growing chains are continuously displaced by ethylene it is possible to use catalytic amounts of aluminum. The α -olefin chain length distribution can be varied by adapting the process such that the chain growth and the displacement reactions occur simultaneously in the same reactor. In this adapted process the α -olefins are recycled to the chain growth step where transalkylation occurs, resulting in higher molecular weight chains. The alkyl chains are thus displaced *in situ* by lower

2. Literature Background

molecular weight α -olefins rather than with ethylene. Although the recycling of the olefins is effective in changing the chain length distribution, it can introduce unwanted branching into the products.



Scheme 2.1: Ziegler ethylene oligomerization

The Shell Higher Olefin Process (SHOP) comprises of three steps: oligomerization, isomerization and metathesis.⁴ The oligomerization step in the SHOP process employs a nickel chelate complex in a polar solvent as catalyst. The α -olefins produced are insoluble in the polar solvent which simplifies the separation and recycling of the homogeneous catalyst. The α -olefins with undesirable chain lengths are fractionated and isomerized to internal olefins. These olefins are subsequently metathesized in further process steps to yield a more desired olefin distribution.

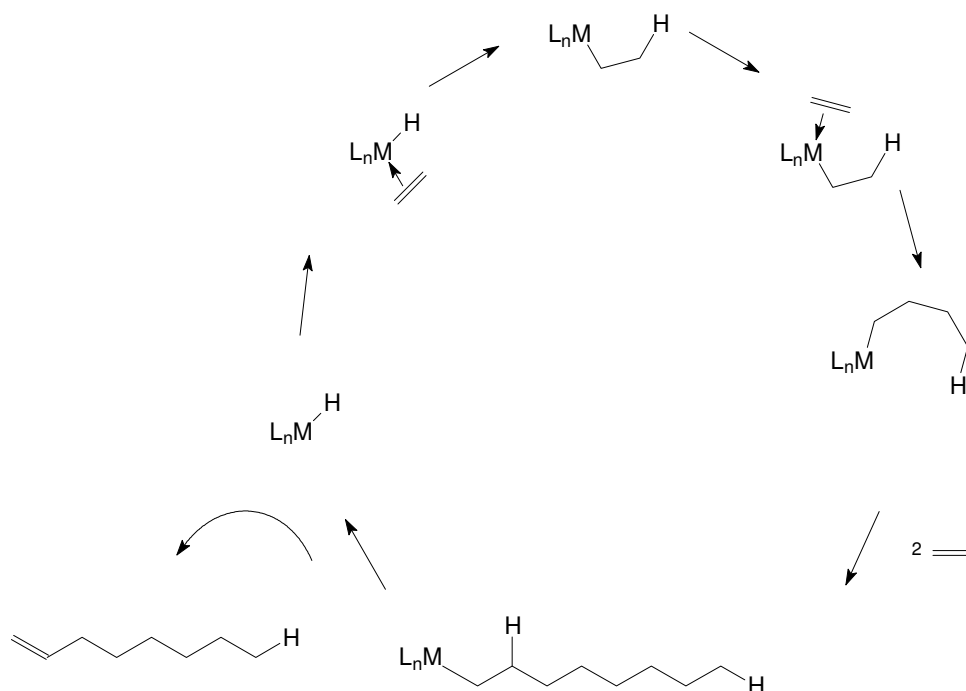
Although the product distributions in the two oligomerization processes mentioned above can be manipulated to adjust the carbon number distribution, the product slate still does not match market demand, especially with regard to the lower α -olefins required as comonomers for the production of LLDPE.¹ In recent years research focussed on the development of more selective ethylene oligomerization catalysts.⁵ Industrial processes for selective ethylene oligomerization include the Alphabutanol process from IFP for the production of 1-butene and the Chevron-Phillips trimerization process for 1-hexene.⁶ The Alphabutanol process utilizes the titanium catalyst, $\text{Ti}(\text{OR})_4/\text{AlEt}_3$, while the Chevron-Phillips process employs a chromium catalyst with a pyrrole ligand.

2.3 Homogeneous ethylene oligomerization catalysts and oligomerization mechanism

2.3.1 Non-selective ethylene oligomerization catalyst systems

Several transition metal complexes are known to oligomerize ethylene to produce a range of longer chain α -olefins.^{7,8,9} Oligomerization is commonly defined according to the number of molecules that react to form the polyolefin chain before chain termination occurs.⁸ When the number of molecules is more than 100 it becomes classified as polymerization (see also Section 2.6).

It is generally agreed that linear chain growth proceeds through ethylene insertion into an alkyl-transition metal bond according to the classical Cossee-Arleman mechanism.¹⁰ This mechanism involves coordination, migration and insertion of ethylene (Scheme 2.2). Chain transfer can occur through β -hydrogen elimination to yield α -olefins.



Scheme 2.2: Cossee-Arleman mechanism

2. Literature Background

The chain lengths in non-selective oligomerization reactions usually obey a Schulz-Flory distribution, which can be described by the α parameter (Equation 1).⁷ Lower α values indicates the production of fewer higher α -olefins.

$$\begin{aligned} \alpha &= \text{rate of propagation}/(\text{rate of propagation} + \text{rate of chain transfer}) \\ &= \text{moles of } C_{n+2}/\text{moles of } C_n \end{aligned} \quad (1)$$

Various factors have an effect on the rate of propagation relative to chain transfer and thereby the molecular weight of the oligomerization products.^{7,11} These factors include the kind of metal and its oxidation state, electronic properties and steric bulk of the ligands attached to the metal, reaction temperature and pressure, monomer concentration, nature of the solvent and molecular weight moderators.

Literature frequently reports on ethylene oligomerization with late transition metal catalysts based on nickel, palladium, iron and cobalt complexes utilizing different ligand types.^{7, 8, 11} It is supposed that late transition metal complexes have a strong tendency to undergo β -hydrogen elimination at the central metal which would induce ethylene oligomerization instead of polymerization. Variation of both steric and electronic environments around the central metal through ligand tailoring can affect both the catalytic activity and the olefin distribution obtained with these metals.^{7,8, 11}

The well-known, monoanionic bidentate phosphorous oxygen donor ligand in combination with nickel (Figure 2.1) is employed as the oligomerization catalyst in the SHOP process.¹²

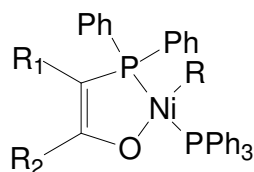
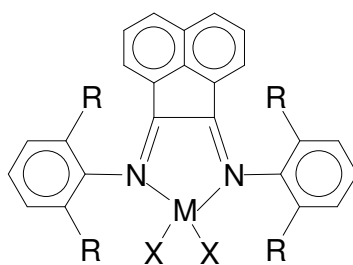


Figure 2.1: Nickel complex-type employed in the SHOP process

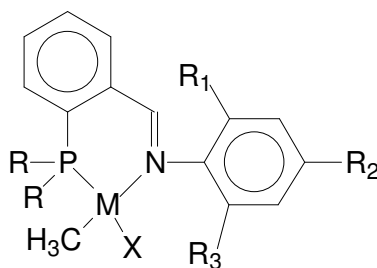
Figure 2.2 displays examples of some of the most active oligomerization catalyst types. These metal complexes have the ability to act as ethylene oligomerization or polymerization catalysts, depending on the steric properties of the ligand substituents. Nickel and palladium complexes with α -diimine and iminophosphine ligands are known as active catalysts for olefin oligomerization.¹³ Likewise, five-

2. Literature Background

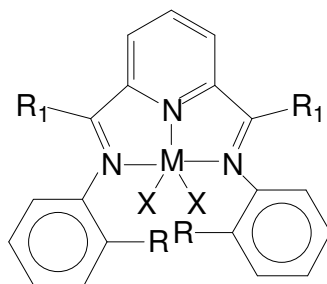
coordinated 2,6-bis(arylimino)pyridyl iron(II) and cobalt(II) dihalides are reported in various examples of ethylene oligomerization.^{7,14} Such dihalide catalysts are activated by methyl aluminoxane (MAO). MAO is a poorly defined, partial hydrolysis product of Al_2Me_6 , which serves two purposes; as an alkyl transfer reagent to the transition metal and as a Lewis acid which abstracts one alkyl group to generate a vacant coordination site.¹⁵



α -diimine complex



iminophosphine complex



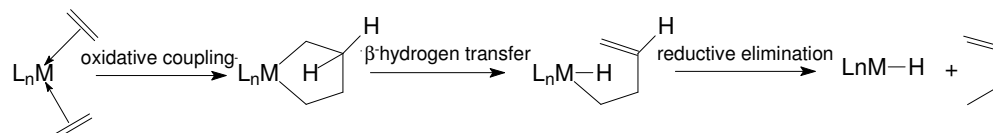
2,6-bis(arylimino)pyridyl complex

Figure 2.2: Examples of general structures for oligomerization catalysts producing Schulz-Flory distributions of α -olefins

2. Literature Background

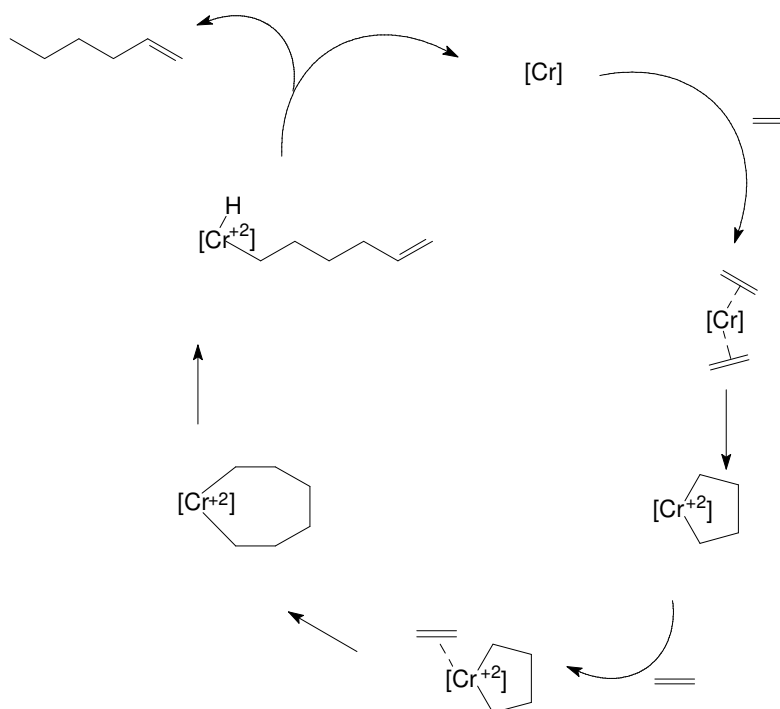
2.3.2 Selective ethylene oligomerization catalyst systems

Selective ethylene dimerization occurs when two molecules of ethylene, coordinated to the metal centre, undergo oxidative coupling to form a metallocyclopentane, followed by β -hydrogen transfer and reductive elimination (Scheme 2.3).¹⁶ Numerous nickel- and titanium-based systems are reported to selectively dimerize ethylene.^{8,11,17}



Scheme 2.3: Proposed pathway for selective ethylene dimerization

Selectivity to produce ethylene trimers is believed to occur through the coordination and insertion of a further ethylene molecule which results in a stable, seven membered metallocycle (Scheme 2.4).¹⁸



Scheme 2.4: Proposed mechanism for selective trimerization of ethylene

2. Literature Background

Numerous homogeneous catalysts have been reported for the selective production of 1-hexene since the late 1980's. A review by Morgan and coworkers⁵, summarizing the advances in selective ethylene trimerization, points out that the more active and selective catalytic systems are based on chromium, titanium and tantalum transition metals. Among these metals which catalyze the trimerization of ethylene, chromium occupies a prominent position. Figure 2.3 shows a catalyst and ligand structures successfully employed in selective ethylene trimerization reactions. Half sandwich titanium complexes (Figure 2.3a) are also reported to be very selective and active trimerization catalysts, but a drawback is the large excess of methyl aluminoxane necessary for activation.¹⁹

The Phillips catalyst, which forms the basis of the Chevron-Phillips trimerization process, is based on a chromium precursor, a pyrrole ligand (2,5-dimethylpyrrole) (Figure 2.3b) and trialkylaluminum as cocatalyst.^{5,20} Various aromatic compounds were investigated as ligands for chromium after the discovery of the Phillips catalyst, most with low or moderate activity or with significant polyethylene formation.⁵ Multidentate heteroatomic ligands with nitrogen, phosphorous (Figure 2.3c) or nitrogen, sulfur donors (Figure 2.3 d) in combination with chromium and a methyl aluminoxane (MAO) cocatalyst were studied, but the discovery of mixed phosphorous and nitrogen donor ligands of the type $\text{Ph}_2\text{PN}(\text{R})\text{PPh}_2$ (Figure 2.3e and Figure 2.3f) in combination with chromium and MAO yielded catalysts with exceptional activity, selectivity and stability together with low polyethylene formation.^{5,21} Multidentate ligands based on mixed sulphur and nitrogen donors were also shown to have promise as active and selective ethylene trimerization ligands (Figure 2.3d).²²

2. Literature Background

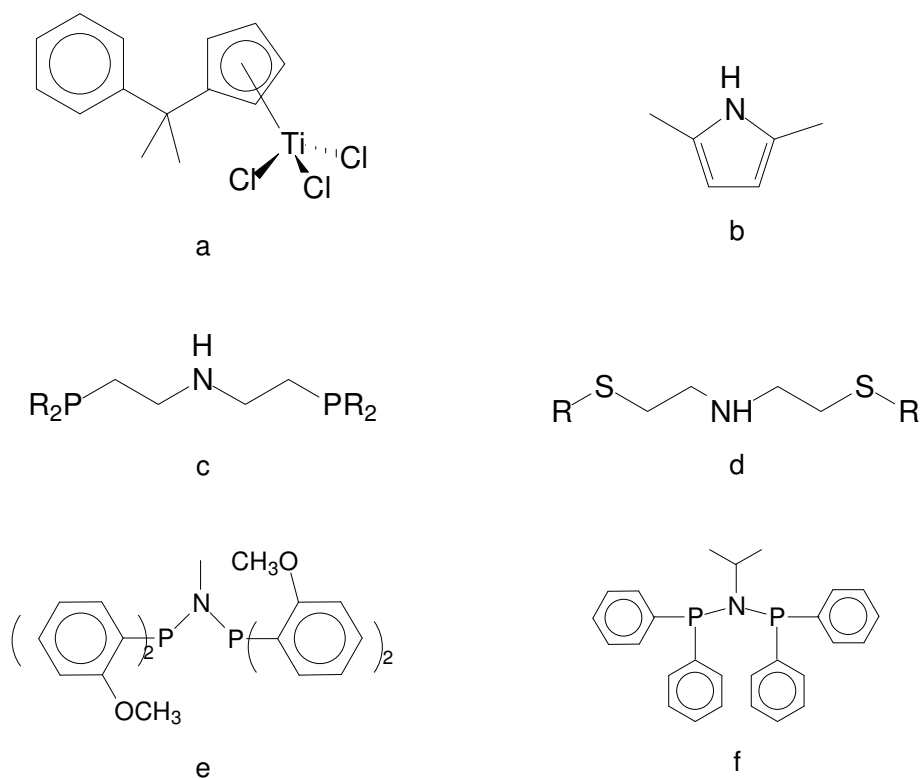


Figure 2.3: Examples of highly active and selective trimerization ligands and a catalyst precursor

While many selective trimerization systems are known, a selective tetramerization system to obtain 1-octene selectively remains a rarity. Until recently it was believed that high selectivity for an ethylene tetramer cannot be achieved, since the formation of a nine membered metallocycle would theoretically not be stable, when the last ethylene molecule is inserted.²³ Researchers at Sasol reported in 2004 that selectivity towards ethylene tetramer formation could be achieved when certain $\text{Ph}_2\text{PN}(\text{R})\text{PPh}_2$ -type ligands were used.²⁴ A mechanistic study confirmed the intermediary metallacyclic species in the formation of 1-octene and a mechanism was proposed to account for the primary and secondary products formed in a typical tetramerization reaction.²⁵ Although selectivities for 1-octene of up to 70% can be obtained, significant quantities of other products are also formed, including 1-butene, 1-hexene, methylcyclopentane, methylene-cyclopentane, 2-propenylcyclopentane, n-propylcyclopentane, C_{10} - C_{36} α -olefins, C_4 - C_{20} alkanes as well as a complex mixture of C_{10} , C_{12} and C_{14} secondary oligomerization products.

2. Literature Background

Selectivity shows a strong dependence on the steric and coordinative properties of the $\text{Ph}_2\text{PN(R)PPh}_2$ type of ligand.^{24,26} A ligand with a methyl group at the nitrogen and no substitution on the aromatic rings shows selectivity to tetramerization, while substitution in the *ortho* position with an oxygen donor group shifts the selectivity towards trimerization. BP reported greater than 85 % selectivity to 1-hexene for a chromium/PNP-type system with *ortho* methoxy groups.²¹ The authors observed that ligands with *ortho* methoxy groups are active catalysts while those with *ortho* ethyl substituents are completely inactive (*this was later to be contradicted by the Sasol group*^{24,26}) and suggested that the *ortho* methoxy groups act as pendant donors, resulting in an increase in the coordinative saturation of the chromium centre. Bollmann et al^{24,26} reported high selectivity for trimerization using chromium with PNP-type ligands containing *ortho* substitution, but without an oxygen donor group. The inclusion of steric bulk in the *ortho* position leads to an increase in trimerization while tetramerization selectivity decreases. It was found that the 1-hexene/1-octene ratio is directly affected by an increase in the steric bulk (total amount of *ortho* groups and the nature of the substituent on the nitrogen). Figure 2.3e and Figure 2.3f show the structures of the PNP-type ligands that are selective towards 1-hexene and 1-octene, respectively.

The trimerization catalyst with *ortho* methoxysubstituents (Figure 2.3e) is reported to be thermally stable and little deactivation over time is observed.²¹ Catalysts that contain *ortho* ethyl substituents, are shown to be highly active trimerization catalysts at lower temperatures, but at higher temperatures the selectivity changes to low molecular weight polyethylene.²⁷ This is probably caused by conformational changes in the absence of an actual donor group.

2.4 Co-oligomerization

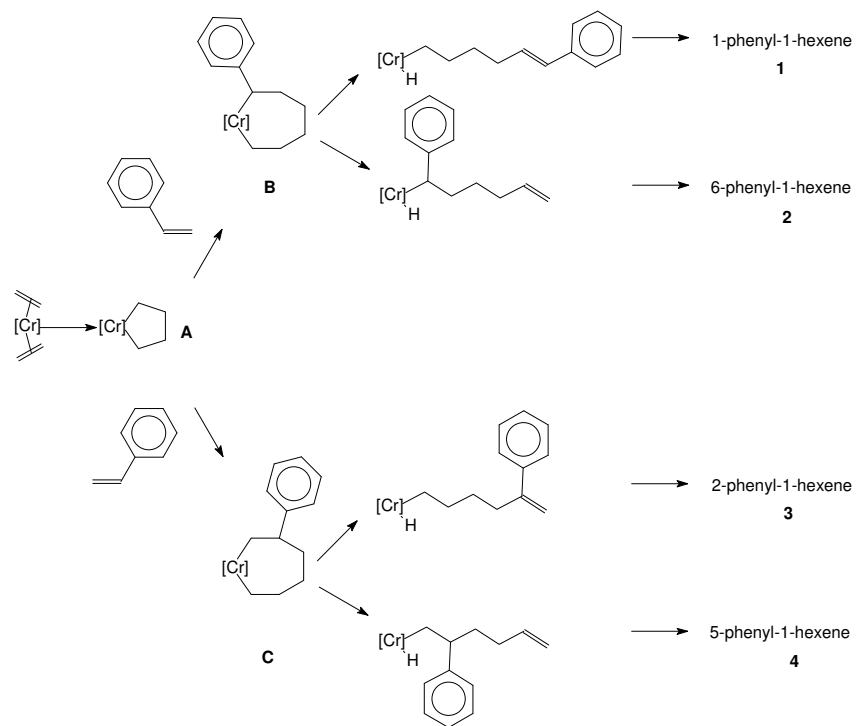
The co-oligomerization products of ethylene and α -olefins are observed as byproducts of the ethylene tri- and tetramerization reactions and result from the coordination of the formed α -olefins to the active metal centre, followed by incorporation into the metallacycle intermediate.²⁵ Such side reactions are undesirable, since it affects the selectivity of the reaction negatively. The incorporation of the formed α -olefins can be eliminated to some extent by using a ligand with steric bulk to minimize the coordination of the α -olefins.

2. Literature Background

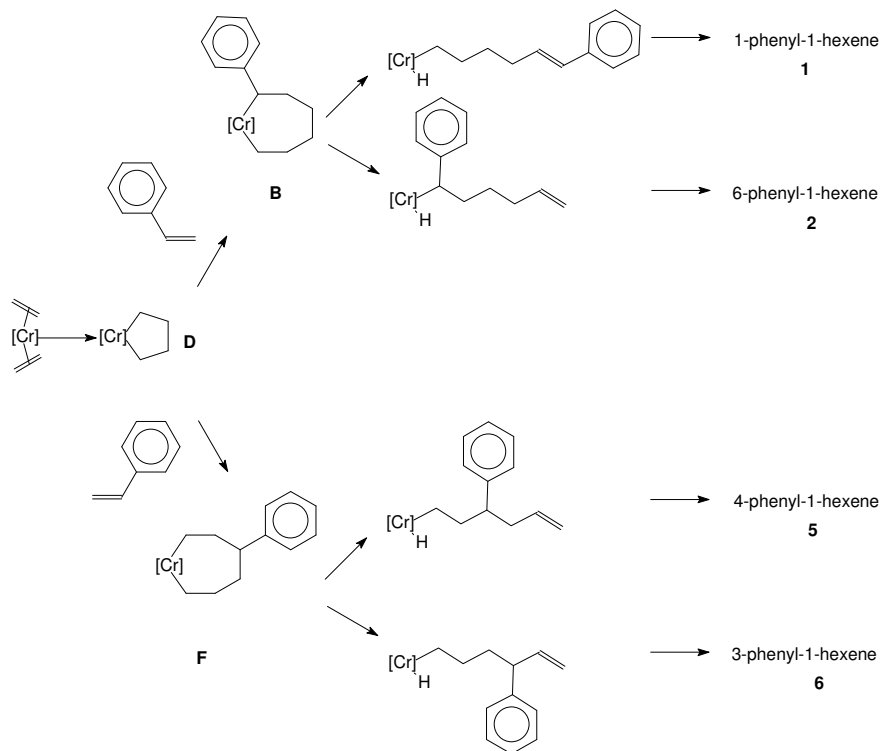
The co-oligomerization of ethylene and a second α -olefin is, however, a potential route to obtain new types of polar comonomers. The use of PNP-type ligands in combination with chromium for the selective cotrimerization of ethylene and styrene was reported by Bowen and Wass.²⁸ Different isomers, containing two ethylene molecules and one styrene unit, were reported to form exclusively. Isomers resulting from two styrene units with one ethylene molecule were not detected in the co-oligomerization reaction mixture. Homo-oligomerization of styrene was also not found. Scheme 2.5 indicates various possible reaction routes for ethylene-styrene co-trimerization. Route 1 involves the coordination of ethylene to the metal centre to form a five membered metallocycle (A) followed by the coordination of a styrene molecule in a 1,2 or a 2,1 fashion. The resulting seven membered metallocycles (B and C) can undergo reductive elimination on either side of the metallocycle to form the final cotrimerization products 1-4. In Routes 2 and 3 a styrene molecule and ethylene molecule can coordinate first with the metal centre to form a four membered metallocycles (D or E) followed by coordination with a further ethylene molecule from either side of the metallocycle. This will lead to the formation of three different seven membered metallocycles (B, C and F) which can result in any of the products 1-6.

The cotrimerization of ethylene and styrene has been reported using the ligand (*o*-OMeC₆H₄)₂PN(CH₃)P(*o*-OMeC₆H₄)₂ in combination with CrCl₃(THF)₃. Here the activity was found to be much lower than reported for the same ligand in ethylene homo-trimerization reactions.²¹ The main co-oligomerization products are 1-phenyl-1-hexene and 6-phenyl-1-hexene, while 3-phenyl-1-hexene and 4-phenyl-1-hexene also form in lesser amounts. The co-oligomerization product distribution indicated that 2,1- insertion of styrene is favoured above 1,2-insertion of styrene. 2-Phenyl-1-hexene and 5-phenyl-1-hexene, which can result only from 1,2-insertion in either Route 1 or Route 3, are absent. The main products 1-phenyl-1-hexene and 6-phenyl-1-hexene can result from 2,1-styrene insertion in both Route 1 and Route 2. 3-Phenyl-1-hexene and 4-phenyl-1-hexene, the minor products, are possibly formed in Route 2 through 2,1-styrene insertion or 1,2-styrene insertion in Route 3. A preference for 2,1-coordination explains the relative amounts of the cotrimerization isomers.

2. Literature Background



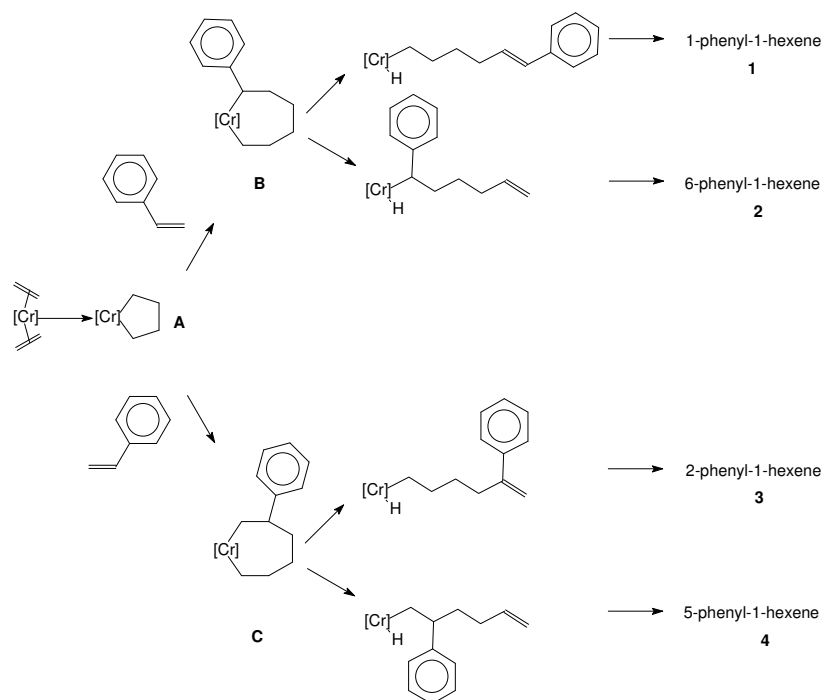
Route 1



Route 2

Scheme 2.5: Possible routes to cotrimercization products (continued on next page)

2. Literature Background



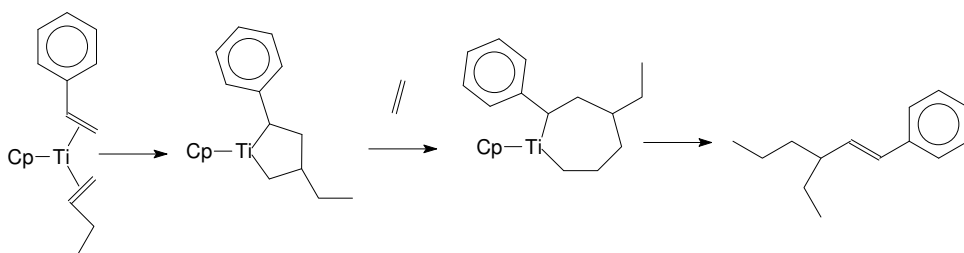
Route 3

Scheme 2.5: Possible routes to cotrimerization products (continued from previous page)

Pellachia *et al.*²⁹ have also reported on the selective co-oligomerization of ethylene and styrene using half-titanocenes. In an initial ethylene-styrene copolymerization study employing $\text{Cp}^*\text{TiMe}_3\text{-B}(\text{C}_6\text{F}_5)_3$ ($\text{Cp}^* = \eta^5\text{-C}_5\text{Me}_5$) the occurrence of 4-phenylbutyl-branched polyethylene was observed. Further investigations have shown the formation of unsaturated ethylene-styrene co-oligomerization products, with 6-phenyl-1-hexene among the main components. 6-Phenyl-1-hexene is subsequently copolymerized with ethylene due to the presence of multi-site titanium systems. (Ti(IV), Ti(III) and Ti(II) organometallic species were detected.) When $\text{Cp}^*\text{TiMe}_3\text{-B}(\text{C}_6\text{F}_5)_3$ is employed the liquid product consists of three major products: 6-phenyl-1-hexene, *cis*-1-phenyl-1-hexene and 3-ethyl-1-phenyl-1-hexene.²⁹ Minor products were found to be *trans*-1-phenyl-1-hexene and 1-phenyl-1-octene. This selective co-oligomerization study have been extended to include $\text{Cp}^*\text{TiCl}_3\text{-MAO}$ as well as different vinyl aromatic comonomers; like *p*-methylstyrene, *m*-methylstyrene, *p*-*tert*-butylstyrene and *p*-chlorostyrene. $\text{Cp}^*\text{TiCl}_3\text{-MAO}$ yields as the major products *trans*-1-phenyl-1-hexene and 6-phenyl-1-hexene and as the minor products, 1-phenyl-1-octene and 6-phenyl-1-octene. Optimization of the co-oligomerization conditions indicates that an increase in styrene-ethylene feed ratio results in an increase in co-oligomer yield, but a decrease in styrene conversion.

2. Literature Background

According to the co-oligomerization product distribution it was proposed that the reaction proceeds through metallocycle intermediates (similar to Scheme 2.5) and comparable to the mechanism of selective ethylene homo-trimerization.²⁹ The occurrence of 3-ethyl-1-phenyl-1-hexene was ascribed to the formation of 1-butene and the subsequent coordination of 1-butene together with a styrene molecule leading to 4-ethyl-2-phenyl-titanacyclopentane (Scheme 2.6). Further insertion of ethylene forms 4-ethyl-2-phenyl-titanacycloheptane and reductive elimination results in 3-ethyl-1-phenyl-1-hexene.



Scheme 2.6: Proposed route for formation of 3-ethyl-1-phenyl-1-hexene during styrene-ethylene-co-oligomerization

Further *in situ* copolymerization reactions have also been described.²⁹ A polymerization catalyst is added to copolymerize the formed co-oligomerization products to yield 4-phenyl-1-butyl branched PE. These copolymers can find application, for example, in polyolefin functionalization (through post polymerization functionalization methods) when *p*-methylstyrene is employed.

In a different study the trimerization catalyst CpTiCl_3 have been activated in the presence of different alkenes.³⁰ The aim of this study was to investigate if the activated titanium compound can be stabilized as Ti(IV) in the presence of the alkene to eliminate the formation of Ti(III) species, which could cause the formation of unfavorable polyethylene as byproduct. During this study it has been found that ethylene can be oligomerized in the presence of 2-norbornene, resulting in unique α -olefins such as 4-norbornyl-1-butene.

2.5 Combined oligomerization-copolymerization (tandem catalysis)

LLDPE is prepared by the copolymerization of ethylene with longer chain linear α -olefins. These α -olefins can be obtained from an ethylene oligomerization process where, in the most cases, a distribution of olefins is produced.^{1,2} After isolation and purification steps a portion of these α -olefins, mainly 1-butene, 1-hexene or 1-octene, is consumed in the manufacturing of LLDPE. A possible way of reducing the cost of LLDPE is to produce α -olefins *in situ* from ethylene using a selective oligomerization catalyst and to copolymerize it with ethylene using a polymerization catalyst in the same reactor.³¹ This eliminates unnecessary purification steps. This process of producing α -olefins from ethylene and copolymerization of the α -olefins with ethylene can be simultaneous or sequential. In the literature it is referred to as tandem catalysis or *in situ* copolymerization. Tandem catalysis in general, where multiple reactions are combined in one process, is applied throughout synthetic chemistry and was recently reviewed by Bazan and coworkers.³² Catalyst compatibility with the solvent, other catalysts and additives from preceding steps need to be considered in sequential tandem catalysis. In an ideal situation there should be no interference between the catalytic species and reactivities should be well matched. One of the main motivations for the use of multiple catalysts in one process/reactor is the prevention of time and yield losses due to isolation and purification of the intermediates. *In situ* generation of harmful chemicals also eliminates the transportation of chemicals over long distances.

A review article on catalytic polymerization points out the difficulty of this approach in the real life of plant operation since '*carefully matching of polymerization rate and time profiles of the different catalysts are prime requirements to prevent the formation of very complex, time and conversion dependent polymer mixtures. Their composition responds to minute variations of the polymerization process parameters*'.³³ It is also noted that the addition of the second catalyst is likely to influence the performance of the first catalyst and that this interaction can affect molecular weights and branch distribution, thus prompting new challenges for reactor engineering, polymer characterization and especially quality control of the resulting products.

As early as 1967 it was documented that butyl branched PE is formed during the polymerization of ethylene with chromium(III)2-ethylhexanoate activated with partially

2. Literature Background

hydrolyzed tri-isobutylaluminum.³⁴ Analysis of the liquid fraction showed that the branches result from α -olefins (mostly 1-hexene) formed during the reaction, which copolymerized with ethylene. Since this discovery various low cost routes to ethylene- α -olefin-copolymers from ethylene as the sole monomer feed were described in patents from Phillips Petroleum Company using supported chromium catalysts.³⁵ In most of these patents the chromium active sites are modified to yield dual site catalytic systems for oligomerization and polymerization of ethylene, respectively. Examples of heterogeneous chromium-based catalysts are numerous and the dual oligomerization and polymerization behaviour of this type of catalysts is, in general, obtained through partial poisoning of the polymerization sites.

Recently the open and patent literature focus more on the use of homogeneous ethylene oligomerization catalytic systems in combination with heterogeneous or homogeneous polymerization catalysts.³⁶⁻⁴⁶ A few of these examples are mentioned in the section below to illustrate the factors of importance when using multiple catalysts in one reactor.

Almost all the non-selective oligomerization catalysts described in the preceding sections have been employed in different *in situ* copolymerization studies. The use of the SHOP-type nickel P⁺O donor catalyst (Figure 2.1, Section 2.3.1) has been reported in combination with a Ziegler polymerization catalyst, titanocene dichloride treated with a mixture of magnesium hydride and α -titanium trichloride.³⁶ The polymerization catalyst was chosen because of its compatibility with the oligomerization catalyst. The oligomerization catalyst is deactivated by alkylaluminum compounds, thus the polymerization catalyst should not require activation with alkylaluminum. It was found that the activity and selectivity of the oligomerization catalyst are not affected by the presence of the polymerization catalyst, but the behaviour of the polymerization catalyst, however, is modified. The polymerization catalyst takes a longer time to reach maximum activity, but remains active for an extended period compared to the situation in the absence of the oligomerization catalyst. Butyl and ethyl branches have been detected in the formed polymer, although the product distribution of the oligomerization catalyst contains also higher α -olefins. One disadvantage of the specific polymerization catalyst is its ability to isomerize α -olefins, forming internal olefins which do not copolymerize. The comonomer response of the polymerization catalyst is also very low, thus it requires a large surplus of α -olefins before copolymer with a higher branching content can be achieved. To produce the large excess of α -olefins in the reactor the oligomerization

2. Literature Background

catalyst concentration has been increased or the copolymerization was started an hour later than the oligomerization reaction. This resulted in a maximum comonomer content of 3 mol%. Metallocenes activated by MAO have been investigated as a means to further increase the comonomer content of the resulting copolymer. The SHOP-type catalyst is active under the reaction conditions employed, but the behaviour of the oligomerization catalyst has been altered.

This study³⁶ shows how important it is to match the compatibility of the oligomerization and polymerization catalyst. The presence of one might affect the catalytic behaviour of the other, or the cocatalyst required for activation of the polymerization catalyst might influence the oligomerization catalyst activity or selectivity.

Subsequent studies also showed that the polymerization catalyst must be able to incorporate the type of oligomer that is produced. When the oligomerization catalyst had selectivity to higher olefins, the resulting macromonomers were copolymerized using the Dow Constrained Geometry catalyst, $[(\eta^5\text{-C}_5\text{Me}_4)\text{SiMe}_2(\eta^1\text{-NCMe}_3)]\text{TiCl}_2$, or metallocenes capable of incorporating longer chain α -olefins.³⁷ Long chain branched LLDPE have been obtained.

The activity of an oligomerization catalyst should be such that it gives rise to a sufficient concentration of comonomer for the formation of polyethylene with the required branching content.^{31,38,39} The activities of the oligomerization and polymerization catalysts should also match under similar reaction conditions. Bis(arylimino)pyridyl complexes of cobalt and iron (Figure 2.2, Section 2.3.1) have oligomerization productivities as high as that of metallocenes and are consequently reported as suitable candidates for tandem catalysis in various examples.^{7,40,41} Detailed ¹³C NMR studies are reported characterizing the branching types and amount of these *in situ* produced copolymers. Both long chain branches and mixed ethyl and butyl branches are present, since this type of oligomerization catalyst produces a Schulz-Flory distribution of α -olefins.³⁸ The structure of the copolymers can be regulated by the ratio of the catalysts and the reaction conditions.

The preparation of branched polyethylene from the combination of three different catalysts has been reported by Bazan and co-workers.⁴² The branched polymer structures have been obtained using a combination of two oligomerization catalysts together with the Dow Constrained Geometry catalyst. The one oligomerization catalyst employed was a nickel diimine catalyst (Figure 2.2, Section 2.3.1) which

2. Literature Background

produces a Schulz-Flory distribution of oligomers and the other was a nickel P[^]O donor complex which primarily produces 1-butene. These triple tandem reactions were shown to generate unique polymers with different melting temperatures, branching contents and molecular weights directly from ethylene by variation of the catalyst components.

The use of more selective oligomerization catalysts which produce α -olefins of certain chain lengths will provide the best control over polymer structure and properties and a match of current commercially produced copolymers may be possible. Several studies combining selective trimerization systems with polymerization catalysts to yield butyl branched copolymers have been published and are discussed below.

These 1-hexene producing catalytic systems include the chromium/PNP-type based catalysts from BP, the chromium/SNS donor systems from Sasol and various CpTi-based catalytic systems.⁴³⁻⁴⁶ The highly active and selective chromium/PNP-type trimerization system described by BP is based on PNP-type ligands with *ortho* methoxysubstituted phenyl groups. Selectivity to 1-hexene is greater than 85% and the catalyst is extremely stable, thermally robust and no deactivation over time occurs.²¹ This oligomerization system is very suitable for use in tandem with polymerization catalysts to produce LLDPE from ethylene alone due to its high activity and selectivity and such an example is reported in a patent.⁴³ In this example the oligomerization catalyst was used in combination with a Ziegler Natta polymerization catalyst. Alternatively, a supported version of the trimerization catalyst was combined with a metallocene to obtain a butyl branched copolymer. The use of CpTi-trimerization systems is described in combination with the Dow Constrained Geometry polymerization catalyst or metallocenes.⁴⁴ These tandem reactions yielded a variety of butyl branched copolymers by adjustment of the reaction conditions and catalyst ratios. Trimerization with bis(2-dodecylsulfanyl-ethyl)amine (SNS) and CrCl₃(THF)₃ was investigated in combination with different metallocenes. Copolymers with different levels of 1-hexene incorporation, depending on the specific metallocene used as well as the way of introducing the catalysts, were obtained.⁴⁵

A mathematical model has subsequently been developed to describe ethylene-1-hexene copolymerization with the chromium/SNS catalytic system.⁴⁶ Broad DSC curves are observed at high oligomerization to polymerization catalyst ratios and the

2. Literature Background

model elucidate that this is due to composition drift and accumulation of 1-hexene during copolymerization. A short pre-trimerization time is used to improve the homogeneity and to minimize the broadening of the DSC curves.

Most of the published work on tandem catalysis demonstrates the use of different combinations of homogenous oligomerization catalysts and polymerization catalysts to achieve the production of branched polyethylene. The mole fraction of the oligomerization catalyst is varied in the majority of the studies to produce copolymers with a wide range of melting temperatures. This illustrates how the branching content of the copolymers increase as the concentration of the oligomerization catalyst increases relative to the polymerization catalyst and more 1-hexene is produced. Not much emphasis is placed on the actual comonomer content distributions of the resulting products, while only the melting points have been listed as indication that comonomer incorporation has occurred.

It is clear from the literature that the production of branched polyethylene is highly possible by combination of an oligomerization and a polymerization catalyst and that the branching types and amounts are inherently dependant on the selectivity and activity of the oligomerization catalyst. The most important considerations are the compatibility of the two catalysts under the reaction conditions and the absence of chemical interference between the active sites. The two catalysts must also have comparable tolerance to the activators. The polymerization catalyst must have a suitable comonomer response to the carbon chain lengths produced by the oligomerization catalyst.

2.6 Homogeneous chromium catalysts selective to higher oligomers or polymers

Several non-metallocene, homogeneous, transition metal coordination complex catalysts are known which produce either oligomers or higher molecular weight materials, ranging from waxes to polymers, according to the classical Cossee-Arman mechanism.⁴⁷ Depending on the reaction conditions, steric nature and electronic properties of the ligand the products can be oligomers (less than 100 molecules), polymers or both. Examples of catalysts include various coordination complexes of $\text{CrCl}_3(\text{THF})_3$ with neutral ligands as described in the literature for the production of polyethylene.^{47,49,50} Research at Sasol Technology during the last decade led to the

2. Literature Background

development of the bis(diphenylphosphino)amine (PNP) type of chromium catalysts for 1-hexene and 1-octene production (as described in the preceding sections) and it was found that some of these catalysts are selective to produce low molecular weight polyethylenes under specific reaction conditions.⁴⁸ Another source describes chromium complexes with bis(benzimidazolyl)pyridine derivative ligands which show combined oligomerization and polymerization selectivity with MAO as cocatalyst, while only polymerization occurs in the presence of diethylaluminum chloride.⁴⁹ In the MAO activated catalyst system an increase in temperature results in a decrease in polymerization selectivity relative to oligomerization, indicating a mechanism different to that of the chromium/PNP-type system where the polymerization activity increases with an increase in temperature. GPC curves show bimodal or even multimodal behaviour, and also show that the molecular weight is dependent on the ligand environment. In complexes with low steric bulk the polymer is waxlike. The authors stated that the steric bulk is not sufficient to prevent associative displacement of the growing chain and the electron affinity in the chromium centre facilitates the chromium induced abstraction of a β -hydride from the growing chain. These combined effects result in a rapid chain transfer process and low molecular weight polymer chains. Complexes with more steric bulk result in higher molecular weight polyethylene, although the fraction of lower molecular weight polyethylene is also present. ¹³C NMR analyses show that linear chains are formed with mainly vinyl end groups.

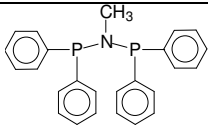
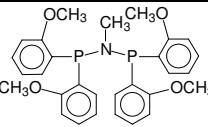
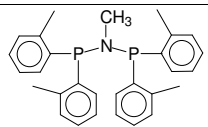
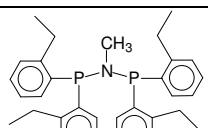
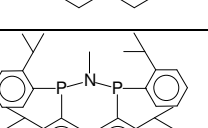
Bis(imino)pyridyl chromium complexes in combination with MAO or triisobutylaluminum have also been investigated for the polymerization of ethylene.⁵⁰ The substituents on the ligands influence the catalytic behaviour of the complexes with regard to both the activity and the molecular weight of the resulting polyethylene. The most active complexes are those bearing two *ortho* methyl groups on the phenyl groups, but an increase in steric bulk in these positions result in a decrease of activity. The presence of donor groups, such as methoxy, in the *ortho* position, causes inactivity in catalysts. A polyethylene fraction and a lower molecular weight wax fraction have been observed. It was also found that ligands with bulkier *ortho* substituents on the phenyl groups give rise to higher molecular weights. An increase in reaction temperature yields a decrease in catalyst activity, although the amount of wax increases. The polymers obtained from these chromium complexes are highly linear. Vinyl, isopropyl and methyl terminal groups have been detected by ¹³C NMR spectroscopy and their origin is explained. Vinyl end groups denote β -hydrogen

2. Literature Background

elimination or β -hydrogen transfer to the monomer, while isopropyl end groups signify chain transfer to the aluminum cocatalyst. Methyl end groups have several origins and can form in the initial methylation step, due to chain transfer to MAO followed by hydrolysis during work-up or the insertion of ethylene into the Cr-H bond formed after β -hydrogen elimination.

Research at Sasol Technology has investigated different PNP-type ligand structures and it has been found that ligands with *ortho* alkyl substituents on the phenyl rings are remarkably active catalyst for wax synthesis at 120 °C.⁴⁸ These catalysts are selective 1-hexene producing catalysts at 60 °C, but switch to polymerization catalysts at higher reaction temperatures. Table 2.1 gives an indication of the relative activities of selected ligand structures. Molecular weights of the products are also compared (1-Pentene was used as comonomer in these reactions).

Table 2.1: Effect of ligand structure on wax synthesized at 120 °C⁴⁸

Ligand	Wax Yield g	$\langle M_n \rangle$	$\langle M_w \rangle$
	2	not available	not available
	5	65 680	137 480
	98	3 100	5 360
	94	2830	8950
	108	4 660	10 360

From the examples listed in Table 2.1 it can be seen that catalysts with ligands without *ortho* substituents or with strong donor groups in these positions are poor

2. Literature Background

wax-producing catalysts. The ligands with the more bulky *ortho* substituents produce the highest molecular weight.

Nickel complexes bearing PNP-type ligands were described for the polymerization of ethylene by Wass and coworkers.⁵¹ The catalysts compared in their study contained methyl, ethyl or isopropyl substituents, respectively, in the *ortho* position of the phenyl rings. It was also found that the more sterically encumbered isopropyl substituent produces the highest molecular weight polyethylene. The branching observed was consistent with a chain walking mechanism, but the level of branching was low.

In the abovementioned study at Sasol Technology, using the chromium/PNP-type catalysts for wax synthesis, the effects of the reaction temperature and ethylene pressure were investigated. The PNP-type ligand, (o-ethylC₆H₄)₂P₂N(CH₃), was used in combination with Cr(acac)₃. As already mentioned, lower temperatures result in mainly 1-hexene. Table 2.2 summarizes the observed effect of temperature and pressure on wax synthesis.

Table 2.2: Effect of the reaction temperature and pressure on wax synthesis using chromium/PNP-type catalysts

Temp °C	Pressure bar	Activity 10 ³ g.(g _{Cr}) ⁻¹	<M _n >	<M _w >
80	20	192	16 150	51 030
100	20	441	5 740	17 380
120	20	507	3 260	10 370
120	30	562	3 900	9 500
120	10	294	3 820	9 450

It was found, as expected, that the molecular weight decreases with increasing reaction temperature due to an increase in the rate of chain transfer reactions. The molecular weight was not found to be significantly dependent on the ethylene pressure. ¹³C NMR analysis showed 1-2 % methyl branches present in the waxes. Only a small fraction of vinyl end groups was observed. The molecular weight and, consequently the wax viscosity, decreased in subsequent reactions with the addition of hydrogen as a chain transfer agent.

2.7 References

1. Developments in Alpha Olefin Production Technology (97/98S14), PERP report, Nexant Chem. Systems
2. Vogt, D. in Applied Homogeneous Catalysis with Organometallic Compounds, Cornils, B., Hermann, W. A., VCH, New York, 1996, volume 1, page 245-258; Wittcoff, H., Reuben, B. G., Plotkin, J. S. in Industrial Organic Chemicals, Wiley-VCH Publishers, 1996, page 114-118
3. Ziegler, K., Martin, H., US Patent 2943125, 1954, Al-Jarallah, A. M., Anabtawi, J. A., Siddiqui, M. A. B., Aitani, A. M., Catalysis Today, 1992, 14, 1; Kirk-Othmer Encyclopedia of Chemical Technology, third edition, volume 16, page 485, Lappin, G. R., Sauer, J. D in Alphaolefins Applications Handbook, Marcel Decker Inc., Berkley, CA, 1989
4. Keim, W., Angewandte Chemie, International Edition, 121, 1990, 235; Keim, W., Kowaldt, F. H., Goddard, R., Kruger, C., Angewandte Chemie, International Edition, 17, 1978, 466
5. Dixon, J. T., Hess, F. M., Morgan, D. H., Journal of Organometallic Chemistry, 2004, 689, 3641
6. Weissermel, K., Arpe, H. J. in Industrial Organic Chemistry, Wiley-VCH Publishers, 1998, page 74; Chauvin, Y., Olivier, H., in Applied Homogeneous Catalysis with Organometallic Compounds, Cornils, B., Hermann, W. A., Eds., VCH, New York, 1996, volume 1, page 245-258; 1-Hexene From Ethylene By The Phillips Trimerization Technology (9518), PERP report, Nexant Chem. Systems; Reagan, W. K., Freeman, J. W., Conroy, B. K., Pettijohn, T. M., Benham, E. A., EP 0608447 to Phillips Petroleum Company, 1994
7. Bianchini, C., Giambastiani, G., Rios, I. G., Montovani, G., Meli, A., Segarra, A. M., Coordination Chemistry Reviews, 2006, 250, 1391
8. Skupinska, J., Chemical Reviews, 1991, 91, 613
9. Speiser, F., Braunstein, P., Saussine, L., Accounts of Chemical Research, 2005, 38, 784

2. Literature Background

10. Tobisch, S., Ziegler, T., *Organometallics*, 2003, 22, 5392; Cossee, P. J., *Journal of Catalysis*, 1964, 3, 80; Arlman, E. J., Cossee, P. J., *Journal of Catalysis*, 1964, 3, 99
11. Ittel, S. D., Johnson, L. K., Brookhart, M., *Chemical Reviews*, 100, 2000, 1169
12. Keim, W., Hoffmann, B., Lodewick, R., Peuckert, M., Schmidt, J., *Molecular Catalysis*, 1979, 6, 79; Keim, W., Kowaldt, F. H., Goddard, R., Kruger, C., *Angewandte Chemie, International Edition*, 17, 1978, 466
13. Johnson, L. K., Killian, C. M., Brookhart, M., *Journal of the American Chemical Society*, 117, 1995, 6414; Svejda, S. A., Johnson, L., Brookhart, M., *Journal of the American Chemical Society*, 121, 1999, 10634; Daugulis, O., Brookhart, M., *Organometallics*, 21, 2002, 5926; Guan, Z. B., Marshall, W. J., *Organometallics*, 21, 2002, 3580
14. Reardon, D., Conan, F., Gambarotta, G., Yap, Q., Wang, Q., *Journal of the American Chemical Society*, 121, 1999, 9318; Schmidt, R., Das, P. K., Welch, M. B., Knudsen, J., Gottfried, S., Alt H. G., *Journal of Molecular Catalysis, A: Chemistry*, 222, 2004, 27
15. Hill, A. F. in *Organotransition Metal Chemistry*, Royal Society of Chemistry, Cambridge, 2002, page 138
16. Bernardi, F., Bottoni, A., Rossi, I., *Journal of the American Chemical Society*, 1998, 120, 7770
17. Muthukumar, S. P., Ravindranathan, M., Sivaram, S., *Chemical Reviews*, 1986, 86, 353
18. Briggs, J. R., *Journal of the Chemical Society Chemical Communications*, 1989, 674; Emrich, R., Heinemann, O., Jolly, P. W., Kruger, C., Verhovnik, G. P. J., *Organometallics*, 1997, 16, 1511; Meijboom, N., Schaverien, C., Orpen, A. G., *Organometallics*, 1990, 9, 774
19. Deckers, P. J. W., Hessen, B., Teuben, J. H., *Organometallics*, 21, 2002, 5122
20. Reagan, W. K., Freeman, J. W., Conroy, B. K., Pettijohn, T. M., Benham, E. A., EP 0608447 to Phillips Petroleum Company, 1994

2. Literature Background

21. Carter, A., Cohen, S. A., Cooley, N. A., Murphy, A., Scutt, J., Wass, D. F., *Chemical Communications*, 2002, 858
22. McGuinness, D. S., Wasserscheid, P., Keim, W., Morgan, D. H., Dixon, J. T., Bollman, A., Maumela, H., Hess, F. M., Englert, U., *Journal of the American Chemical Society*, 125, 2003, 5272
23. Yu, Z. X., Houk, K. N., *Angewandte Chemie, International Edition*, 2003, 42, 808, Blok, A. N. J., Budzelaar, P. H. M., Gal, A. W., *Organometallics*, 2003, 22, 2564
24. Bollmann, A., Blann, K., Dixon, J. T., Hess, F. M., Kilian, E., Maumela, H., McGuinness, D. S., Morgan, D. H., Neveling, A., Otto, S., Overett, M., Slawin, A., Wasserscheid, P., Kuhlmann, S, *Journal of the American Chemical Society*, 2004, 126, 14712
25. Overett, M., Blann, K., Bollmann, A., Dixon, J. T., Haasbroek, D., Killian, E., Maumela, H., McGuinness, D. S., Morgan, D. H., *Journal of the American Chemical Society*, 2005, 127, 10723
26. Bollmann, A., Blann, K., Dixon, J. T., Hess, F. M., Killian, E., Maumela, H., Morgan, D.H., Neveling, A., Otto, S., Overett, M. J., *Chemical Communications*, 2005, 620; Killian, E., Blann, K., Bollmann, A., Dixon, J. T., Kuhlmann, S., Maumela, M. C., Maumela, H., Morgan, D. H., Nongodlwana, P., Overett, M. J., Pretorius, M., Höfener, K., Wasserscheid, P., *Journal of Molecular Catalysis, A: Chemistry*, 2007, 270, 214
27. Blann, K., De Wet-Roos, D., Joubert, D. J., Killian, E., Dixon, J. T., Phelembe, N. J., Du Toit, A., US Patent 7285607 to Sasol Technology, 2007
28. Bowen, L. E., Wass, D. F., *Organometallics*, 2006, 25, 555
29. Pellecchia, C., Mazzeo, M., Gruter, G. J., *Macromolecular Rapid Communications*, 1999, 20, 337; Pellecchia, C., Pappalardo, D., Oliva, L., Mazzeo, M., Gruter, G. J., *Macromolecules*, 2000, 33, 2807
30. Hagen, H., Kretschmer, W. P., Van Buren, F., Hessen, B., Van Oeffelen, D. A., *Journal of Molecular Catalysis, A: Chemistry*, 2006, 248, 237
31. Komon, Z. J. A, Bazan, G. C., *Macromolecular Rapid Communications*, 2002, 22, 467

2. Literature Background

32. Wasilke, J., Obrey, S. J., Baker, T., Bazan, G. C., *Chemical Reviews*, 2005, 105, 1001
33. Mulhaupt, R., *Macromolecular Chemistry and Physics*, 2003, 204, 289
34. Manyik, R. M., Walker, W. E., Wilson, T. P., *Journal of Catalysis*, 1977, 47, 197
35. Reagen, W. K., Freeman, B. K., Conroy, B. K., Pettijohn, T. M, EP 0608447 to Phillips Petroleum Company, 1994
36. Denger, C., Haase, U., Fink, G., *Makromolekular Rapid Communications*, 1991, 12, 697
37. Sperber, O., Kaminsky, W., *Macromolecules*, 2003, 36, 9014
38. Gallard, G. B., Quijada, R., Rojas, R., Bazan, G., Komon, Z. J. A., *Macromolecules*, 2002, 35, 339
39. Barnhart, R. W., Bazan, G. C., *Journal of the American Chemical Society*, 1998, 120, 1082
40. Wang, H., Ma, A., Ke, Y., Hu, Y., *Polymer International*, 2003, 52, 1546
41. Quijada R., Rojas R., Bazan G., Komon Z.J.A., Mauler G.B., Gallard G. B., *Macromolecules*, 2001, 34, 2411
42. Komon, A. J. A., Diamond, G. M., Leclerc, M. K., Murphy, V., Okazaki, M., Bazan, G. C., *Journal of the American Chemical Society*, 2002, 124, 15280
43. Wass, D. F., WO patent 02/04119 to BP Chemicals, 2002
44. Ye, Z., Al'Obaidi, F., Zhu, S., Subramanian, R., *Macromolecular Chemistry and Physics*, 2005, 206, 2096; Ye, Z., Al'Obaidi, F., Zhu, S., Subramanian, R., *Macromolecular Rapid Communications*, 2004, 25, 647
45. De Wet- Roos, D., Dixon, J. T., *Macromolecules*, 2004, 37, 9314
46. Zhang, J., Fan H., Li, B., Zhu, J., *Chemical Engineering Science*, 2008, 63, 2057; Zhang, J., Fan H., Li, B., Zhu, J., *Journal of Polymer Science, Part A: Polymer Chemistry*, 2007, 45, 3562

2. Literature Background

47. Gibson, V. C., Spitzmesser, S. K., *Chemical Reviews*, 2003, 103, 283
48. Phelembe, N., De Wet-Roos, D., Sasol Technology unpublished results, 2006; Blann, K., De Wet-Roos, D., Joubert, D. J., Killian, E., Dixon, J. T., Phelembe, N. J., Du Toit, A., US Patent 7285607 to Sasol Technology, 2007
49. Zhang, W., Sun, W., Zhang, S., Hou, J., Wedeking, K., Schultz, S., Frohlich, R., Song, H., *Organometallics*, 2006, 25, 1961
50. Estruelas, M. A., Lopez, A. M., Mendez, L., Oliván, M., Onate, E., *Organometallics*, 2003, 22, 395; Small, B. L., Carney, M. J., Holman, D. M., O'Rourke, C. E., Halfen, J. A., *Macromolecules*, 2004, 37, 4375
51. Cooley, N. A., Green, S. M., Wass, D. F., *Organometallics*, 2001, 20, 4769; Carter, A., Cooley, N. A., Pringle, P. G., Scutt, J., Wass, D. F., *Polymer Materials Science and Engineering*, 2002, 86, 314

3 Tetramerization tandem catalysis

3.1 Introduction

Previous studies showed that the production of branched polyethylene is highly possible by combination of an oligomerization and a polymerization catalyst in one reactor, but the two catalysts should be compatible under the same reaction conditions.¹ Factors affecting these tandem catalysed systems were mentioned in Chapter 2. Usage of a selective oligomerization catalyst will lead to a well defined copolymer.

The ligand $\text{Ph}_2\text{PN}\{\text{CH}(\text{CH}_3)_2\}\text{PPh}_2$ (Figure 3.1) in combination with a chromium source is an active catalyst for ethylene oligomerization with high selectivity to 1-octene (68 %) at 45 °C and 45 bar ethylene pressure.² It was decided to investigate tandem copolymerization employing this specific ligand together with chromium due to its high reported activity and 1-octene selectivity, in combination with a metallocene in order to produce LLDPE with primarily hexyl branches. During this study the oligomerization catalyst was generated *in situ* by combination of $\text{Cr}(\text{acac})_3$, $\text{Ph}_2\text{PN}\{\text{CH}(\text{CH}_3)_2\}\text{PPh}_2$ and the cocatalyst, methyl aluminoxane (MAO).

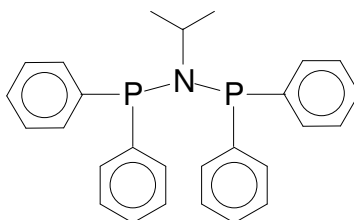


Figure 3.1: Structure of the selective tetramerization ligand $\text{Ph}_2\text{PN}\{\text{CH}(\text{CH}_3)_2\}\text{PPh}_2$

Key elements were identified that could affect both the oligomerization and polymerization reactions. A systematic study was performed to look into these aspects which include:

- temperature,

3. Tetramerization tandem catalysis

- reaction time, and
- catalyst and cocatalyst ratios.

These issues are addressed in the discussion that follows. Additionally, the effects of the individual components of the *in situ* generated tetramerization catalyst, $\text{Cr}(\text{acac})_3$ and the PNP-type ligand, on the polymerization catalyst performance were investigated. A second goal of the study was the comparison of copolymers obtained through the tandem route with conventionally prepared commercial copolymers.

3.2 Experimental

3.2.1 Materials

Metallocene catalysts were obtained from Boulder Scientific, $\text{Cr}(\text{acac})_3$ from Aldrich, MAO from Crompton and $\text{Ph}_2\text{PN}\{\text{CH}(\text{CH}_3)_2\}\text{PPh}_2$ from Cytec. All reagents were used as received. Ethylene (99.5 %) was obtained from Afrox and used without further purification. Methylcyclohexane and a C_7/C_8 paraffin solvent were received from Aldrich and Sasol Wax, respectively. Solvents were purified by passing it through an aluminum oxide column and were stored on molecular sieves (4 Å).

3.2.2 Oligomerization and polymerization procedures

Reactions were conducted under inert conditions in either a 1 L Buchi reactor or a 1 L Parr reactor equipped with mechanical stirring and temperature control. Solvent and MAO were first added to the reactor followed by the catalysts. Catalysts were dissolved in dry toluene under nitrogen atmosphere in a glove box. Reactions were initiated by starting the ethylene flow to the reactor. Reactor pressures of 30 bar were used unless otherwise stated. Reactions were terminated by venting the ethylene followed by the addition of acetone. The polymers were washed with acetone and dried under vacuum at 60 °C for 12 h.

3.2.3 Thermal analysis

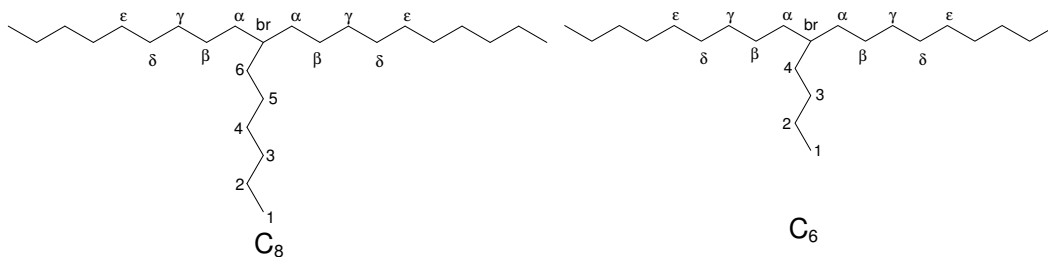
Differential Scanning Calorimetry (DSC) analyses were performed on a Mettler Toledo DSC822, a TA Q200 or a Perkin Elmer Pyris 1 instrument. Instruments were calibrated using indium as standard. Samples were first melted at 180 °C to remove the thermal history followed by crystallization and melting at 10 °C.min⁻¹. The melting temperature obtained from the latter heating run is reported. Temperature

3. Tetramerization tandem catalysis

dependent crystallinity curves were calculated from DSC data according to a method in the literature, using the reference crystalline and amorphous specific enthalpies from the ATHAS data bank.³

3.2.4 Quantitative ¹³C NMR analysis

The polymer (60 mg) was dissolved in 0.6 mL deuterated 1,1,2,2-tetrachloroethane (6 wt%) stabilized with 2,6-di-*tert*-butyl-4-methylphenol (BHT). The sample was placed in a ventilated oven to homogenize at 130 °C for approximately 2 hours. Quantitative ¹³C NMR experiments were performed at 150 MHz using a 5 mm PFG switchable/broadband probe (¹H -¹⁹F, ¹⁵N - ³¹P) on a Varian UNITY/INOVA 600 MHz spectrometer at 120 °C. 90° Pulse widths of approximately 6 μs and delay times between pulses of 15 s were used with an acquisition time of 1.8 s. The number of scans was set to 5040, but the signal-to-noise parameter was set to 2000. Therefore either 5040 scans were acquired or the acquisition was stopped after the required signal-to-noise was reached. Consequently the analysis time ranged from 3 -10 hours. Chemical shifts were referenced internally to the main backbone methylene carbon resonance (30 ppm). Numbering nomenclature (Scheme 3.1) was used as described in the literature⁴. Chemical shifts obtained from the literature⁴ were used for the identification of peaks.



Scheme 3.1: Numbering scheme⁴ for carbons in the copolymer framework

The methine carbon at the branching position (br in Scheme 3.1) at 38.2 ppm was used for quantitative evaluation of the comonomer content. Equation 1 was used to determine the sum of the α -olefins incorporated while the peaks at 23.4 ppm ($2C_6$) and 22.9 ppm ($2C_8$) were used to approximate the 1-octene to 1-hexene ratio since the resonances of brC₈ and brC₆ overlap.

3. Tetramerization tandem catalysis

$$\frac{\sum \int 2[\text{Methene Carbon of Comonomer}]}{\sum \int [\text{Backbone Carbons}]} \times \frac{100}{1} = \text{Total comonomer present (mole\%)} \quad (1)$$

3.2.5 GC analysis

Analysis of the liquid product was performed using a Shimadzu GC-FID equipped with a CP Sil PONA column (100 m x 250 μm x 0.50 μm). The carrier gas was hydrogen at a flow rate of 5 mL.min⁻¹. The oven temperature program comprised a 5 minutes isothermal step at 35 °C followed by a ramp to 260 °C at a rate of 5 °C.min⁻¹. Nonane was used as internal standard.

3.2.6 High Temperature GPC analysis

Molecular weight determinations were carried out on a Waters Alliance GPC system with a refractive index detector. Styragel HTGE and HT2 columns from Waters were used. The instrument was calibrated with narrow polydispersity polystyrene standards (EasyCal) from Polymer Laboratories. 1,2,4-Trichlorobenzene, stabilized with 0.0125 % 2,6-di-*tert*-butyl-4-methylphenol, was used as solvent at 140 °C with a flow rate of 1 mL.min⁻¹. Samples were dissolved at a concentration of 2 mg.mL⁻¹ in the stabilized 1,2,4- trichlorobenzene and homogenized for 2 hours at 140 °C prior to the analysis.

3.2.7 Melt flow index determination

Melt flow indexes were determined on a Ceast Melt Flow Indexer. The melt flow index of polyethylene was measured at 190 °C, using a 2.16 kg force and a die of 8 mm length having a 2.01 mm inside diameter.

3.2.8 CRYSTAF analysis

CRYSTAF analyses were performed on a Polymer Char combination CRYSTAF-TREF apparatus fitted with an IR detector using 1,2,4-trichlorobenzene as solvent. Samples (20 mg maximum) were first dissolved in 30 mL solvent at 160 °C after which the temperature was decreased to 100 °C and stabilized for 30 minutes. The temperature was then decreased from 100 °C to 30 °C at a controlled rate of 0.2 °C.min⁻¹ while the change in the polymer concentration was recorded.

3. Tetramerization tandem catalysis

When analyzing higher comonomer content copolymers the cooling was achieved by connecting liquid nitrogen to the instrument. The temperature was decreased from 100 °C to 0 °C at a controlled rate of 0.2 °C.min⁻¹. 1,2-Dichlorobenzene was used as the solvent.

3.2.9 Tensile measurements

Samples for tensile property measurements were moulded on a Ray-Ran injection moulding machine with a melt temperature of 190 °C and a mould temperature of 50 °C. Tensile properties of the injection-moulded test pieces were determined on a Hounsfield tensile testing apparatus. The modulus was measured at a strain rate of 1 mm.min⁻¹. The extension rate was increased to 5 mm.min⁻¹ when a force of 5 MPa was reached, after which the tensile strength at break was measured.

3.3 Results and discussion

3.3.1 The effect of temperature

The effect of temperature on the type of polymer produced when combining the chromium/PNP-type oligomerization catalyst system with the metallocene catalyst, diphenylmethylenedicyclopentadienyl(9-fluorenyl)zirconiumdichloride ($\text{Ph}_2\text{C}(\text{Cp})(9\text{-Flu})\text{ZrCl}_2$) (Figure 3.2), in one reactor was investigated. Tandem reactions were conducted at constant temperatures for a period of 1 hour. Temperatures of 40, 60, 80 and 100 °C were employed. Control experiments were done under similar conditions with only the oligomerization or polymerization catalyst present in the reactor. Hydrogen was added (see Section 3.3.1.1 for amounts) to reduce the molecular weight in order to increase the solubility of the polymer for solution phase analyses.

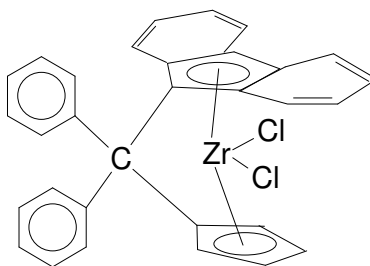


Figure 3.2: Structure of $\text{Ph}_2\text{C}(\text{Cp})(9\text{-Flu})\text{ZrCl}_2$

3. Tetramerization tandem catalysis

3.3.1.1 Reaction conditions

Tandem reactions at all temperatures were conducted with $\text{Ph}_2\text{C}(\text{Cp})(9\text{-Flu})\text{ZrCl}_2$ (3×10^{-7} mol), $\text{Cr}(\text{acac})_3$ (5.5×10^{-6} mol), $\text{Ph}_2\text{PN}\{\text{CH}(\text{CH}_3)_2\}\text{PPh}_2$ (6.3×10^{-6} mol) and MAO (3.2×10^{-3} mol) as cocatalyst in a 1L Parr reactor with 300 mL solvent (C_7/C_8 paraffin). Reaction time was 1 hour at an ethylene pressure 30 bar. The quantity of hydrogen added depended on the reaction temperature: 40 °C (450 mg), 60 °C (400 mg), 80 °C (200 mg) and 100 °C (100 mg). These concentrations of $\text{Cr}(\text{acac})_3$, $\text{Ph}_2\text{PN}\{\text{CH}(\text{CH}_3)_2\}\text{PPh}_2$ and MAO were also used in reactions with only the oligomerization catalyst present. Oligomerization reference reactions were also done under the same reaction conditions, but without the addition of hydrogen.

The polymerization catalyst and cocatalyst concentrations were decreased to 2.3×10^{-7} mol and 2.4×10^{-3} mol, respectively, in reactions without the oligomerization catalyst present. The reactions were done in a 1L Parr reactor with 300 mL solvent (C_7/C_8 paraffin). Reaction time was 1 hour at an ethylene pressure 30 bar. The comonomers were added by means of a HPLC pump in reactions where this was necessary; 40 °C (15 g C6; 35 g C8), 60 °C (11 g C6; 20 g C8), 80 °C (10 g C6; 14 g C8), 100 °C (5 g C6; 5 g C8) over the reaction time. Hydrogen was added according to the reaction temperature: 40 °C (450 mg), 60 °C (400 mg), 80 °C (200 mg) and 100 °C (100 mg).

3.3.1.2 Results

The distribution of the main products formed in the tandem reactions at different temperatures are graphically displayed in Figure 3.3 while more detailed results are shown in Table 3.1. GC-FID showed that 1-hexene and 1-octene formed as the main oligomerization products. Solid polymer is obtained in both the oligomerization and the tandem reaction. The product distribution is highly dependent on the reaction temperature.

The relative amounts of the main oligomer products, i.e. 1-hexene and 1-octene, and the polymer fraction are expressed as a mass fraction in Figure 3.3. The byproducts are not included in this product distribution. GC-FID analyses showed that small quantities (~10 % in total) of 1-butene, methylcyclopentane, methylenecyclopentane, 2-propenylcyclopentane, n-propylcyclopentane, $\text{C}_{10}\text{-C}_{36}$ α -olefins, $\text{C}_4\text{-C}_{20}$ alkanes as

3. Tetramerization tandem catalysis

well as a complex mixture of C₁₀, C₁₂ and C₁₄ secondary oligomerization products are also present.

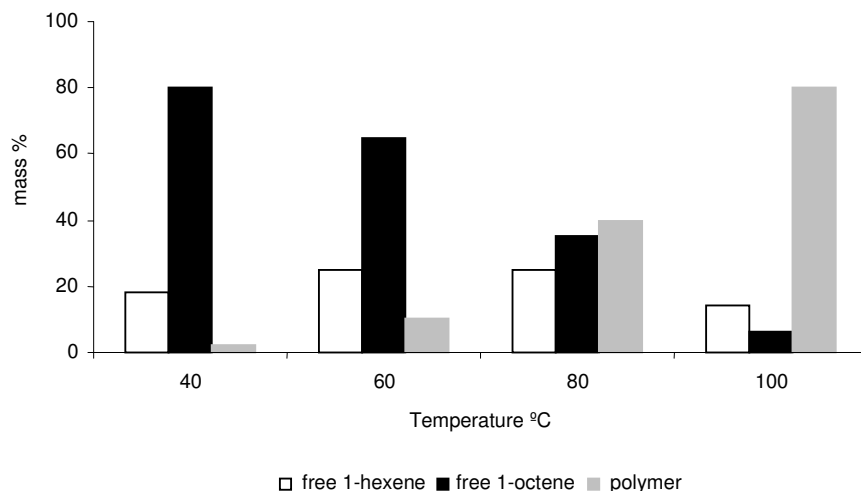


Figure 3.3: Effect of temperature on the main product distribution of tandem reactions

Table 3.1: Effect of temperature on solid formation in the tandem and oligomerization reactions

Temp. °C	Polymer yield Oligo. g	Polymer yield Tandem g	Comonomer content mol%		
			Tandem copolymer		
			1-hexene	1-octene	total
40	1	1	_ ^a	_ ^a	_ ^a
60	1.6	3	0.6	1.5	2.1
80	1.4	12	0.5	1.0	1.5
100	5	40	0.2	0.2	0.4

^anot measured due to low solubility

The amount of solid material produced during the tandem reaction increased with an increase in reaction temperature while the total amount of α -olefins produced decreased (Figure 3.3). GC analysis of the liquid fraction showed an increase in the 1-hexene to 1-octene ratio. The decrease in α -olefin production is reflected in the decreased comonomer content of the resulting polymer as determined by ¹³C NMR analysis (Table 3.1). The ease of incorporation of the α -olefins at the lower reaction temperatures could also contribute to this observation.⁵

3. Tetramerization tandem catalysis

CRYSTAF analyses of the tandem copolymers were done to determine their chemical composition distributions and the results are displayed in Figure 3.4a to Figure 3.4d. The CRYSTAF traces of the polymers obtained by tandem catalysis at temperatures below 100 °C show bimodal chemical composition distributions comprising of fractions of distinctly different crystallinities. This is a direct consequence of the differences in ethylene sequence lengths (ESL). Long ethylene sequences will form more stable crystallites at higher temperatures compared to short sequences where nuclei and possible resulting crystallites become stable only at reduced temperatures.⁶

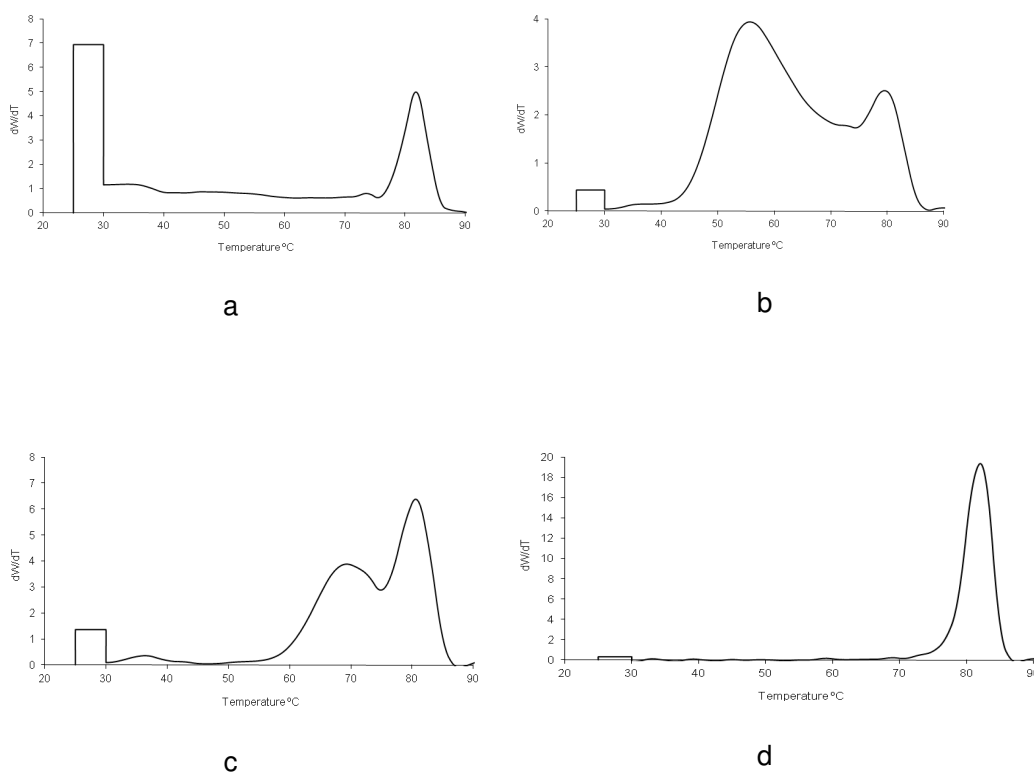


Figure 3.4: CRYSTAF traces of tandem copolymers produced at (a) 40 °C; (b) 60 °C; (c) 80 °C; (d) 100 °C

The more crystalline fraction precipitating at 82 °C is similar for all polymers and is ascribed to the mostly linear polyethylene forming during the initial stages of the reaction when the α -olefin concentration is still low. During the reaction at 100 °C, where conditions are not favourable for oligomerization, the polyethylene that is formed is almost exclusively linear; hence its mostly monomodal profile. At progressively lower temperatures, oligomerization is favoured (Figure 3.3) and the

3. Tetramerization tandem catalysis

overall comonomer content of the resulting polymer increases (decreased ESL). This would result in lower crystallization temperatures and we clearly see a bimodal distribution developing at the lower reaction temperatures. A copolymer prepared at a reaction temperature of 80 °C has a fraction of lower crystallinity at 70 °C in the CRYSTAF trace, while a crystallization peak at 55 °C is observed for the polymer prepared at 60 °C. A large fraction of the copolymer is still in solution at the end of the CRYSTAF analysis of the copolymer prepared at a reaction temperature of 40 °C, while the soluble fractions are smaller for the polymers prepared at 60 °C and 80 °C, and essentially non-existent for the polymer produced at 100 °C. The fact that the crystallization peak at 82 °C persists in the CRYSTAF traces for all the polymers is a clear indication that we have two competing reactions. In the first place the production of essentially linear polyethylene predominates during the initial stages of polymerization, while the formation of copolymers occur when the production of oligomers commence. Eventually a gradient mixture of polymers results, varying from crystalline polyethylene to less crystalline and non-crystalline copolymers.

Polymers were also synthesized through conventional copolymerization by feeding the same concentrations of 1-octene and 1-hexene as that formed during the tandem reactions (see experimental section). In this way the conditions during tandem polymerization could be simulated in the absence of the tetramerization catalyst precursors. CRYSTAF traces of the conventional copolymerization products are displayed in Figure 3.5a to Figure 3.5d.

3. Tetramerization tandem catalysis

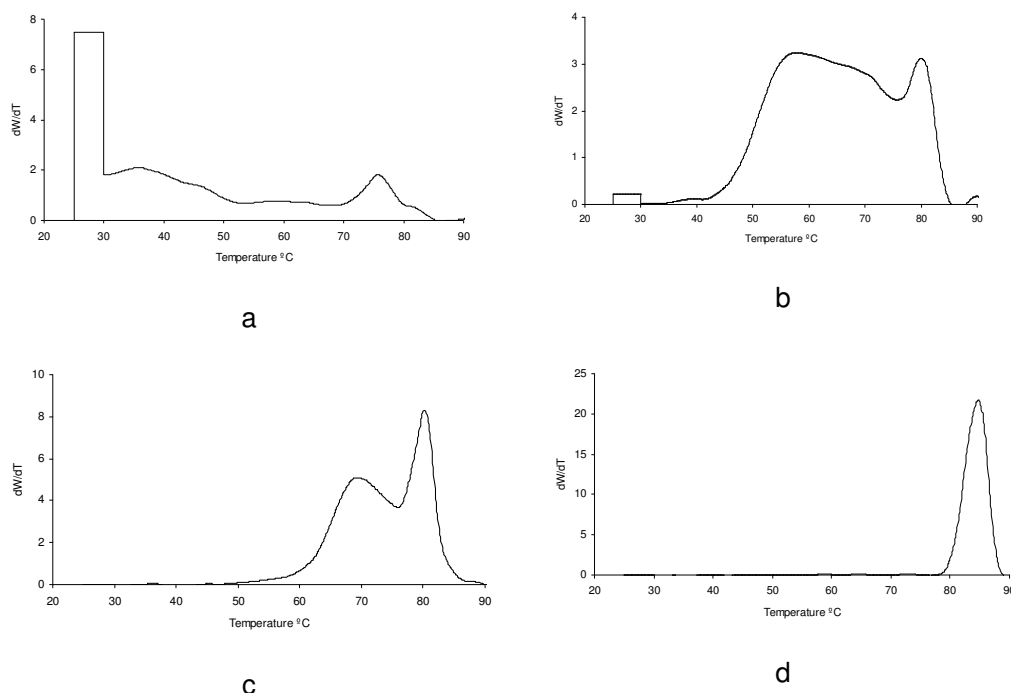


Figure 3.5: CRYSTAF traces of conventional copolymers produced at (a) 40 °C; (b) 60 °C; (c) 80 °C; (d) 100 °C

CRYSTAF traces of these products show similar chemical composition distribution profiles compared to those of the tandem reactions, but with minor differences in the lower temperature region and also with regard to the relative more high density material which is present for the 40 °C tandem reaction. The high density component in the conventional reaction can also be ascribed to the initial low concentration of comonomer present during the tandem reaction. The prominent high density component present in the copolymer synthesized in the 40 °C tandem reaction can be explained by the results obtained in the oligomerization reference reactions, and bears out the assumption that a mixture of polymers are made during the tandem reaction.

Figure 3.6 shows the bimodal chemical composition distribution in the CRYSTAF traces of the polymers obtained from the oligomerizations reactions alone, conducted at different temperatures.

3. Tetramerization tandem catalysis

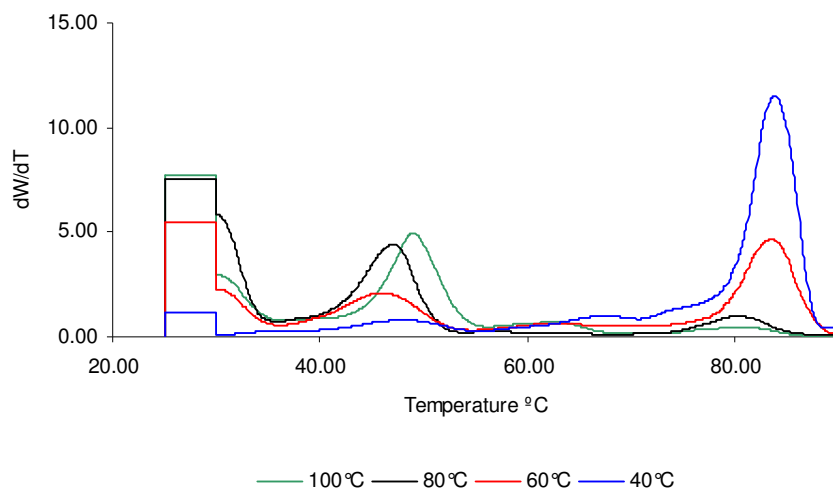


Figure 3.6: CRYSTAF traces of polymers obtained from oligomerization reactions at different temperatures

The prominent component present at 82 °C in the CRYSTAF trace of the tandem copolymer is clearly also formed during oligomerization. The amount of this material is a maximum at a reaction temperature of 40 °C and decreases with increasing reaction temperature. The low crystallinity component in this case appears at a significant lower temperature. An increase in the less crystallisable material which includes the soluble fraction is also observed.

Comparisons of the molecular weight distributions of the tandem and conventional copolymers were done by GPC analyses and are displayed in Table 3.2. (Different amounts of hydrogen were added to the reactions to compensate for the effect of temperature on molecular weight.)

3. Tetramerization tandem catalysis

Table 3.2 : GPC results from tandem copolymerization, oligomerization and conventional copolymerization

	Tandem Catalysis		Copoly- merization	Oligomerization	
	Peak 1	Peak 2	Peak 1	Peak 1	Peak 2
Reaction temperature 40 °C					
M _p	140	110	143	117	380, 138
<M _n >	32	124	25	94	275
<M _w >	142	133	136	220	602
PI	4.4	1.1	5.4	2.3	2.19
Reaction temperature 60 °C					
M _p	133	trace present *	129	112	169
<M _n >	74		70	46	184
<M _w >	138		133	267	286
PI	1.9		1.9	5.8	1.6
Reaction temperature 80 °C					
M _p	160	133	160	104	131
<M _n >	107	141	91	45	158
<M _w >	175	175	181	145	201
PI	1.6	1.2	2	3.3	1.3
Reaction temperature 100 °C					
M _p	147	104	166	-	192
<M _n >	89	119	99	-	172
<M _w >	162	136	181	-	572
PI	1.82	1.2	1.83	-	3.3

* traces present, but not integrated

GPC data (Table 3.2) of the polymers obtained by tandem catalysis show a bimodal distribution with high (~140 000 g.mol⁻¹) as well as low (~1000 g.mol⁻¹) molecular weight peaks, the latter presumably results from the polymer formed by the oligomerization catalyst. Copolymers obtained through conventional copolymerization show only the high molecular weight peaks in the same region as the tandem catalysis experiments.

From the preceding results it is clear that the optimum temperature for oligomerization (1-octene synthesis) is much lower than that of polymerization. At

3. Tetramerization tandem catalysis

the lower temperatures, 1-octene yield is high, but the polymer yield is low. To produce LLDPE in high yields with high 1-octene content it is therefore necessary to first produce the α -olefins at the optimum oligomerization temperature and then increase the temperature to above 100 °C to initiate the production of the copolymer. Consequently, the effect of producing LLDPE using a temperature gradient was investigated.

3.3.2 The effect of a temperature gradient

3.3.2.1 Reaction conditions

The reactions were executed in a 5 L Buchi reactor with $\text{Ph}_2\text{C}(\text{Cp})(9\text{-Flu})\text{ZrCl}_2$ (4.5×10^{-6} mol), $\text{Cr}(\text{acac})_3$ (1.2×10^{-4} mol), $\text{Ph}_2\text{PN}\{\text{CH}(\text{CH}_3)_2\}\text{PPh}_2$ (1.4×10^{-4} mol) and MAO (21.4×10^{-3}) mol in 1.5 L solvent (C_7/C_8 paraffin cut) and at an ethylene pressure of 28 bar. Samples were removed at a sampling port at the bottom of the reactor. Reactions were carried out by starting at 50 °C for 30 minutes before increasing the temperature slowly in 10 minute intervals to 100 °C. Samples were obtained at 50, 70 and 100 °C, respectively.

3.3.2.2 Results

CRYSTAF analyses (Figure 3.7) illustrate the change in chemical composition distribution during the course of a reaction performed with a temperature gradient from 50 °C to 100 °C. It is clear that a wide range of products are produced.

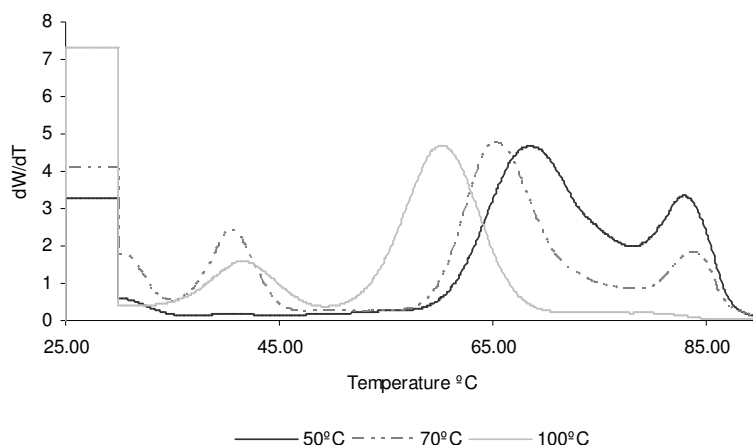


Figure 3.7: CRYSTAF traces of fractions obtained from a tandem copolymerization reaction when sampling at different temperature intervals

A more crystalline component (peak at 80 °C) and a less crystalline component (peak at 70°C) are present in the sample obtained at 50 °C. The peak at 80 °C in the

3. Tetramerization tandem catalysis

CRYSTAF traces can be ascribed to the product formed by the oligomerization catalyst (see Figure 3.6) as well as the initial low concentration of α -olefins during the tandem reaction. With an increase in time and temperature the concentration of α -olefins increases and the lower crystallization peak in the CRYSTAF trace shifts from 70 °C to 60 °C. More α -olefins are now available for copolymerization, and similarly the intensity of the crystallization peak around 80 °C decreases as more polymer with a higher comonomer content is formed at higher temperatures. An additional crystallization peak, at 40 °C, becomes apparent in the CRYSTAF traces as the reaction temperature increases. The presence of this peak could be ascribed to the action of the oligomerization catalyst as seen from the study at constant temperatures (Figure 3.6). The soluble fraction also increases with time and temperature, consistent with Figure 3.6.

3.3.3 The effect of catalyst and cocatalyst ratios

Methylaluminoxane (MAO) is used as cocatalyst to activate both the polymerization and oligomerization catalysts. Varying the ratio of MAO to oligomerization catalyst and that of the oligomerization catalyst to polymerization catalyst affects the amount of α -olefin produced during the low temperature oligomerization reactions. The effect of changes in the catalyst and cocatalyst ratio on the resulting copolymer was investigated in a set of experiments.

The metallocenes *rac*-ethylenebis(indenyl)zirconiumdichloride ($\text{EtIn}_2\text{ZrCl}_2$) (Figure 3.8) and $\text{Ph}_2\text{C}(\text{Cp})(9\text{-Flu})\text{ZrCl}_2$ (Figure 3.2) were employed in this study.

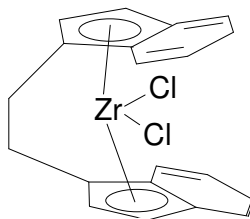


Figure 3.8: Structure of $\text{EtIn}_2\text{ZrCl}_2$

3.3.3.1 Reaction Conditions

The first set of experiments was done using $\text{EtIn}_2\text{ZrCl}_2$ (2.5×10^{-6} mol). The ratios of metallocene to oligomerization catalyst and MAO used are given in Table 3.3. The

3. Tetramerization tandem catalysis

solvent was methylcyclohexane (300 mL) and the ethylene pressure was 36 bar. All reactions were done in a 1 L Parr reactor. The temperature was kept below 50 °C for 30 minutes after which it was increased to above 100 °C. The total reaction time was 1 hour.

The second set of experiments used $\text{Ph}_2\text{C}(\text{Cp})(9\text{-Flu})\text{ZrCl}_2$ (2.5×10^{-7} mol) as polymerization catalyst in a 1L Parr reactor. The ratio of metallocene to oligomerization catalyst and MAO used are given in Table 3.4. The solvent was methylcyclohexane (300 mL) and the ethylene pressure was 40 bar. The temperature was kept below 50 °C for 30 minutes, after which it was increased to above 100 °C. The total reaction time was 1 hour.

3.3.3.2 Results

A change in α -olefin production affects the crystallinity of a copolymer due to different amounts of the α -olefin incorporated. The comonomer disrupts the crystallization of the copolymer and the more comonomer incorporated, the lower the degree of crystallinity and the lower the melting temperatures should become.⁷ The enthalpy of melting (Δh_m) should be lower when the crystallinity decreases. The melting peak maximum temperatures (DSC) and enthalpy of melting were consequently used to evaluate the effect of catalyst and cocatalyst ratios on the copolymer (Table 3.3).

Table 3.3: Effect of catalyst and cocatalyst ratios on tandem reactions with the metallocene $\text{EtIn}_2\text{ZrCl}_2$

$\text{Cr}(\text{acac})_3$: $\text{EtIn}_2\text{ZrCl}_2$	MAO: $\text{EtIn}_2\text{ZrCl}_2$	MAO: $\text{Cr}(\text{acac})_3$	Polymerization Activity $\text{kg} \cdot (\text{g}_{\text{Zr}}\text{h})^{-1}$	DSC mp °C	Δh_m $\text{J} \cdot \text{g}^{-1}$
36:1	2 160:1	60:1	53	130	200
36:1	4 320:1	120:1	426	114	135
36:1	8 640:1	240:1	615	113	105
12:1	2 880:1	240:1	580	116	110
4:1	960:1	240:1	396	117	150

In the first three reactions in Table 3.3 the MAO concentration was increased relative to the chromium concentration. The reaction with a 60:1 MAO: $\text{Cr}(\text{acac})_3$ ratio yielded a polymer with a relative high crystallinity as evident from the melting peak maximum at 130 °C and Δh_m of $200 \text{ J} \cdot \text{g}^{-1}$ compared to the polymers produced at higher ratios that afforded lower values. An increase to 120:1, for example, yielded a copolymer

3. Tetramerization tandem catalysis

with a melting peak maximum at 114 °C and a Δh_m of 135 J.g⁻¹. An additional increase in the MAO:Cr(acac)₃ ratio had only a minor effect on the polymer melting temperatures, but the Δh_m decreases further to 105 J.g⁻¹. The polymerization catalyst activity consistently increases with an increase in cocatalyst concentration.

By decreasing the amount of tetramerization catalyst relative to the polymerization catalyst less comonomer is formed and an increase in polymer melting temperature was observed. The CRYSTAF traces in Figure 3.9 and Figure 3.10 show the change in chemical composition distribution of the different copolymers produced when using EtIn₂ZrCl₂. With an increase in cocatalyst concentration and oligomerization catalyst concentration more comonomer is formed and consequently incorporated in the backbone as is evident from the considerable decrease in the crystalline fraction.

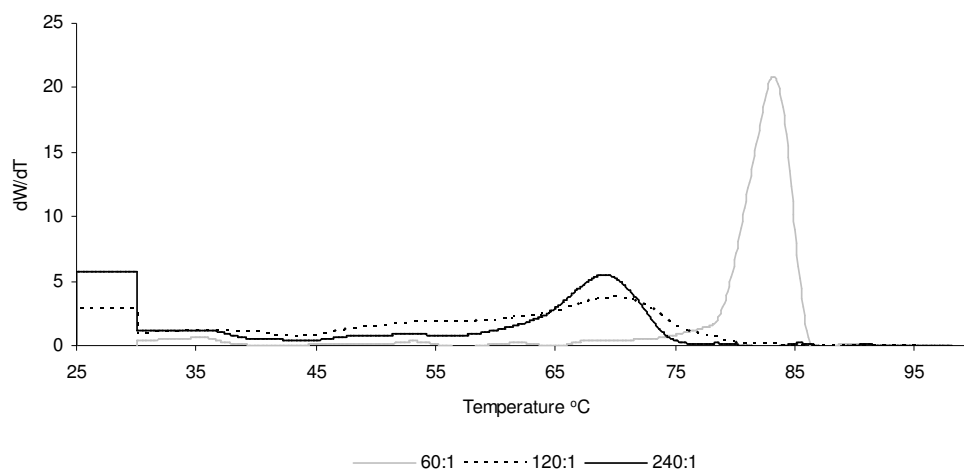


Figure 3.9: CRYSTAF traces of tandem copolymers prepared at varying co-catalyst to oligomerization catalyst ratios [Cr(acac)₃:EtIn₂ZrCl₂ fixed at 36:1]

3. Tetramerization tandem catalysis

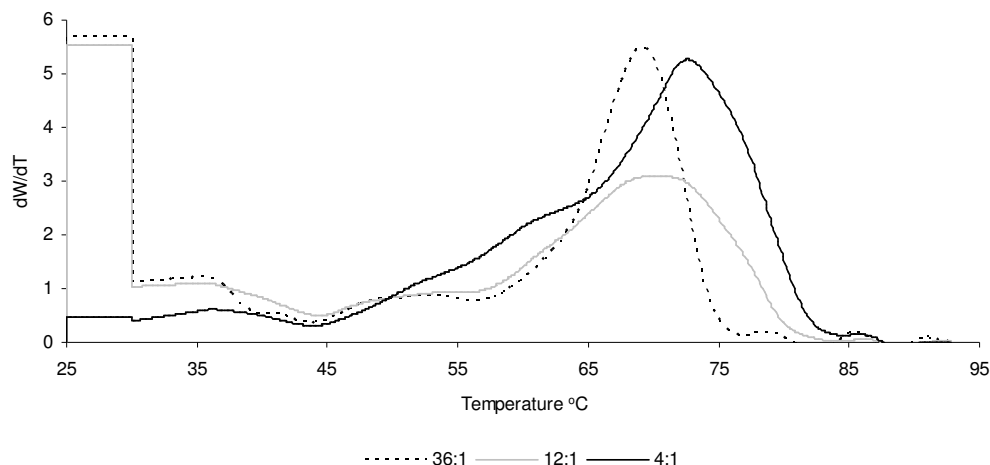


Figure 3.10: CRYSTAF traces of tandem copolymers prepared using $\text{EtIn}_2\text{ZrCl}_2$ at varying tetramerization catalyst to polymerization catalyst ratios [$\text{MAO}:\text{Cr}(\text{acac})_3$ fixed at 240:1]

Additional experiments were conducted with the metallocene $\text{Ph}_2\text{C}(\text{Cp})(9\text{-Flu})\text{ZrCl}_2$ to investigate the effect of the $\text{Cr}(\text{acac})_3:\text{Ph}_2\text{C}(\text{Cp})(9\text{-Flu})\text{ZrCl}_2:\text{MAO}$ ratios on the polymerization activity and copolymer properties, the results of which are summarized in Table 3.4.

Table 3.4: Effect of catalyst and cocatalyst ratios on tandem reactions with the metallocene $\text{Ph}_2\text{C}(\text{Cp})(9\text{-Flu})\text{ZrCl}_2$

$\text{Cr}(\text{acac})_3:[\text{Zr}]^*$	$\text{MAO}:[\text{Zr}]^*$	$\text{MAO}:\text{Cr}(\text{acac})_3$	Polymerization Activity $\text{kg} \cdot (\text{g}_z \cdot \text{h})^{-1}$	DSC mp $^\circ\text{C}$	Δh_m $\text{J} \cdot \text{g}^{-1}$
36:1	12 840	357	1405	82	60
12:1	12 840	1070	1538	124	120
12:1	4 280	357	747	116	105
4:1	4 280	1070	967	134	200

* $[\text{Zr}] = \text{Ph}_2\text{C}(\text{Cp})(9\text{-Flu})\text{ZrCl}_2$

Table 3.4 illustrates the changes in polymerization activity, melting peak maximum temperatures and melting enthalpy with respect to changes in the tetramerization catalyst and cocatalyst ratios. With a decrease in the $\text{Cr}(\text{acac})_3:\text{Ph}_2\text{C}(\text{Cp})(9\text{-Flu})\text{ZrCl}_2$ ratio at a constant MAO concentration less comonomer is produced, resulting in more linear copolymers with longer crystallizable ethylene sequences, thicker lamellae and thus higher melting temperatures. A decrease in the MAO

3. Tetramerization tandem catalysis

concentration at the same $\text{Cr}(\text{acac})_3:\text{Ph}_2\text{C}(\text{Cp})(9\text{-Flu})\text{ZrCl}_2$ ratio causes a decrease in the polymerization activity. Table 3.4 also shows that a decrease in polymerization activity results when the $\text{Cr}(\text{acac})_3:\text{Ph}_2\text{C}(\text{Cp})(9\text{-Flu})\text{ZrCl}_2$ ratio increases.

3.3.4 Chemical compatibility

3.3.4.1 The effect of the oligomerization catalyst on the activity of the polymerization catalyst

Chemical compatibility is a prerequisite for successful tandem catalysis.¹ Results in Table 3.4 indicate that the polymerization activity is affected by the presence of the oligomerization catalyst. It is known that the comonomer concentration influences polymerization activity; this phenomenon is described in the literature as the comonomer effect.⁸ The observed loss in activity during tandem catalysis could thus also be due to the higher comonomer concentration when the $\text{Cr}(\text{acac})_3:\text{Ph}_2\text{C}(\text{Cp})(9\text{-Flu})\text{ZrCl}_2$ ratio increases. Therefore, the effect of the oligomerization catalyst on the polymerization catalyst activity was investigated further by varying the $\text{Cr}(\text{acac})_3:\text{Ph}_2\text{C}(\text{Cp})(9\text{-Flu})\text{ZrCl}_2$ ratio while keeping the amount of 1-octene constant. In order to compensate for the reduced amount of 1-octene synthesized due to the decreased tetramerization catalyst concentration, a pre-determined amount of 1-octene was added to make up for this loss. When a continuous reactor is employed the excess comonomer can be recycled to minimize the amount of oligomerization catalyst added to the reactor. The effect of the $\text{Cr}(\text{acac})_3:\text{Ph}_2\text{C}(\text{Cp})(9\text{-Flu})\text{ZrCl}_2$ ratio on the chemical composition distributions of the formed copolymers was determined. A temperature gradient was used while investigating the effect of the $\text{Cr}(\text{acac})_3:\text{Ph}_2\text{C}(\text{Cp})(9\text{-Flu})\text{ZrCl}_2$ ratio on the chemical composition distribution at a constant comonomer concentration.

3.3.4.1.1 Reaction conditions

The amount of $\text{Cr}(\text{acac})_3$ was decreased in steps from 0.006 mmol to zero while the $\text{Ph}_2\text{C}(\text{Cp})(9\text{-Flu})\text{ZrCl}_2$ to MAO ratio was kept constant. A constant amount of the polymerization catalyst $\text{Ph}_2\text{C}(\text{Cp})(9\text{-Flu})\text{ZrCl}_2$ (0.003 mmol) was used in all reactions, except for the reaction without chromium, where the amount was lowered to ensure better temperature control. Varying amounts of 1-octene were added in order to obtain copolymers with similar incorporation of α -olefins. The ligand: $\text{Cr}(\text{acac})_3$ ratio was 1.3:1 in all experiments and a constant amount of hydrogen (40 mg) was added. Reactions were started at 40 °C (15 min) after which the temperature was increased to 150 °C.

3. Tetramerization tandem catalysis

3.3.4.1.2 Results

The changing $\text{Cr}(\text{acac})_3:\text{Ph}_2\text{C}(\text{Cp})(9\text{-Flu})\text{ZrCl}_2$ ratio affects the polymerization activity significantly. The influence of the tetramerization catalyst on the polymerization catalyst activity is illustrated in Figure 3.11 while more results - melt flow index (MFI) and DSC meltingpeak maximum temperatures (DSC mp) - are displayed in Table 3.5. Figure 3.12 shows the CRYSTAF traces of the resulting copolymers.

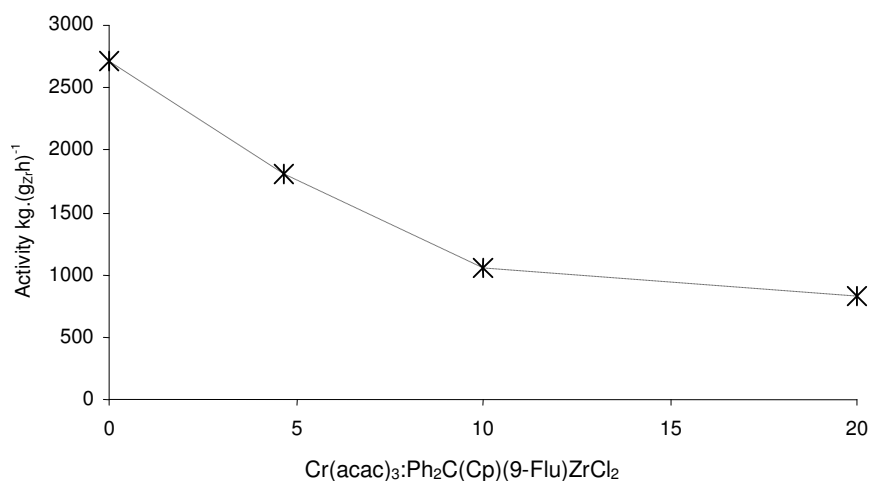


Figure 3.11: Effect of $\text{Cr}(\text{acac})_3:\text{Ph}_2\text{C}(\text{Cp})(9\text{-Flu})\text{ZrCl}_2$ on polymerization activity at constant comonomer concentration

Table 3.5: Effect of $\text{Cr}(\text{acac})_3:\text{Ph}_2\text{C}(\text{Cp})(9\text{-Flu})\text{ZrCl}_2$ on copolymer properties at constant comonomer concentration

$\text{Cr}(\text{acac})_3$ mmol	$\text{Cr}(\text{acac})_3:\text{[Zr]}^*$	1-octene mL	MFI $\text{g}(10\text{min})^{-1}$	DSC mp $^{\circ}\text{C}$
0.006	20:1	0	2	111
0.003	10:1	15	2	111
0.0014	5:1	40	1	109
0	0:1	40	1	114

*[Zr]= $\text{Cr}(\text{acac})_3:\text{Ph}_2\text{C}(\text{Cp})(9\text{-Flu})\text{ZrCl}_2$

3. Tetramerization tandem catalysis

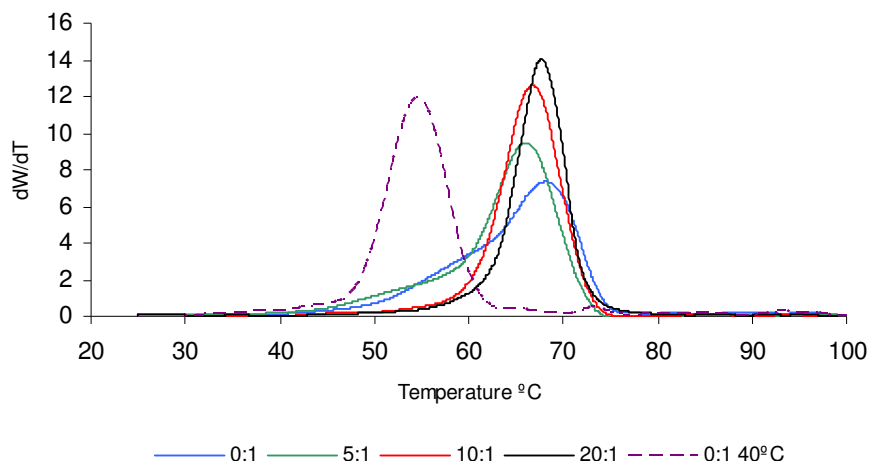


Figure 3.12: CRYSTAF traces showing the effect of $\text{Cr}(\text{acac})_3:\text{Ph}_2\text{C}(\text{Cp})(9\text{-Flu})\text{ZrCl}_2$ on chemical composition distribution at constant comonomer concentration

Figure 3.11 confirms that the polymerization activity drops with an increasing ratio of the oligomerization catalyst to polymerization catalyst. Broader comonomer content distributions are noticeable in Figure 3.12 with a decreasing $\text{Cr}(\text{acac})_3:\text{Ph}_2\text{C}(\text{Cp})(9\text{-Flu})\text{ZrCl}_2$ ratio, probably because of the added comonomer which was present from the start of the reaction at the lower temperature. A conversion at a constant temperature of 40 °C (stopped after 15 minutes) resulting in the CRYSTAF trace (0:1 40 °C) in Figure 3.12, confirming that the broader comonomer distribution are because of the increased comonomer incorporation at the 40 °C. The small variations in melting peak maximum positions (DSC mp) can be ascribed to small variations in the total comonomer concentration in the different reactions. Table 3.5 shows the melt flow index (MFI) increased from 1 to 2 $\text{g}(10\text{min})^{-1}$ at low $\text{Cr}(\text{acac})_3:\text{Ph}_2\text{C}(\text{Cp})(9\text{-Flu})\text{ZrCl}_2$ ratios to higher $\text{Cr}(\text{acac})_3:\text{Ph}_2\text{C}(\text{Cp})(9\text{-Flu})\text{ZrCl}_2$ ratios, indicating a change in molecular weight distributions (GPC results not available).

3.3.4.2 The effect of the individual oligomerization catalyst components on the polymerization catalyst activity

The decrease in polymerization catalyst activity was further investigated by varying the concentrations of the individual tetramerization catalyst components relative to the polymerization catalyst, $\text{EtIn}_2\text{ZrCl}_2$, at a constant temperature. A constant amount of 1-octene was added to match the comonomer concentration in the tandem reactions in the absence of the functional tetramerization catalyst.

3. Tetramerization tandem catalysis

3.3.4.2.1 Reaction conditions

Reactions were performed in a 1 L Buchi reactor using $\text{EtIn}_2\text{ZrCl}_2$ (2.3×10^{-8} mol) and MAO (1.1×10^{-3} mol) in a C₇/C₈ paraffin cut as solvent (300 mL). Ethylene pressure was 30 bar. 1-Octene (30 mL) was added to all reactions. The individual catalyst components, $\text{Cr}(\text{acac})_3$ and $\text{Ph}_2\text{PN}\{\text{CH}(\text{CH}_3)_2\}\text{PPh}_2$, were added to the reactions according to the $\text{Cr}(\text{acac})_3:\text{EtIn}_2\text{ZrCl}_2$ and ligand: $\text{EtIn}_2\text{ZrCl}_2$ ratios displayed in Table 3.6 and Table 3.7. The reactor temperature was kept at 100 °C.

3.3.4.2.2 Results

In Figure 3.13 and Figure 3.14 the marked effects of varying the $\text{Ph}_2\text{PN}\{\text{CH}(\text{CH}_3)_2\}\text{PPh}_2$ and chromium relative to the polymerization catalyst at 100 °C are depicted in terms of the melting peak maximum temperature and molecular weight. In addition to the loss in activity, an increase in the weight average molecular weight, accompanied by a slight increase in the peak melting temperatures was observed. These results are summarized in Table 3.6 and Table 3.7.

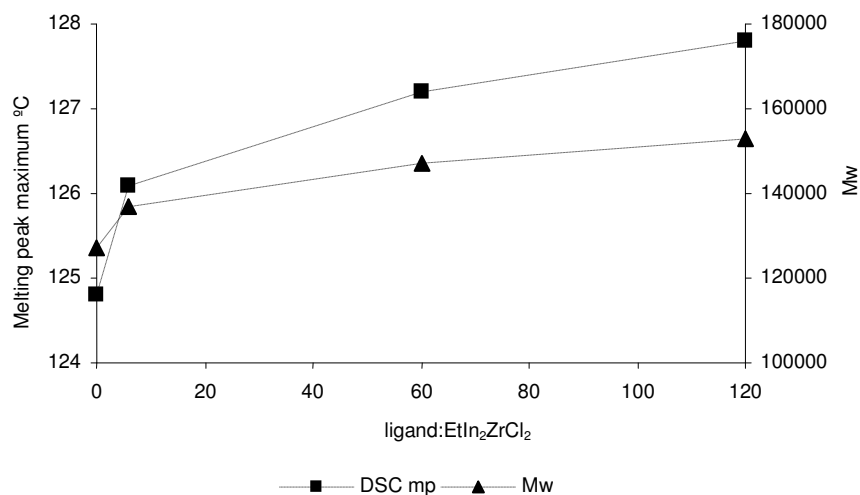


Figure 3.13: Effect of varying the PNP-type ligand to polymerization catalyst ratio at 100 °C on copolymer properties

3. Tetramerization tandem catalysis

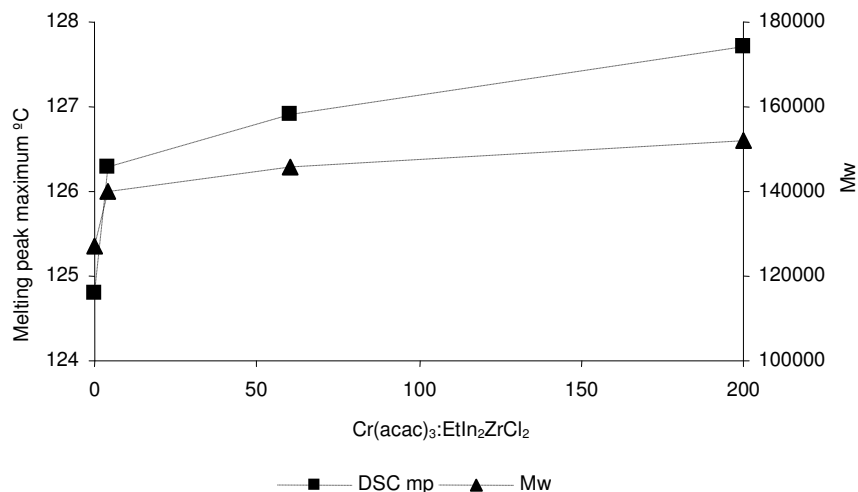


Figure 3.14: Effect of varying the Cr(acac)₃ to polymerization catalyst ratio at 100 °C on copolymer properties

Table 3.6: Effect of varying the PNP-type ligand to polymerization catalyst ratio at 100 °C on copolymer properties

ligand: [Zr]*	Activity kg.(g _{Zr} h) ⁻¹	DSC mp °C	<M _n >	<M _w >	PI
0:1	17 787	124.8	61	127	2.1
6:1	19 565	126.1	65	137	2.1
60:1	11 117	127.2	72	147	2.0
120:1	7 115	127.8	68	153	2.3

*[Zr]=EtIn₂ZrCl₂

Table 3.7: Effect of varying the Cr(acac)₃ to polymerization catalyst ratio at 100 °C on copolymer properties

Cr(acac) ₃ : [Zr]*	Activity kg.(g _{Zr} h) ⁻¹	DSC mp °C	<M _n >	<M _w >	PI
0:1	17 787	124.8	61	127	2.1
4:1	97 826	126.3	60	140	2.3
60:1	6 670	126.9	57	146	2.5
200:1	4 447	127.7	62	152	2.4

*[Zr]=EtIn₂ZrCl₂

3. Tetramerization tandem catalysis

On the basis of these observations, the premise that the tetramerization catalyst operates entirely separate from the polymerization catalyst does not seem correct. The proposition that the ligand or metal act as chain transfer agents also does not seem likely, since the molecular weight increases in the presence of the tetramerization catalyst components. Rather, it would seem that in both cases, some kind of competitive mechanism prevails between the components of the oligomerization catalyst and the monomers for the active polymerization site. From the decreased activity (Table 3.6 and Table 3.7) and increased molecular weights and peak melting temperatures observed, one can visualize the active polymerization sites shielded by the PNP-type ligands in competition with the bulky comonomers. The usual coordination, propagation and transfer reactions of the copolymerization process can become severely restricted.

3.3.5 Comparative study of tandem copolymers with commercial 1-octene copolymers

Copolymers were prepared by means of tandem catalysis for comparison with commercial copolymers. The available commercial copolymers have 1-octene contents of 4 and 6 mol%. The data sheets of the commercial ethylene-1-octene copolymers stated that the copolymers were prepared by a metallocene catalyst in solution phase.⁹ A series of tandem copolymers with total comonomer contents between 3 and 8 mol% were prepared for this comparison. The commercial copolymers have melt flow indexes of 1 and 3 g(10min)⁻¹, respectively. The molecular weights of the tandem copolymers were targeted to have their melt flow indexes in this range by the addition of hydrogen.

The metallocene catalyst Ph₂C(Cp)(9-Flu)ZrCl₂ (Figure 3.2) was used in the tandem reactions together with the chromium/PNP-type system. Ph₂C(Cp)(9-Flu)ZrCl₂ was chosen due to its ability to incorporate high quantities of 1-octene while still producing very high molecular weight polyethylene.¹⁰ A reaction temperature of 40 °C was used until the desired amount of comonomers were produced, after which the temperature was increased to above 100 °C for polymerization. The Cr(acac)₃:Ph₂C(Cp)(9-Flu)ZrCl₂ ratio used was determined by the required comonomer content. The lower comonomer content copolymers were thus prepared by changing the oligomerization catalyst amount and reaction time.

3. Tetramerization tandem catalysis

3.3.5.1 Microstructure comparison

3.3.5.1.1 Reaction conditions

Reactions were executed in a 1L Parr reactor in 300 mL solvent (C₇/C₈ paraffin cut) and at an ethylene pressure of 30 bar. Ph₂C(Cp)(9-Flu)ZrCl₂ (3×10⁻⁷ mol), Cr(acac)₃ (5.5×10⁻⁶ mol), Ph₂PN{CH(CH₃)₂}PPh₂ (6.3×10⁻⁶ mol) and MAO (1.6×10⁻³ mol) were used to prepare the copolymers with comonomer content up to 4 mol%. Temperature was kept below 40 °C until the desired amount of α-olefins were produced (estimate from ethylene uptake) after which the temperature was increased to 120 °C. Hydrogen (50 mg) was added at the start of the reaction. The copolymers with the higher comonomer contents were prepared in a similar way but the oligomerization catalyst amount was increased. Cr(acac)₃ (1.1×10⁻⁵ mol), Ph₂PN{CH(CH₃)₂}PPh₂ (1.3×10⁻⁵ mol) and MAO (3.2×10⁻³ mol) were used. A conventional copolymer was produced at 120°C and 30 bar using Ph₂C(Cp)(9-Flu)ZrCl₂ (1×10⁻⁷ mol) and MAO (0.53×10⁻³ mol) and adding 1-octene to the reaction. Hydrogen (50 mg) was added to the reaction.

3.3.5.1.2 Results

A series of copolymers with comonomer contents in the range of the commercial copolymers were obtained. The comonomer contents of the tandem copolymers were calculated from their ¹³C NMR spectra. Figure 3.15 and Figure 3.16 show the spectra of copolymers with 4 mol% and 7 mol% comonomer content, respectively.

3. Tetramerization tandem catalysis

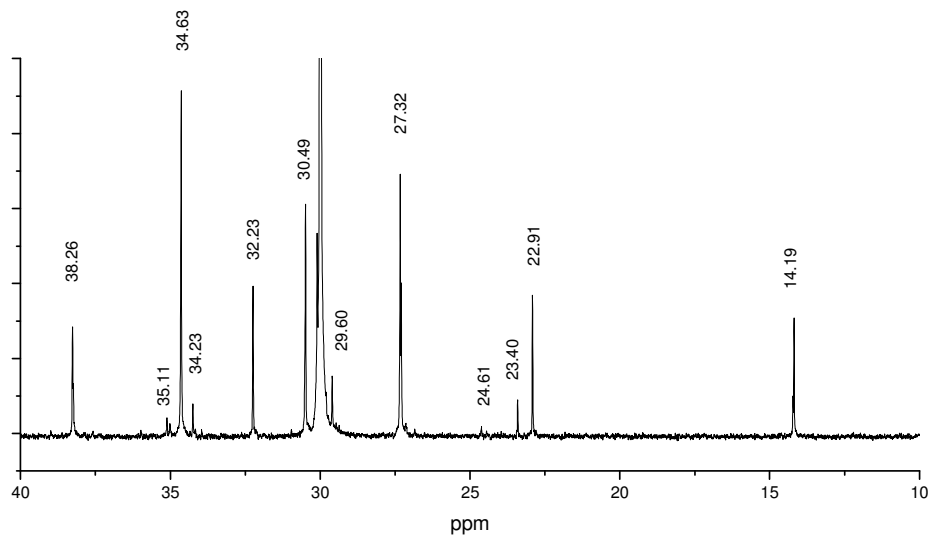


Figure 3.15: ^{13}C NMR spectrum of a copolymer with 4 mol% comonomers (1-hexene and 1-octene)

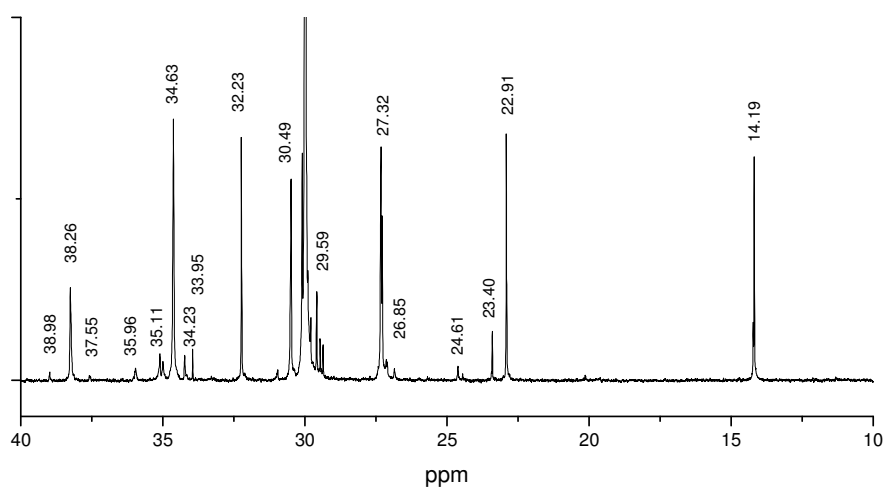


Figure 3.16: ^{13}C NMR spectrum of a copolymer with 6 mol% comonomers (1-hexene and 1-octene)

The ^{13}C NMR spectra of the copolymers produced using the metallocene catalyst $\text{Ph}_2\text{C}(\text{Cp})(9\text{-Flu})\text{ZrCl}_2$ show an increase in the number of peaks as the comonomer content increases from 4 to 6 mol%. These additional peaks can have various possible origins. The specific metallocene catalyst used in this study has a high comonomer response due to its open structure, resulting in it being more prone to clustering of the comonomer at high comonomer concentrations. The increasing

3. Tetramerization tandem catalysis

number of peaks from the 4 to 6 mol% tandem copolymers can thus be attributed to an increasing number of monomer sequences where the branches are not isolated.¹¹ This is also evident in the copolymer produced by conventional copolymerization (Figure 3.17) when adding a fixed amount of 1-octene.

The ^{13}C NMR of the commercial copolymer (Figure 3.18) shows fewer peaks, possibly as a result of less clustering of the branches. This is most likely due to a different metallocene catalyst employed in the synthesis of the copolymers and not as a result of the tandem process. A second reason for the increased number of peaks is the presence of the oligomerization catalyst which form low molecular weight polymer. Prominent end group peaks, e.g. at 29.6 ppm, belonging to the low molecular weight polymer are observed. End groups peaks occur at 32.2, 29.9; 29.6, 22.9 and 14.0 ppm, but most overlap with the resonances of hexyl branches. Allylic carbons are also present at 33.95 ppm (Figure 3.16) and are ascribed to the presence of double bonds in the low molecular weight material. It is also possible that some of the α -olefin byproducts which form in the oligomerization reaction incorporate into the copolymer.

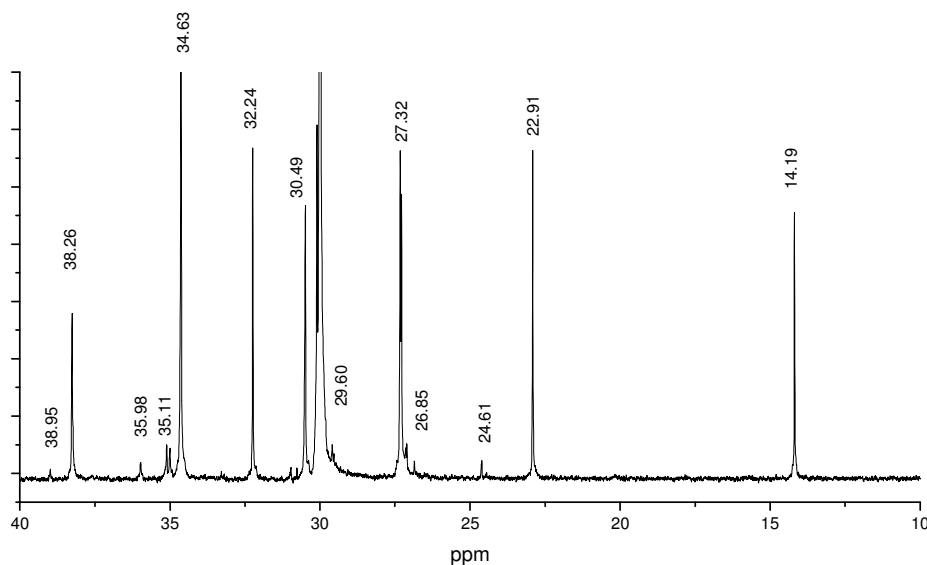


Figure 3.17: ^{13}C NMR spectrum of a copolymer (6 mol% comonomer) prepared by the conventional way of adding 1-octene

3. Tetramerization tandem catalysis

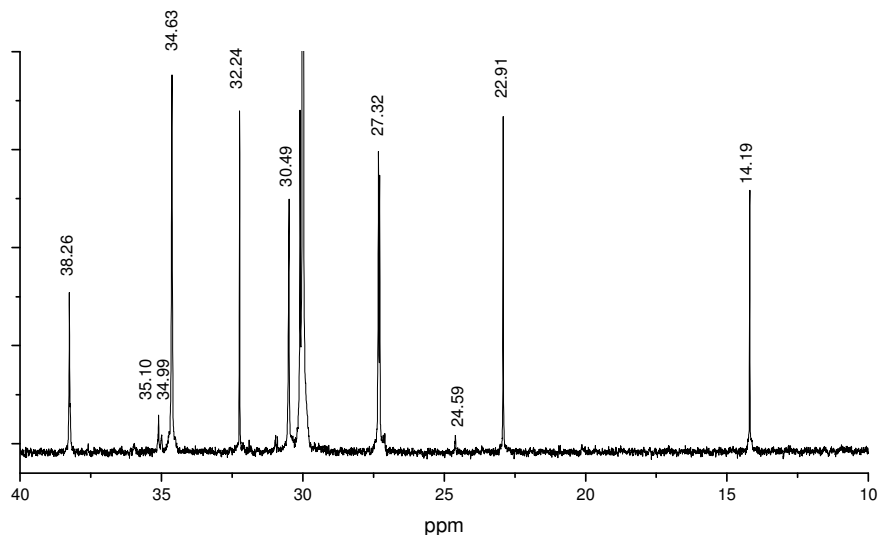


Figure 3.18: ^{13}C NMR spectrum of a commercial 1-octene copolymer with 6 mol% 1-octene

The CRYSTAF traces in Figure 3.19 display a comparison of the chemical composition distribution of the series of tandem copolymers with varying comonomer content. These CRYSTAF analyses were done in 1,2-dichlorobenzene to enable measurements to 0°C , which was not possible using 1,2,4-trichlorobenzene (used in the prior reported analyses) due to its higher melting temperature.

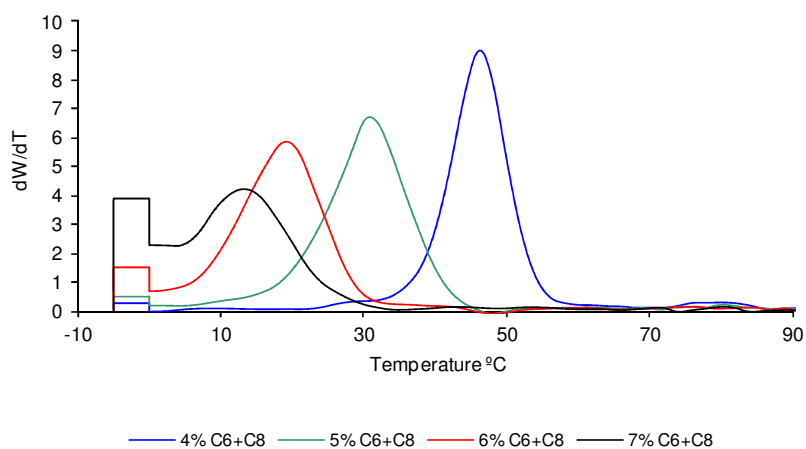


Figure 3.19: CRYSTAF traces of tandem copolymers of varying comonomer content

3. Tetramerization tandem catalysis

A small fraction of high density material is noticeable at 80 °C while the greatest portion of material is crystallizing at much lower temperatures, depending on the comonomer content. The soluble fraction increases with increasing comonomer content. Figure 3.20 and Figure 3.21 compare the CRYSTAF traces of the tandem copolymers and the available commercial copolymers with 1-octene contents of 4 and 6 mol%, respectively. The CRYSTAF measurement used 1,2-dichlorobenzene as solvent to enable low temperature analyses.

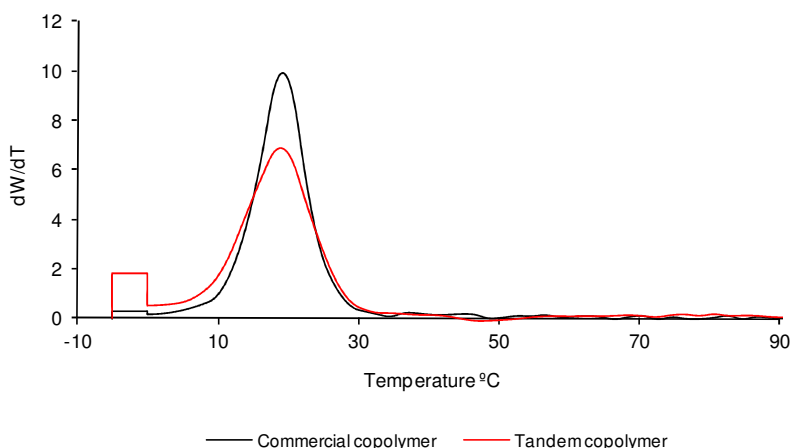


Figure 3.20: Comparison of a commercial copolymer (6 mol% 1-octene) with a tandem copolymer with similar comonomer content

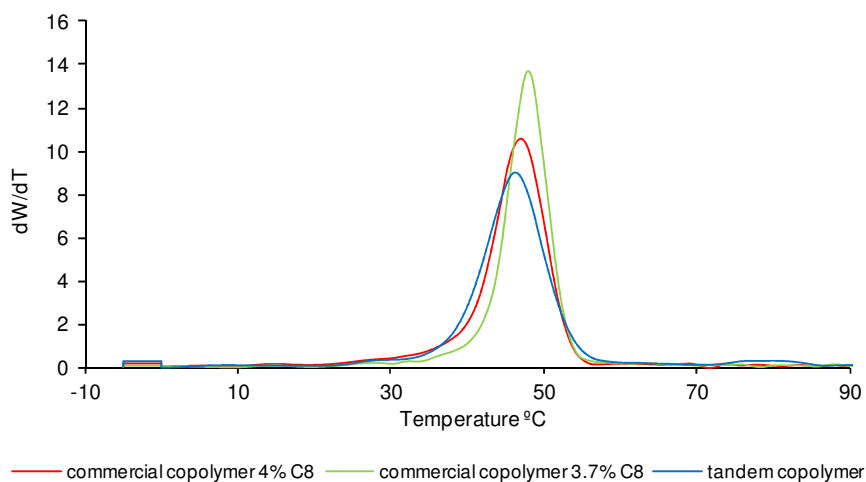


Figure 3.21: Comparison of commercial copolymer (4 mol% 1-octene) with a tandem copolymer with similar comonomer content

3. Tetramerization tandem catalysis

The chemical composition distributions are similar with the main difference the higher soluble fraction in the case of the tandem copolymer. The higher soluble fraction can be ascribed to the presence of the oligomerization catalyst which produces low molecular weight polymer. Both the lower temperature step and the oligomerization catalyst present in the tandem reaction contribute to formation of the solids and thus to the chemical composition distribution in the tandem copolymer (see Section 3.3.2). These contributions were determined in two additional reactions. Figure 3.22a display the CRYSTAF trace of the polymer obtained after running the tandem reaction at a constant temperature of 40 °C for 1 hour (yield; 2 g product). A reaction with only the oligomerization catalyst present in which the same temperature profile as in the tandem reactions was followed, yielded 3 g solids (Figure 3.22b). The complete tandem reaction yielded 45 g product.

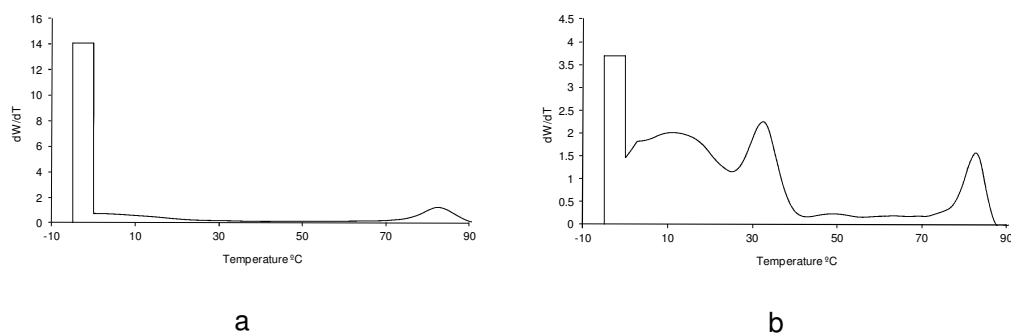


Figure 3.22: (a) Polymer obtained from tandem reaction at 40 °C; (b) Solid obtained from oligomerization reaction at 40 °C for 1 hour followed by heating above 100 °C

The presence of the small amount of additional material present in the tandem copolymer due to the presence of the oligomerization catalyst, the different temperature steps as well as the variation in comonomer content during the reaction will affect the properties of the final product and explain the difference between the tandem and commercial copolymers.

3.3.5.2 Comparison of properties

3.3.5.2.1 Melt flow behaviour

Molecular weight data of selected tandem copolymers in comparison with a commercial copolymer, as determined by GPC and the melt flow index values are listed in Table 3.8. The tandem copolymers display bimodal molecular weight distributions with a high molecular weight component ($\sim 160\,000\text{ g}\cdot\text{mol}^{-1}$) and a second component with low molecular weight ($\sim 1\,000\text{ g}\cdot\text{mol}^{-1}$).

3. Tetramerization tandem catalysis

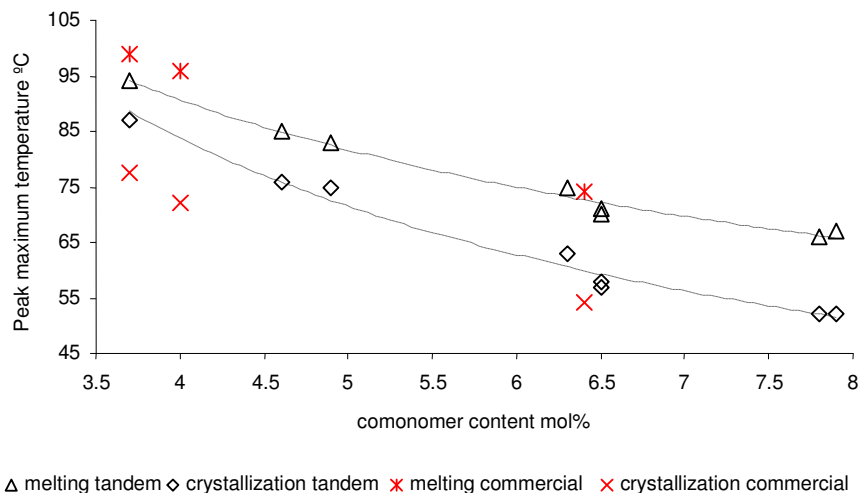
Table 3.8: Comparison of molecular weight distributions and MFI

Copolymer	Comonomer	$\langle M_n \rangle$	$\langle M_w \rangle$	M_p	MFI g.(10min) ⁻¹
	mol%	Peak 1	Peak 1	Peak 2	
Commercial	6.4	73	166	-	1.1
Tandem 1	6.0	87	184	882	1.6
Tandem 2	6.5	97	199	865	1.4
Tandem 3	7.7	91	186	921	1.8

The main difference in the tandem copolymers is the small fraction of low molecular weight material in the GPC diagram produced by the oligomerization catalyst. As a result the melt flow indexes of the tandem copolymers are higher than that of the commercial copolymer even though their molecular weights are higher.

3.3.5.2.2 Thermal behaviour

The thermal behaviour of the series of tandem copolymers with different comonomer contents was investigated by DSC and compared to that of the commercial copolymers. Figure 3.23 displays the melting and crystallization maximum peak values as a function of total comonomer content.

**Figure 3.23:** Melting and crystallization maximum peak maximum temperatures as function of the comonomer content

The crystallization behaviour of the tandem copolymers determined from DSC measurements differs from that of the commercial copolymers. Crystallization

3. Tetramerization tandem catalysis

maximum peak values for the commercial copolymers are lower than those of the tandem copolymers. When comparing the temperature dependent weight fraction crystallinity curves of the tandem copolymers calculated from DSC data³ with those of the commercial copolymers, it is clear that the crystallization behaviour of the copolymers is different (Figure 3.24). The tandem copolymers start to crystallize earlier due to the small amount of linear material present (see Figure 3.7), but at a slower rate.

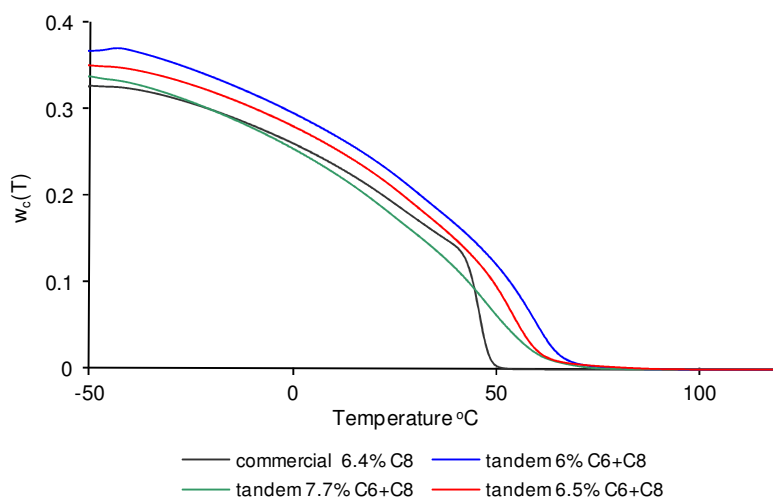


Figure 3.24: Comparison of the temperature dependent weight fraction crystallinity curves of tandem and commercial copolymers (calculated from DSC data as described in the experimental section).

3.3.5.2.3 Tensile properties

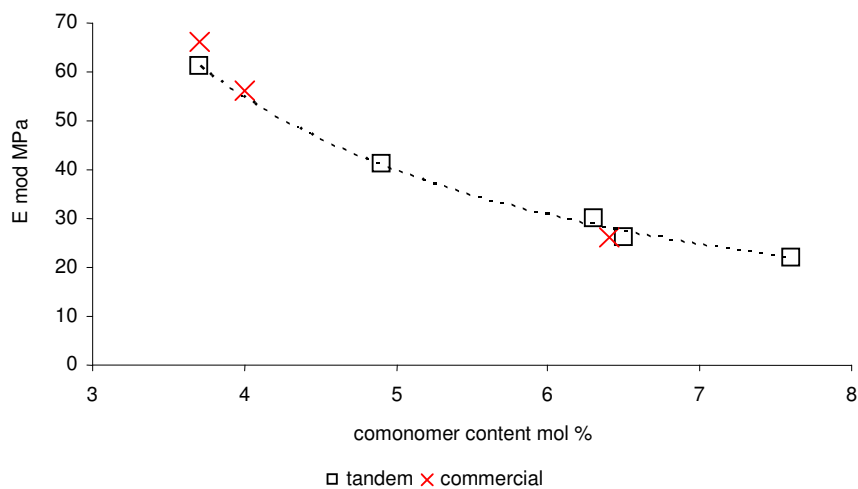
The tensile properties of the tandem and commercial copolymers are summarized in Table 3.9. The melt flow index (MFI) is listed as an indication of the molecular weight differences in the samples. No yield point is observed in the tensile curves of the tandem or the commercial copolymers as expected for copolymers with higher 1-octene content.¹² The modulus was measured as the slope of the stress-strain curve obtained at a strain rate of 1 mm.min⁻¹. The extension rate was increased to 5 mm.min⁻¹ when a force of 5 MPa was reached. Thereafter the tensile strength at break was measured.

3. Tetramerization tandem catalysis

Table 3.9: Comparison of tensile properties of tandem and commercial copolymers

Copolymer	MFI $\text{g}(10\text{min})^{-1}$	Tensile Modulus MPa	Elongation at break %	Tensile strength at break MPa
Commercial 3.7 mol%	3.0	66	185	20
Commercial 4 mol%	1.0	56	256	22
Commercial 6.4 mol%	1.1	26	112	15
Tandem 3.7 mol%	3.5	61	315	23
Tandem 4.9 mol%	3.0	41	234	17
Tandem 6.3 mol%	1.6	30	115	14
Tandem 6.5 mol%	1.4	26	117	14
Tandem 7.7 mol%	1.8	22	102	13

The modulus values and tensile strengths listed in Table 3.9 of the tandem copolymers follow the decreasing trend expected for an increase in comonomer content (Figure 3.25 and Figure 3.26). Commercial copolymers fit into these trends.

**Figure 3.25:** Effect of comonomer content on modulus of the copolymers

3. Tetramerization tandem catalysis

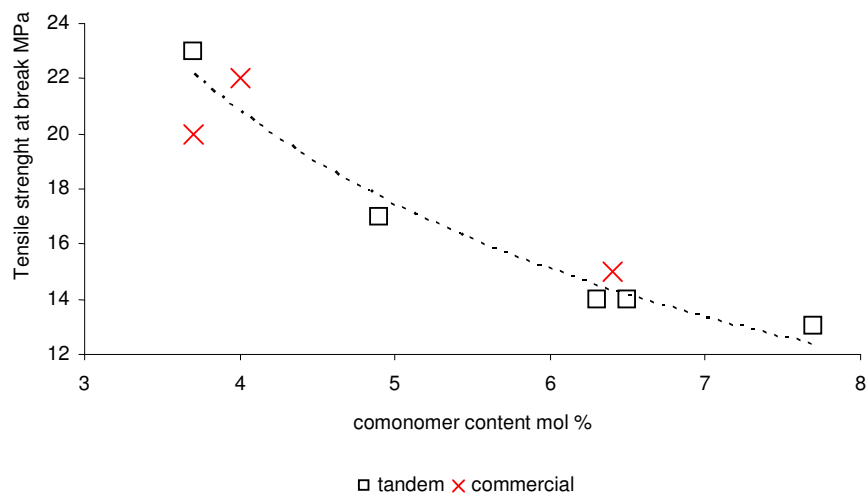


Figure 3.26: Effect of comonomer content on tensile strength at break of the copolymers

3.3.6 Fractionation of tandem copolymers by prep-TREF

The tandem copolymer (3.7 mol% comonomer) was fractionated by prep-TREF (preparative temperature rising elution fractionation) to illustrate the chemical composition distribution. Fractionation using this technique occurs on the basis of crystallisability.¹³ An advantage of prep-TREF is the possibility to collect relative large fractions which can be analysed offline. The molecular weights and comonomer contents of the different fractions can then be established using GPC and ¹³C NMR, respectively.

3.3.6.1 Prep-TREF conditions

The polymer was dissolved in xylene at 130 °C in a glass reactor at a concentration of 10 mg.mL⁻¹. Irganox 1010 was added to the solution as a stabiliser (2 wt%) followed by pre-heated white quartz sand (50-70 mesh). The solution temperature was stabilized at 130 °C for 3 hours, followed by cooling at a rate of 1 °C.h⁻¹ to room temperature. The sand was then transferred to a stainless steel column with an internal diameter of 7 cm and length of 15 cm. The temperature was increased stepwise while the polymer was eluted with xylene at a flow rate of 4 mL.min⁻¹. Fractions were collected at different temperature steps. Xylene was evaporated in a rotary evaporator and the fractions dried under vacuum at 60 °C for 8 h.

3. Tetramerization tandem catalysis

3.3.6.2 Results

Nine fractions of the tandem copolymer with an average comonomer content of 3.7 mol % were collected during the fractionation process. The bulk of material was obtained at 60 °C to 70 °C, but lower and higher temperature fractions were also present. The yields from the various fractions are displayed in Figure 3.27.

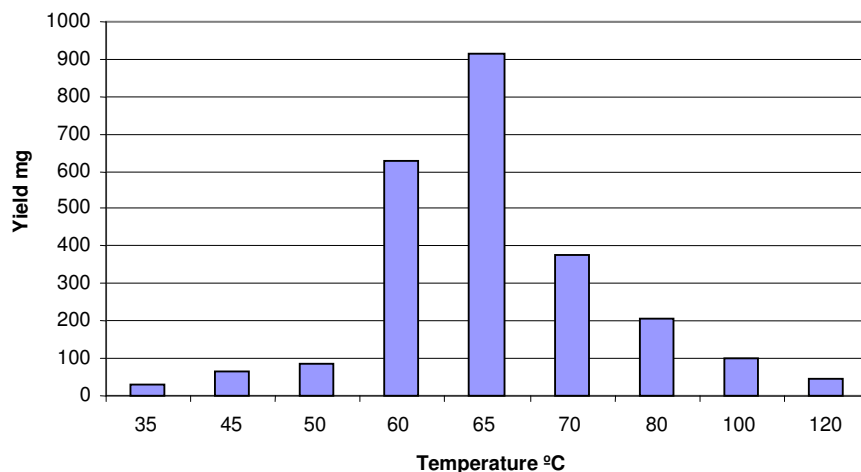


Figure 3.27: Distribution of fractions obtained from the prep-TREF analysis of a tandem copolymer

The fractions were subsequently analysed by DSC, GPC, CRYSTAF and ^{13}C NMR. CRYSTAF analyses in Figure 3.28 illustrate the chemical composition distributions present in the various fractions.

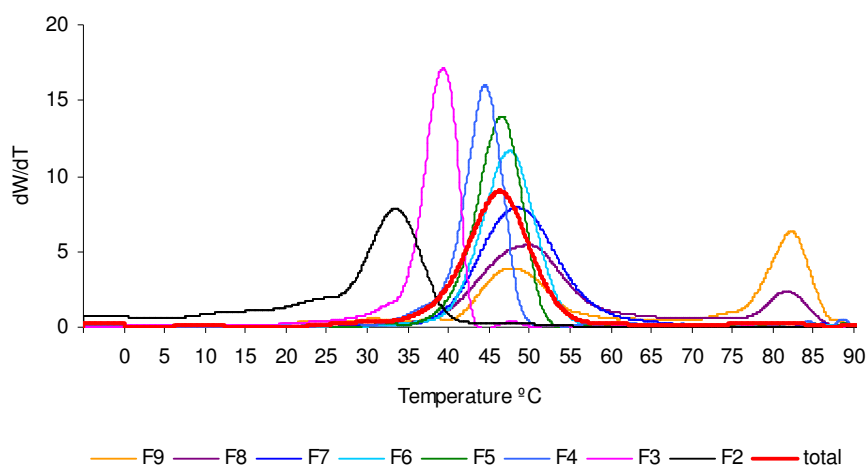


Figure 3.28: Comparison of the chemical composition distributions in different TREF-fractions of a tandem copolymer

3. Tetramerization tandem catalysis

The CRYSTAF results show that fractions 8 and 9 have bimodal distributions. Both fractions consist of a component which crystallizes at 80 °C and one which crystallizes at 47 °C. The fractionation was thus not successful in separating the different components of Fractions 8 and 9.

¹³C NMR analyses (Table 3.10) indicated that the average comonomer contents vary from 3.6 mol% in Fraction 1 to 4.5 mol% in Fraction 4, while Fraction 8 has an average comonomer content of 2.2 mol%. ¹³C NMR analyses of Fractions 1 and 2 show more prominent allylic peaks at 34.0 ppm in comparison to the fractions collected at higher temperatures. Here the end group peaks are also more noticeable, indicating low molecular weight material.

DSC results are tabled in Table 3.10 and GPC data in Table 3.11. The DSC analyses show an increase in melting and crystallization temperature from Fraction 3 upwards. This is as expected due to the fractionation based on crystallisability. GPC results confirm that the fractions collected at the lower temperatures are of low molecular weight.

Table 3.10: DSC data of prep-TREF fractions of a tandem copolymer

Fraction	Comonomer content mol%	DSC cp °C	DSC mp °C	Δh_m J.g ⁻¹
F1	3.6	80.2/63.8	95.4/65.2	115
F2	3.2	74.2	89.2	95
F3	not available	73.8	90.9	90
F4	4.5	76.0	93.9	92
F5	4.5	78.5	95.6	92
F6	3.7	81.5	97.7	95
F7	3.7	87.9	103.4	103
F8	2.2	106.1	120.3/124.16	131
F9	not available	110.2	124.6	147

3. Tetramerization tandem catalysis

Table 3.11: GPC data of prep-TREF fractions of a tandem copolymer

Fraction	$\langle M_n \rangle$	M_p	$\langle M_w \rangle$	PI
F2	7 554	57 645	67 741	9.0
F3	39 176	86 588	120 259	3.1
F4	90 016	145 859	178 103	2.0
F5	105 728	163 387	198 750	1.9
F6	90 358	157 953	187 443	2.1
F7	70 318	144 640	172 275	2.5
F8	63 215	140 508	196 604	3.1
F9	64 570	157 081	246 510	3.8

Although the fractionation by prep-TREF was not 100 % successful in separating the various components completely, it is evident that the tandem copolymer comprises of fractions with distinctly different molecular weight and comonomer content distributions. This broad distribution results from the presence of the oligomerization catalyst which produces solids distinctly different from that produced by the metallocene catalyst. Furthermore, the changing comonomer concentration and the different temperatures during the polymerization reaction also contributed to the different microstructure of the fractions.

3.4 Conclusions

From the preceding results it is clear that the chromium/ $\text{Ph}_2\text{PN}\{\text{CH}(\text{CH}_3)_2\}\text{PPh}_2$ tetramerization catalyst and a metallocene polymerization catalyst are not completely compatible in a tandem catalysis system because of different optimum temperatures for α -olefin production and polymer formation. Successful tandem catalysis is possible when the reactions are performed in a sequential way. Ethylene copolymers of 1-hexene and 1-octene were obtained from a single monomer. The oligomerization to polymerization catalyst ratios, the catalyst to cocatalyst ratios as well as the temperature profile are all factors that influence the amount of α -olefins formed and therefore the type of copolymer produced.

Additionally it was found that the two catalysts interfere chemically. The activity of the polymerization catalyst decreases in the presence of the oligomerization catalyst, possibly because of competitive interactions between the oligomerization catalyst components and the monomers at the active polymerization catalyst centre.

3. Tetramerization tandem catalysis

The main differences between tandem and conventional, commercial copolymers are the presence of a small amount of low molecular weight material produced by the oligomerization catalyst as well as the formation of a linear component. The linear fraction results from the the initial low concentration of α -olefins, but such a component is also produced by the oligomerization catalyst.

3.5 References

1. Wasilke, J., Obrey, S. J., Baker, T., Bazan, G. C., *Chemical Reviews*, 2005, 105, 1001
2. Bollmann, A., Blann, K., Dixon, J. T., Hess, F. M., Kilian, E., Maumela, H., McGuinness, D. S., Morgan, D. H., Neveling, A., Otto, S., Overett, M., Slawin, A., Wasserscheid, P., Kuhlmann, S, *Journal of the American Chemical Society*, 2004, 126, 14712; Walsh, R., Morgan, D. H., Bolmann, A., Dixon, J. T., *Applied Catalysis, A*, 2006, 306, 184
3. Mathot, V. B. F. in *Calorimetry and Thermal Analysis of Polymers*, Hanser Publishers, 1994, Munich, 130-135; ATHAS Databank, <http://web.utk.edu/~athas/databank/alkene/pe/pe.html> and references therein, accessed 2006
4. De Pooter, M., Smith, P. B., Dohrer, K. K., Bennett, K. F., Meadows, M. D., Smith, C. G., Schouwenaars, H. P., Geerards, R. A., *Journal Applied Polymer Science*, 1991, 42, 399; Liu, W., Rinaldi, P. L., *Macromolecules*, 2001, 34, 4757
5. Nomura, K., Fujita, K., Fujika, M., *Journal of Molecular Catalysis, A: Chemistry*, 2004, 220, 133
6. Monrabal, B., Blanco, J., Nieto, J., Soares, J. B. P., *Journal of Polymer Science, Part A: Polymer Chemistry*, 2000, 37, 89
7. Camurati, I., Cavicchi, B., Dall'Occo, T., Piemotesi, F., *Macromolecular Chemistry and Physics*, 2002, 202, 701
8. Awudza, J. A., Tait, P. J. T, *Journal of Polymer Science, Part A: Polymer Chemistry*, 2007, 46, 267; Koivumäki, J., Seppälä, J. V., *Macromolecules*, 1993, 26, 5535

3. Tetramerization tandem catalysis

9. http://www.dexplastomers.com/products/exact/grade/_down/eDS8201.pdf, accessed 2007
10. Yano, A., Akimoto, A. in *Metallocene - Catalyzed Polymers*, Plastic Design Library, New York, 1998, 97
11. Liu, W., Rinaldi, P. L., *Macromolecules*, 2001, 34, 4757
12. Bensason, S., Minick, J., Moet, A., Chum, S., Hiltner, A., Baer, E., *Journal of Polymer Science, Part B: Polymer Physics*, 1998, 34, 1301; Islam, A., Hussein, A. I., *Journal of Applied Polymer Science*, 2006, 100, 5019
13. Anantawaraskul, S., Soares, J. B. P., Wood-Adams, P. M., *Advances in Polymer Science*, 2005, 182, 1; Soares, J. B. P., Hamielec, A. E., *Polymer*, 1995, 36, 1639

4 Trimerization tandem catalysis

4.1 Introduction

Butyl branched polyethylene can be obtained when a selective ethylene trimerization catalyst is used in combination with a polymerization catalyst with ethylene as the monomer.¹ Tandem catalysis studies using selective trimerization catalysts have been reported in the literature and are summarized in Chapter 2.

Bis(diphenylphosphino)amine (PNP) type of ligands with substituents in the *ortho* position are known to have high selectivity in the formation of 1-hexene during ethylene oligomerization reactions. The system $(o\text{-OMeC}_6\text{H}_4)_2\text{PN}(\text{CH}_3)\text{P}(o\text{-OMeC}_6\text{H}_4)_2/\text{CrCl}_3/\text{MAO}$ (Figure 4.1 a) is reported to be an extremely active and selective ethylene trimerization catalyst which produces low amounts of polymer even at temperatures above 100 °C.² A ligand with *ortho* ethyl substituents (Figure 4.1 b) is an active catalyst with tuneable selectivity.³ The catalyst system produces predominantly low molecular weight polyethylene waxes at elevated temperatures, but at temperatures below 60 °C it forms selectively 1-hexene. This result is probably linked to different conformations of $(o\text{-EtC}_6\text{H}_4)_2\text{PN}(\text{CH}_3)\text{P}(o\text{-EtC}_6\text{H}_4)_2$ at different temperatures in solution, while the oxygen atom in $(o\text{-OMeC}_6\text{H}_4)_2\text{PN}(\text{CH}_3)\text{P}(o\text{-OMeC}_6\text{H}_4)_2$ is able to stabilize specific conformations through additional coordination to the chromium centre.

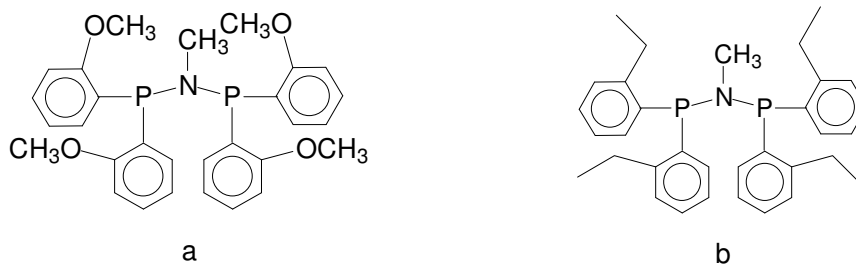


Figure 4.1: Structures of trimerization ligands

The good selectivity, activity and stability of $(o\text{-OMeC}_6\text{H}_4)_2\text{PN}(\text{CH}_3)\text{P}(o\text{-OMeC}_6\text{H}_4)_2/\text{CrCl}_3/\text{MAO}$ in ethylene oligomerization reactions at high temperatures make it ideal for use in tandem catalysis. The activity of this catalyst in trimerization

4. Trimerization tandem catalysis

might be comparable to that of a metallocene polymerization catalyst under the same reaction conditions. Specifically, the optimum reaction temperature for oligomerization might match with that of the metallocene which will facilitate successful tandem catalysis in contrast to the combined tetramerization catalyst system described in Chapter 3.

In this study, this ethylene trimerization system was used in combination with a metallocene polymerization catalyst to produce LLDPE based on 1-hexene and ethylene. The aspects which were investigated are:

- The effect of the PNP-type ligand on the ethylene/1-hexene copolymerization reaction
- The effect of reaction time on the properties of the tandem copolymers
- Comparison of the tandem copolymers with conventional 1-hexene copolymers

Although $(o\text{-EtC}_6\text{H}_4)_2\text{PN}(\text{CH}_3)\text{P}(o\text{-EtC}_6\text{H}_4)_2/\text{CrCl}_3/\text{MAO}$ was not deemed suitable for tandem catalysis due to the high amounts of low molecular weight solids produced at high temperatures, its wax-forming nature is of interest. The second part of this chapter describes the synthesis and characteristics of these low molecular weight polyethylenes (waxes).

4.2 Experimental

4.2.1 Materials

Metallocene catalysts were obtained from Boulder Scientific, $\text{Cr}(\text{acac})_3$ from Aldrich, MAO from Crompton and the PNP-type ligands from Cytec. All reagents were used as received. Pure ethylene was obtained from Afrox. Methylcyclohexane and a C_7/C_8 paraffin cut were obtained from Aldrich and Sasol Wax, respectively, and were used as solvents. Solvents were purified by passing it through an aluminum oxide column and were stored on molecular sieves (4Å).

4.2.2 Oligomerization and polymerization procedures

Reactions were conducted under inert conditions in a 1L Buchi reactor equipped with mechanical stirring and temperature control. Solvent and 50 % of the MAO were first added to the reactor followed by ethylene. Solutions of the catalysts were prepared

4. Trimerization tandem catalysis

under a nitrogen atmosphere in a glove box using dry toluene as solvent. The remaining 50 % of the MAO was added to the catalyst solutions. Reactions were initiated by introducing the activated catalyst solution to the pressurized reactor with high pressure nitrogen. A total reactor pressure of 30 bar was used. Reactions were terminated by the addition of an alcohol followed by cooling and venting of the ethylene. The polymers were washed with acetone and dried under vacuum at 60 °C for 12 h.

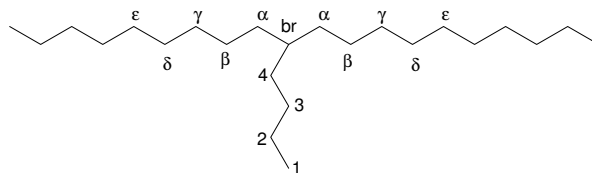
4.2.3 Thermal analysis

Differential Scanning Calorimetry (DSC) analyses were performed on a TA Q200 instrument. The instrument was calibrated using indium as standard. Samples were first melted at 180 °C to remove the thermal history followed by crystallization and melting at 10 °C.min⁻¹. Melting temperatures obtained from the latter heating run are reported.

4.2.4 Quantitative ¹³C NMR analysis

The polymer (60 mg) was dissolved in 0.6 mL deuterated 1,1,2,2-tetrachloroethane (6 wt%) stabilized with 2,6,-di-*tert*-butyl-4-methylphenol. The sample was placed in a ventilated oven to homogenize at 130°C for approximately 2 hours. Quantitative ¹³C NMR experiments were performed at 150 MHz using a 5 mm PFG switchable/broadband probe (¹H -¹⁹F, ¹⁵N - ³¹P) on a Varian ^{UNITY} INOVA 600 MHz spectrometer at 120°C. 90° Pulse widths of approximately 6 μs and delay times between pulses of 15 s were used with an acquisition time of 1.8 s. The number of scans was set to 5040, but a signal-to-noise parameter was set to 2000. Therefore either 5040 scans were acquired or the acquisition was stopped after the required signal-to-noise was reached. Consequently the analysis time ranged from 3 -10 hours. Chemical shifts were referenced internally to the main backbone methylene carbon resonance (30 ppm). Chemical shifts obtained from the literature were used for identification of peaks.⁴ Numbering nomenclature was used as described in the literature.⁴ The methene carbon at 38.2 ppm (br in Scheme 4.1) was used for quantitative evaluation of the comonomer content. Equation 1 was used to determine the amount of the 1-hexene incorporated.

4. Trimerization tandem catalysis

**Scheme 4.1:** Numbering scheme for carbons in the copolymer framework

$$\frac{\sum \int 2[\text{Methene Carbon of Comonomer}]}{\sum \int [\text{Backbone Carbons}]} \times \frac{100}{1} = \text{Total comonomer present (mole\%)} \quad (1)$$

4.2.5 GC analysis

GC-FID analysis of the liquid product was performed using a CP Sil PONA column (100 m x 250 μm x 0.50 μm) with hydrogen as carrier gas (flow rate 5 $\text{mL}\cdot\text{min}^{-1}$) and nonane as internal standard. The oven temperature program comprised a 5 minutes isothermal step at 35 $^{\circ}\text{C}$ followed by a ramp to 260 $^{\circ}\text{C}$ at a rate of 5 $^{\circ}\text{C}\cdot\text{min}^{-1}$.

4.2.6 High Temperature GPC analysis

High temperature GPC analyses were conducted on a PL-GPC 220 high-temperature chromatograph equipped with a differential refractive index detector and four PL gel MIXED-B columns (Polymer Laboratories). The concentration of the samples was 2 $\text{mg}\cdot\text{mL}^{-1}$ in 1,2,4- trichlorobenzene, stabilized with 0.0125 % 2,6-di-*tert*-butyl-4-methylphenol. A flow rate of 1 $\text{mL}\cdot\text{min}^{-1}$ and temperature of 140 $^{\circ}\text{C}$ were maintained for all experiments. The molecular weight calibration was done with monodisperse polystyrene standards (EasiCal from Polymer Laboratories).

High temperature GPC analyses on the polyethylene waxes was performed using a PL-GPC 220 high- temperature chromatograph equipped with a differential refractive index detector. Separation was performed on two 300 x 7.5mm PLgel 5 μm Mixed-D columns (molecular separation range 200 – 400 000 $\text{g}\cdot\text{mol}^{-1}$). The mobile phase was HPLC grade *o*-xylene. The pump, injector and column compartments were programmed to 60 $^{\circ}\text{C}$, 100 $^{\circ}\text{C}$ and 100 $^{\circ}\text{C}$. A flow rate of 1 $\text{mL}\cdot\text{min}^{-1}$ were employed. The concentration of the samples was 0.05 wt% in the *o*-xylene solution. Calibration was performed using *n*-alkanes from C_{12} to C_{60} and polyethylene standards with chain lengths C_{88} and C_{144} .

4.2.7 Melt flow index determination

Melt flow index was determined on a Ceast Melt Flow Indexer. The melt flow index of polyethylene was determined at 190 °C, using a 2.16 kg force and a die of 8 mm length having a 2.01 mm inside diameter.

4.2.8 CRYSTAF analysis

CRYSTAF analyses were performed on a Polymer Char combination CRYSTAF-TREF apparatus fitted with an IR detector using 1,2,4-trichlorobenzene as solvent. Samples (20 mg maximum) were first dissolved in 30 mL solvent at 160 °C after which the temperature was decrease to 100 °C. The temperature was then decreased from 100 °C to 30 °C at a controlled rate of 0.2 °C.min⁻¹ while the change in polymer concentration was recorded. When analyzing low molecular weight polyethylene the cooling was achieved by connecting liquid nitrogen to the instrument. The temperature was decreased from 100 °C to 0 °C at a controlled rate of 0.2 °C.min⁻¹. 1,2-Dichlorobenzene was used as the solvent.

4.2.9 Tensile measurements

Samples for tensile property measurements were moulded on a Ray-Ran injection moulding machine with a melt temperature of 190 °C and a mould temperature of 50 °C. Tensile properties of the injection-moulded test pieces were determined on a Hounsfield tensile testing apparatus. The modulus was measured at a rate of 1 mm.min⁻¹. The extension rate was increased to 5 mm.min⁻¹ when a force of 5 MPa was reached, after which the tensile strength at break was measured.

4.2.10 Viscosity measurements

Viscosity measurements were performed using a Brookfield viscometer with a number 18 spindle. Samples were first melted at 150 °C and homogenize in an oven, before it was transferred to the viscometer. The viscosity was measured at 135 °C.

4.3 Results and Discussion

4.3.1 The effect of the PNP-type ligand on 1-hexene copolymerization

In Chapter 3 it was described that the activity of the polymerization catalyst had been influenced by the PNP-type ligand. It also seemed that the incorporation of 1-octene was negatively affected by an increase in PNP-type ligand concentration. The effect of the PNP-type ligand on the 1-hexene copolymerization behaviour of $\text{EtIn}_2\text{ZrCl}_2$ was therefore also investigated. The ligand to $\text{EtIn}_2\text{ZrCl}_2$ ratio was increased and a constant amount of 1-hexene was added. The PNP-type ligand structure was also varied at a fixed ligand to $\text{EtIn}_2\text{ZrCl}_2$ ratio. The PNP-type ligands with *o*-methoxy (Figure 4.1 a), *o*-ethyl (Figure 4.1 b) or no substituents on the phenyl rings were employed in these reactions.

4.3.1.1 Reaction conditions

Reactions were conducted with $\text{EtIn}_2\text{ZrCl}_2$ (4×10^{-8} mol) and MAO as cocatalyst (1.65×10^{-3} mol) in a 1 L Buchi reactor at 100 °C with 300 mL solvent (C_7/C_8 paraffin). The ethylene pressure was 30 bar. The reaction time was 30 minutes. The concentration of the ligand (*o*-OMe C_6H_4) $_2$ PN(CH $_3$)P(*o*-OMe C_6H_4) $_2$ was varied such that the ligand: $\text{EtIn}_2\text{ZrCl}_2$ ratio was 10, 40, 50 and 80 in the different experiments. The ligands (*o*-Et C_6H_4) $_2$ PN(CH $_3$)P(*o*-Et C_6H_4) $_2$ and $\text{Ph}_2\text{PN}(\text{CH}_3)\text{PPh}$ were also tested at a ligand: $\text{EtIn}_2\text{ZrCl}_2$ ratio of 1:50 under the same reaction conditions.

4.3.1.2 Results

Figure 4.2 shows the effect of the PNP-type ligand concentration on the polymer yield. The polymer yield decreases with an increase in the ligand: $\text{EtIn}_2\text{ZrCl}_2$ ratio. No significant difference can be observed in the polymer yield when the substituent on the ligand was changed.

4. Trimerization tandem catalysis

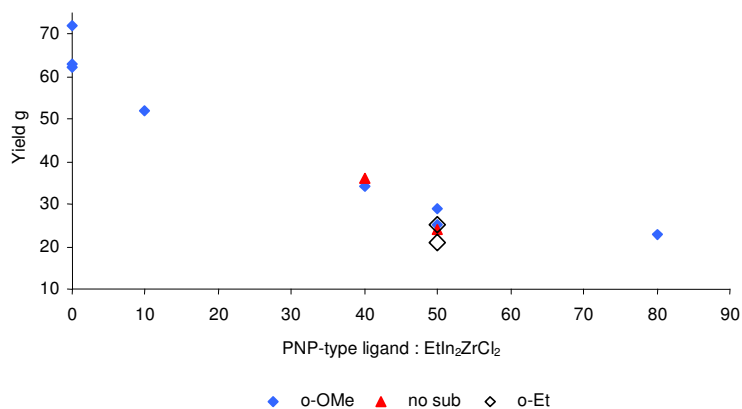


Figure 4.2: Effect of the substituents on PNP-type ligand and ligand:EtIn₂ZrCl₂ molar ratio on the polymer yield

Although the polymerization activity decreased when the ligand:EtIn₂ZrCl₂ ratio increased, no clear trend in the DSC melting peak maximum temperatures were observed. 1-Octene copolymerization using the metallocene EtIn₂ZrCl₂ in the presence of a PNP-type ligand was revisited following the results obtained from the 1-hexene study. Previous results showed that the 1-octene incorporation decreased (as evident from the increase in DSC melting peak maximum temperature) with an increase in ligand:EtIn₂ZrCl₂ ratio, indicating competitive coordination between PNP-type ligands and monomers for the active polymerization site (Section 3.3.5.2). This restricts the incorporation of the bulky 1-octene to some extent. The previous 1-octene copolymerization behaviour in the presence of a PNP-type ligand was confirmed by the results of the repeat experiments. The previous differences observed in the copolymerization behaviour between 1-octene and 1-hexene may be ascribed to the different sizes of the two comonomers. The more bulky 1-octene may be restricted to a greater extent than 1-hexene from coordination in the presence of the PNP-type ligand.

4.3.2 The effect of reaction time

Tandem copolymerization reactions were conducted using (*o*-OMePh)₂PN(CH₃)P(*o*-OMePh)₂/Cr(acac)₃/MAO in combination with EtIn₂ZrCl₂ at a constant temperature of 100 °C to produce 1-hexene copolymers. Reactions were stopped at different intervals to investigate the effect of reaction time on polymer yield and composition.

4. Trimerization tandem catalysis

4.3.2.1 Reaction conditions

Tandem reactions were conducted with $\text{EtIn}_2\text{ZrCl}_2$ (4×10^{-8} mol), $\text{Cr}(\text{acac})_3$ (3×10^{-6} mol), $(o\text{-OMePh})_2\text{PN}(\text{CH}_3)\text{P}(o\text{-OMePh})_2$ (3.3×10^{-6} mol) and MAO as cocatalyst (1.65×10^{-3} mol) in a 1 L Buchi reactor at 100 °C with 300 mL solvent (C_7/C_8 paraffin). The ethylene pressure was 30 bar. Reactions were terminated by addition of an alcohol. Reaction times were 5, 15 and 30 minutes.

4.3.2.2 Results

Figure 4.3 illustrates the quantity of 1-hexene and polymer formed at the different reaction times. The thermal properties of the copolymers are displayed in Table 4.1.

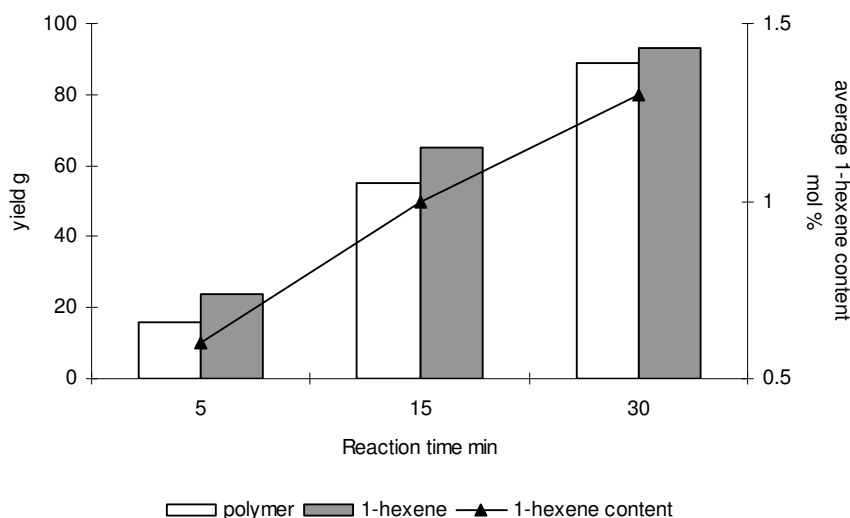


Figure 4.3: Effect of reaction time on the tandem copolymerization reactions

Table 4.1: Thermal properties of tandem copolymers obtained after 5, 10 and 15 minutes

Reaction time min	Comonomer content mol %	DSC mp °C	DSC cp °C
5	0.1	123.7	112.1
15	1.0	121.1	109.6
30	1.3	120.2	108.5

The DSC melting and crystallization peaks temperatures shift to slightly lower values as the reaction proceeds. An illustration of the effect of reaction time on the copolymer composition can be seen in the CRYSTAF traces. The comonomer

4. Trimerization tandem catalysis

content increases with an increase in the reaction time due to the increasing amount of 1-hexene accumulating in the reactor. CRYSTAF traces are shown in Figure 4.4.

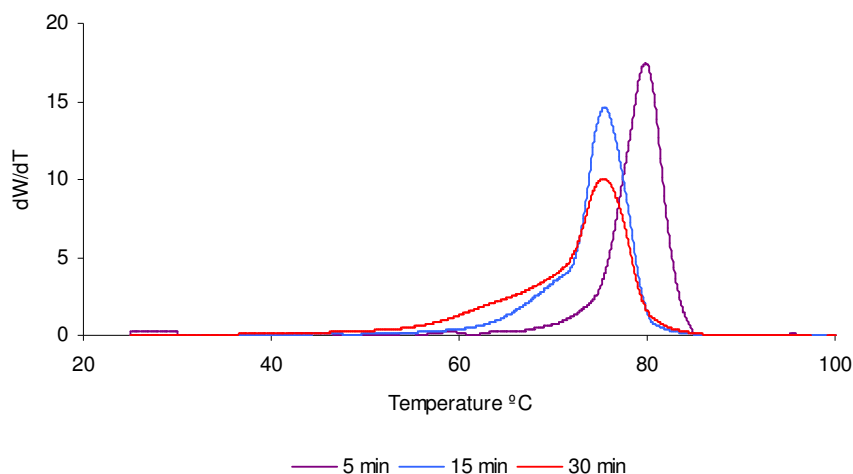


Figure 4.4: CRYSTAF trace showing the effect of reaction time on the chemical composition distribution of the tandem copolymers

The CRYSTAF peak temperature shifts to a lower value and broadens, when the reaction time increases from 5 to 15 minutes. After a further 15 minutes a tail of higher comonomer content material is present in the CRYSTAF trace due to the increasing amount of 1-hexene present. The GPC analyses (Table 4.2) show a significant change in the molecular weight with time.

Table 4.2: Variation in tandem copolymer molecular weights with an increase reaction time

Reaction time min	$\langle M_n \rangle$	$\langle M_w \rangle$	M_p	PI
5	61	120	105	2.0
15	68	152	127	2.2
30	70	158	134	2.2

The molecular weight increases as the reaction proceeds from 5 to 15 minutes. This observation is unexpected, because the comonomer concentration increases as the reaction time increases. It is known that high comonomer concentrations result in lower molecular weight copolymers due to chain transfer to the monomer.⁵ In this

4. Trimerization tandem catalysis

case the lower molecular weight polymer produced in the first five minutes of the reaction is probably a result of the increased temperature during the first part of the reaction when the oligomerization catalyst is most active and the reaction temperature overshoots the set point. The molecular weight distribution also became slightly broader after five minutes, but not significantly so. No significant change in the molecular mass distribution between 15 and 30 minutes occurred.

4.3.3 Comparative study of tandem copolymers with conventional 1-hexene copolymers

Tandem copolymers were compared to conventionally prepared copolymers. In these conventional copolymerization reactions a constant amount of 1-hexene was added to the reactor. The chemical composition distribution, molecular mass distributions and tensile properties of these tandem and conventional copolymers were compared.

4.3.3.1 Chemical composition distribution

4.3.3.1.1 Reaction conditions

The tandem copolymers (Polymer 1 and Polymer 2) were prepared with $\text{EtIn}_2\text{ZrCl}_2$ (4×10^{-8} mol), $\text{Cr}(\text{acac})_3$ (3×10^{-6} mol), $(o\text{-OMePh})_2\text{PN}(\text{CH}_3)\text{P}(o\text{-OMePh})_2$ (3.3×10^{-6} mol) and MAO as cocatalyst (1.65×10^{-3} mol) in a 1 L Buchi reactor at 100 °C with 300 mL solvent (C_7/C_8 paraffin).

The conventional copolymers (Polymer 3 and Polymer 4) were prepared using $\text{EtIn}_2\text{ZrCl}_2$ (4×10^{-8} mol) and MAO (1.65×10^{-3} mol) in 300 mL solvent (C_7/C_8 paraffin) and 30 bar ethylene. 1-Hexene (35 g and 60 g, respectively) was added at the start of the two reactions. A third copolymer (Polymer 5) was prepared using the same catalyst amounts, but 100 g 1-hexene was added during the course of the reaction via a HPLC pump.

4.3.3.1.2 Results

Figure 4.5 compares the chemical composition distributions of a tandem copolymer with that of two conventionally prepared copolymers. Different quantities of 1-hexene

4. Trimerization tandem catalysis

were added to the two conventional copolymers. Table 4.3 displays the thermal properties of the copolymers.

Table 4.3: Comparison of thermal properties of the copolymers

	Comonomer content mol %	DSC mp °C	Δh_m J.g⁻¹	DSC cp °C
Polymer 1	1.3	120.2	173	108.5
Polymer 3	not available	120.0	140	109.6
Polymer 4	not available	118.5	124	103.1

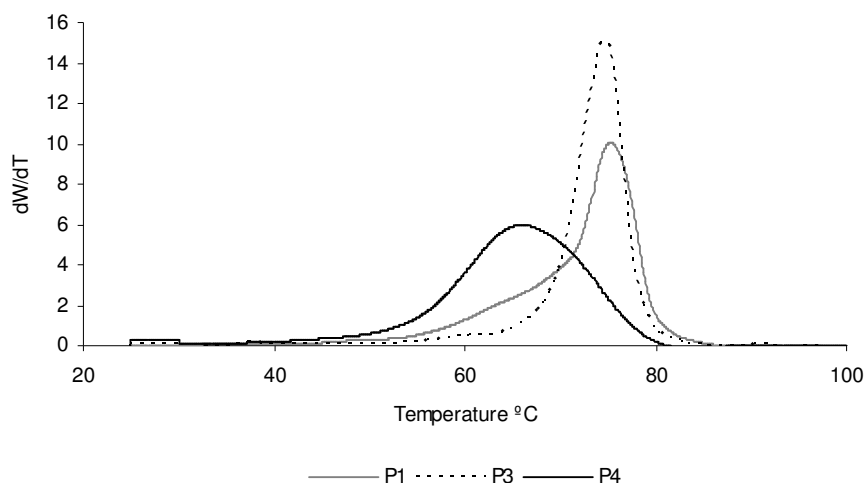


Figure 4.5: Comparison of CRYSTAF traces of tandem (P1) and conventional copolymers (P3 and P4)

The CRYSTAF trace of the tandem copolymer (Polymer 1) has a prominent crystallization peak at ~75 °C and a tail of less crystallisable material. This can be explained by the varying comonomer concentration during the course of the reaction. The tandem polymer, Polymer 1, has a broad chemical composition distribution, almost what one would expect of a commercial LLDPE produced by heterogeneous transition metal catalysts. The copolymers, Polymer 3 (P3) and Polymer 4 (P4), prepared by adding 1-hexene at the start of the reaction, exhibit uniform chemical composition distribution, with a variation in peak crystallization temperature as well as in the broadness of the peak. These phenomena can be related to the amount of 1-hexene incorporated in the polymer.

4. Trimerization tandem catalysis

It is believed that the chemical composition distribution resulting from the tandem copolymerization is mainly caused by the varying comonomer concentration during the course of the reaction. In Section 4.3.1 it was shown that the presence of the PNP-type ligand does not influence 1-hexene incorporation. A copolymerization reaction was conducted where 1-hexene was introduced during the course of the reaction using a HPLC pump to simulate the production of 1-hexene in the absence of the trimerization catalyst. In such a way it could be confirmed that the varying comonomer concentration is the only reason for the observed chemical composition distribution. Figure 4.6 displays the CRYSTAF trace of the resulting copolymer, Polymer 5, compared to that of two tandem copolymers (Polymers 1 and 2).

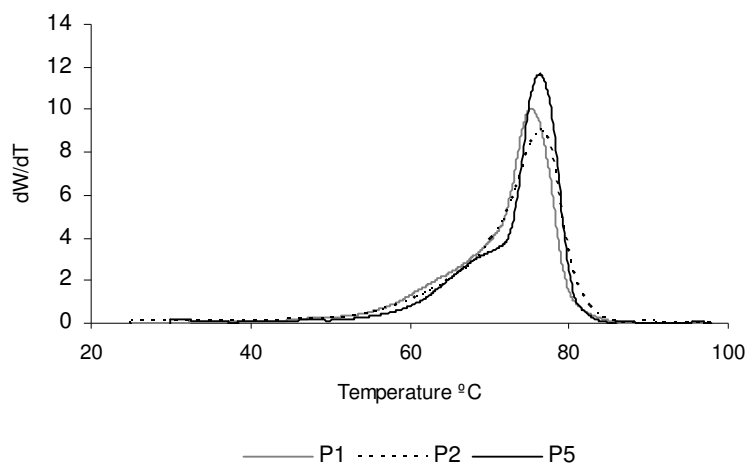


Figure 4.6: CRYSTAF comparison of tandem copolymers and the copolymer obtained by feeding 1-hexene during a copolymerization reaction

No significant difference is observed in the chemical composition distributions of the products when comparing the CRYSTAF traces. GPC analyses of the copolymers are compared in Table 4.4. Molecular weight values are also comparable.

Table 4.4: Molecular weight data of the different copolymers

Copolymer	$\langle M_n \rangle$	$\langle M_w \rangle$	M_p	PI
Polymer 1	70	157	134	2.3
Polymer 2	71	158	134	2.2
Polymer 5	71	154	129	2.2

4. Trimerization tandem catalysis

4.3.3.2 Tensile properties

The tensile properties (Table 4.5) of the polymers were measured and were found to be almost identical when comparing polymers with the same molecular weight and chemical composition distributions.

Table 4.5: Tensile properties of tandem and conventional copolymers

Sample	Tensile Modulus Mpa	Yield Strength Mpa	Elongation at break %
Polymer 1	204	89	489
Polymer 2	202	89	504
Polymer 3	209	94	461
Polymer 4	131	71	452
Polymer 5	200	86	494

The tandem copolymers, Polymers 1 and 2, and the copolymer obtained by adding 1-hexene during the reaction, Polymer 5, have modulus and yield values in the range of the two conventional copolymers, Polymers 3 and 4, consistent with their comonomer distributions. Polymer 4 with the highest comonomer content displays the lowest modulus because of its lower crystallinity.

4.3.3.3 Addition of the polymerization catalyst at a later stage

A copolymer with a higher comonomer as well as a more homogenous comonomer distribution was prepared by adding the polymerization catalyst $\text{EtIn}_2\text{ZrCl}_2$ after 30 minutes were allowed for the trimerization reaction. A substantial amount of 1-hexene was already formed when the copolymerization reaction started.

4.3.3.3.1 Reaction conditions

Oligomerization reactions were conducted with $\text{Cr}(\text{acac})_3$ (3×10^{-6} mol), $(o\text{-OMePh})_2\text{PN}(\text{CH}_3)\text{P}(o\text{-OMePh})_2$ (3.3×10^{-6} mol) and MAO (1.65×10^{-3} mol) in a 1 L Buchi reactor at 100 °C with 300 mL solvent (C_7/C_8 paraffin). The ethylene pressure was 30 bar. $\text{EtIn}_2\text{ZrCl}_2$ (4×10^{-8} mol) was added after 30 minutes with high pressure nitrogen. The reaction was conducted for a further 15 minutes to yield copolymers, Polymer 6 and Polymer 7. Polymer 8, was obtained using $\text{EtIn}_2\text{ZrCl}_2$ (4×10^{-8} mol) and MAO (1.1 mmol). 1-Hexene (120 g) was added at the start of the reaction.

4. Trimerization tandem catalysis

4.3.3.3.2 Results

A substantial amount of 1-hexene was already formed when the copolymerization reaction started which resulted in a more homogeneous distribution of the comonomer. Figure 4.7 compares the CRYSTAF traces of the copolymers, Polymers 6 and 7, with that of a conventional copolymer, Polymer 8.

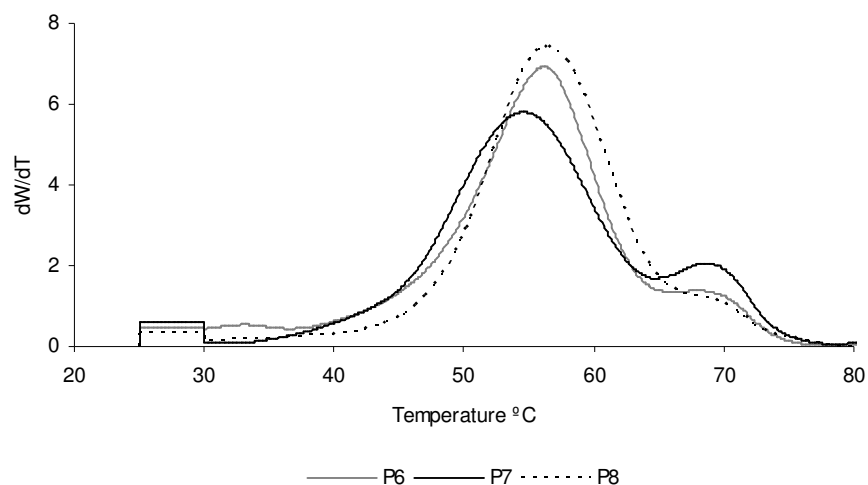


Figure 4.7: CRYSTAF traces of tandem copolymers with delayed addition of the polymerization catalyst and a conventional copolymer

Copolymers with much lower crystallinity were obtained due to the higher concentration of 1-hexene present at the stage when the polymerization catalyst is added to the reactor. The GPC data is displayed in Table 4.6. The CRYSTAF traces and GPC analyses of tandem copolymers, Polymers 6 and 7, are comparable to that of a 1-hexene copolymer, Polymer 8, which was prepared by addition of the 1-hexene at the start of the reaction.

Table 4.6: Molecular weight data of copolymers

Polymer	$\langle M_n \rangle$	$\langle M_w \rangle$	M_p	PI
Polymer 6	60	131	113	2.2
Polymer 7	62	123	108	2.0
Polymer 8	63	139	116	2.2

No major differences in polymer characteristics are observed when copolymerizing *in situ* produced 1-hexene and ethylene in the presence of $(o\text{-OMePh})_2\text{PN}(\text{CH}_3)\text{P}(o\text{-OMePh})_2$.

4. Trimerization tandem catalysis

OMePh)₂ relative to a conventional copolymerization. The peculiar shoulder at 70 °C present in the CRYSTAF traces (Figure 4.7) of both the tandem and conventional copolymers may be ascribed to catalyst decomposition towards the end of the reaction.

In summary, the results show that the differences observed in 1-hexene copolymers obtained from tandem catalysis compared to that of copolymers prepared by the addition of 1-hexene are basically a result of the varying comonomer content during the course of the reaction.

These results are in accordance with that obtained in a previous tandem study using the trimerization catalyst, bis(2-dodecylsulfanyl-ethyl)amine (SNS)/CrCl₃, where broad DSC curves were observed. Additionally, the current study shows the effect on the chemical composition distributions as determined by CRYSTAF analyses. A more complete comparison with conventionally prepared copolymers was made in this study to illustrate the differences in chemical composition distribution obtained with the tandem catalyst system.

4.4 Wax formation with the trimerization catalyst, (*o*-EtC₆H₄)₂PN(CH₃)P(*o*-EtC₆H₄)₂/CrCl₃/MAO, at high temperatures

The trimerization catalyst, (*o*-EtC₆H₄)₂PN(CH₃)P(*o*-EtC₆H₄)₂/CrCl₃/MAO, produce low molecular weight polyethylene at temperatures above 60 °C which makes it unsuitable for use in tandem reactions to produce LLDPE, but the wax-like product remains of interest. The effect of reaction conditions, MAO and hydrogen concentration, on the type of material produced was subsequently investigated.

4.4.1 The effect of MAO concentration

Reactions were performed at different Cr(acac)₃:MAO ratios to investigate the effect of the cocatalyst levels on the amount and the type of material synthesized. It is well known that the MAO to Cr(acac)₃ ratio impacts on the molecular weight of polymers produced with homogeneous transition metal catalysts, with higher MAO

4. Trimerization tandem catalysis

loadings yielding lower molecular weight polyethylene due to chain transfer to aluminum.⁶

4.4.1.1 Reaction conditions

The reactions were performed in a 5L Buchi reactor using $\text{Cr}(\text{acac})_3$ (1.5 mmol) and $(o\text{-EtC}_6\text{H}_4)_2\text{PN}(\text{CH}_3)\text{P}(o\text{-EtC}_6\text{H}_4)_2$ (1.7 mmol) in a C_7/C_8 paraffin solvent (1200 g). Hydrogen (300 mg) was added to all the reactions. The reactor pressure was 30 bar. The catalyst concentration was fixed in all experiments while the MAO concentration was varied according to the ratios in Table 4.7.

4.4.1.2 Results

Significant differences were observed in the properties of the material prepared at the different MAO concentrations. Table 4.7 summarizes the yields and characteristics of the waxes obtained in these experiments.

Table 4.7: Effect of MAO concentration on wax yield and characteristics

$\text{Cr}(\text{acac})_3:\text{MAO}$	Yield g	Crystallization onset °C	Δh_c J.g ⁻¹	Viscosity (135°C) cP
1:70	90	110	240	380
1:140	250	105	200	210
1:210	210	104	220	160
1:280	220	104	210	140
1:420	220	103	230	140
1:550	230	103	220	130

The results in Table 4.7 show a minimum yield at the lowest MAO concentration. The yield increases when the MAO is doubled, but with a further increase in the MAO amount the yield stays relatively constant. The viscosity (used as a measure of the molecular weight) is the highest at the low MAO concentration and decreases upto a ratio of 1:210, hereafter the viscosity is not affected to a large extent by the $\text{Cr}(\text{acac})_3:\text{MAO}$ ratio. The crystallization behaviour is also influenced by the changing $\text{Cr}(\text{acac})_3:\text{MAO}$ ratio, but only at low MAO concentrations. The onset of crystallization shift to lower temperature when the MAO is increased. The effect of the changing MAO concentrations is more noticeable in the melting curves. The

4. Trimerization tandem catalysis

DSC curves in Figure 4.8 illustrate the change in the melting behaviour of the waxes at different cocatalyst concentrations.

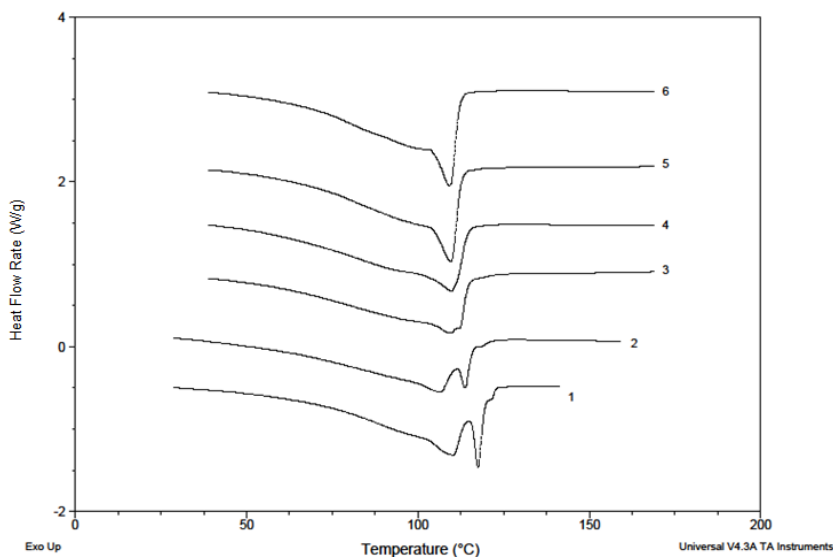


Figure 4.8: DSC curves of waxes prepared using different MAO ratios (*Curve 1* $\text{Cr}(\text{acac})_3$:MAO 1:70, *Curve 2* 1:140, *Curve 3* 1:210, *Curve 4* 1:280, *Curve 5* 1:420 and *Curve 6* 1:550)

The DSC melting curves show clearly a distinct higher melting fraction when the $\text{Cr}(\text{acac})_3$:MAO ratio is less than 1:280 (Curves 1, 2 and 3). At ratios of 1:280 and higher (Curves 4, 5 and 6) a single melting peak is observed. The observation of the second higher melting fraction at lower $\text{Cr}(\text{acac})_3$:MAO ratios, corresponds with the higher viscosity observed at these lower MAO concentrations. It is thus expected that this fraction is of higher molecular weight.

4.4.2 The effect of hydrogen concentration

Chain transfer agents, e.g. hydrogen, are used to lower the molecular weight of polyethylene waxes in order to control their viscosities for different applications. The effect of an increased hydrogen concentration was investigated in subsequent reactions. A constant MAO ratio of 1:280 maintained in the reactions.

4.4.2.1 Reaction conditions

The hydrogen concentration was varied at a fixed $\text{Cr}(\text{acac})_3$:MAO ratio (1:280). The reactions were performed in a 5L Buchi reactor using $\text{Cr}(\text{acac})_3$ (1.5 mmol) and (*o*-

4. Trimerization tandem catalysis

$\text{EtC}_6\text{H}_4)_2\text{PN}(\text{CH}_3)\text{P}(\text{o-EtC}_6\text{H}_4)_2$ (1.7 mmol) in a C_7/C_8 paraffin solvent (1200 g). The hydrogen concentration was varied according to the values displayed in Table 4.8.

4.4.2.2 Results

The effect of hydrogen concentration on the wax formation and product properties is displayed in Table 4.8. The changing hydrogen concentration affects the yield and the properties of the waxes.

Table 4.8: Effect of H_2 on the wax yield and properties

H_2 mg	Yield g	Crystallization onset °C	Δh_c J.g ⁻¹	Viscosity (135°C) cP
0	170	104	220	288
300	240	104	230	195
800	220	104	210	140
1300	230	103	215	110
1500	210	101	165	84
2200	100	100	188	49

The yield increases with hydrogen addition up to 300 mg, thereafter it stays more or less constant before it decreases sharply at the highest hydrogen concentration. Increases and decreases in catalyst activity caused by the presence of hydrogen are described in the literature.⁷ The increase in wax yield can be ascribed to a faster regeneration of the active catalytic site on the metal-hydride, after chain elimination. The decrease in activity at the highest hydrogen amount is probably due to the low ethylene partial pressure in the reactor, or blocking of the active sites by hydrogen.⁷

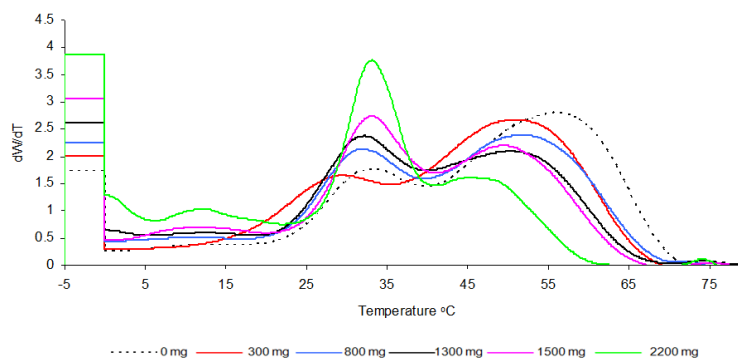
The viscosity decreases dramatically with the increased hydrogen concentration, but it seems that the crystallinity (approximated by the heat of crystallization, Δh_c) might be influenced negatively. The molecular weight data obtained from GPC analyses of selected waxes are displayed in Table 4.9. The molecular weight decreases with an increasing amount of hydrogen and the polydispersity index (PI) becomes narrower at the higher hydrogen concentration.

4. Trimerization tandem catalysis

Table 4.9: Molecular weight data of waxes synthesized at varying H₂ concentrations

H ₂ mg	M _p	<M _n >	<M _w >	PI	Viscosity (135°C) cP
1300	2233	1 295	2 252	1.74	110
1500	1911	1 526	2 234	1.46	84
2200	1475	1 119	1 570	1.40	49

CRYSTAF traces are displayed in Figure 4.9 to show the chemical composition distributions in the waxes. This technique is more informative than DSC to investigate structural differences in the waxes. It differentiates between fractions with different microstructures present in the wax, because co-crystallization between fractions is minimized when the waxes are crystallized from dilute solutions.⁸ In the case of high molecular weight polyethylene this solution crystallization profile is mainly influenced by branching, but the crystallization of low molecular weight material is influenced by both branching and molecular weight.⁹

**Figure 4.9:** Comparison of CRYSTAF traces at changing hydrogen concentrations

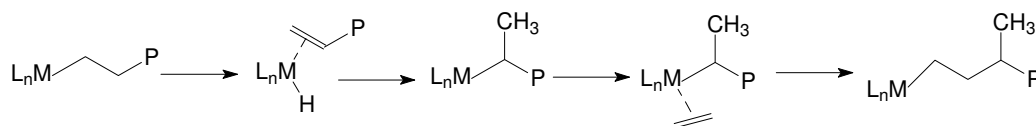
All the waxes display a bimodal CRYSTAF trace. The amount of soluble material at the end of the analyses increases with an increasing hydrogen concentration. The onset of crystallization is the lowest for the highest hydrogen amount while the relative amounts of the fractions crystallizing around 35°C and 55°C also follow a trend. The amount of material which crystallizes around 55°C decreases, while the fraction crystallizing around 35°C increases with an increasing amount of hydrogen.

An increase in hydrogen concentration was successful in lowering the molecular weight and thus the viscosity, but the observed decrease in crystallisability of the wax will affect application-based properties, i.e. hardness, negatively.

4. Trimerization tandem catalysis

^{13}C NMR analysis of the fraction extracted from such a wax confirms that the structure of the poorly crystallisable material is highly branched. Methyl branches (~4 mol%) are detected in the extracted fraction and very prominent end groups, verifying the low molecular weight of this fraction, are observed. The remaining wax contains 1.5 mol% methyl branches in comparison to the 2.5 mol% methyl branches in the bulk wax. Traces of ethyl branches are present.

The methyl branching in the waxes can occur due to a chain isomerisation or a chain walking mechanism.¹⁰ Methyl branches are observed in ethylene homopolymerization reactions using heterogeneous chromium catalysts. Mechanistic studies indicate the presence of chromium bonded to a secondary carbon atom within the polymer chain.¹⁰ A hydrogen atom is transferred from the α -carbon to the β -carbon through an olefin-chromium-hydride intermediate. Propagation from the isomerized site gives a methyl branch. Ethyl branches can be explained by repeated isomerization. Similarly, a chain walking mechanism is commonly observed in polyethylene prepared using late transition metal complexes. Scheme 4.2 illustrates such a mechanism to generate a methyl branch.¹⁰



Scheme 4.2: Proposed mechanism for methyl branching

Several catalyst conformations can exist in solution due to rotation of the phenyl groups of the coordination complex and this can probably explain the broad chemical composition distribution observed in these waxes under specific reaction conditions.¹¹ (The fluxional behaviour of the catalyst could not be confirmed by NMR spectroscopy due to the paramagnetic nature of the chromium centre.) Certain conformations may result in the formation of catalytic sites more prone to chain isomerization, enhancing the formation of methyl branches and thus the observed poorly crystallisable fraction. Further ligand development to design more rigid coordination complexes may help to establish if such a mechanism is operating.

4.5 Conclusions

The preceding results confirm that the PNP-type of ligands reduce the activity of the polymerization catalyst significantly during ethylene polymerization reactions,

4. Trimerization tandem catalysis

although a change in the ligand substituents does not have a marked effect. It seems likely that the trimerization catalyst interferes chemically with the polymerization catalyst.

The tandem copolymerization reactions performed using the chromium/(*o*-OMeC₆H₄)₂PN(CH₃)P(*o*-OMeC₆H₄)₂ trimerization system illustrate the effect of increasing reaction time on the chemical composition distribution because of the increasing amount of 1-hexene produced. A tail of higher comonomer content material is present with an increase in reaction time, due to 1-hexene accumulating in the reactor.

Comparison of CRYSTAF traces of tandem copolymers with conventional copolymers shows that the tandem copolymers have a broader chemical composition distribution. Addition of 1-hexene during the course of a conventional copolymerization reaction produces copolymers with similar chemical composition distributions to that of the tandem copolymers. Later addition of the polymerization catalyst to the oligomerization reaction produces copolymers with higher comonomer content, similar to conventional copolymers.

The wax forming nature of the temperature switchable catalyst, chromium/(*o*-EtC₆H₄)₂PN(CH₃)P(*o*-EtC₆H₄)₂, was investigated at different MAO and hydrogen concentrations. The dependence of viscosity, crystallization behaviour and wax yields on these variables was determined: low MAO concentrations resulted in multiple melting peaks, while higher concentrations display single melting peaks and lower viscosity values. The wax yields increase upto a chromium:MAO ratio of 1:140, whereafter an increase in the ratio does not increase the wax yield. An increase in poorly crystallisable material is apparent from CRYSTAF at high hydrogen concentrations and NMR data indicate increased methyl branching which points to a chain isomerisation mechanism. An increase in the fluxional behaviour of the catalyst conformation at certain reaction conditions is postulated, which could be responsible for the different microstructures obtained.

4.6 References

1. De Wet-Roos, D., Dixon, J. T., *Macromolecules*, 2004, 37, 9314; Ye, Z., Al'Obaidi, F., Zhu, S., Subramanian, R., *Macromolecular Chemistry and Physics*, 2005, 206, 2096; Ye, Z., Al'Obaidi, F., Zhu, S., Subramanian, R., *Macromolecular Rapid Communications*, 2004, 25, 647
2. Cartern A., Cohen, S. A., Cooley, N. A., Murphy, A., Scutt, J., Wass, D. F., *Chemical Communications*, 2002, 858
3. Blann, K., Bollmann, A., Dixon, J. T., Hess, F. M., Killian, E., Maumela, H., Morgan, D.H., Neveling, A., Otto, S., Overett, M. J., Sasol Technology, WO 2004/056477, 2004; Blann, K., De Wet-Roos, D., Du Toit, A., Joubert, D. J., Phelembe, N. J., Sasol Technology, US 2006/0020091, 2006
4. De Pooter, M., Smith, P. B., Dohrer, K. K., Bennett, K. F., Meadows, M. D., Smith, C. G., Schouwenaars, H. P., Geerards, R. A., *Journal of Applied Polymer Science*, 1991, 42, 399; Liu, W., Rinaldi, P. L., *Macromolecules*, 2001, 34, 4757
5. Camurati, I., Cavicchi, B., Dall'Occo, T., Piemotesi, F., *Macromolecular Chemistry and Physics*, 2002, 202, 701
6. Sarzotti, D. M., Marshman, D. J., Ripmeester, W. E., Soares, J. B. P., *Journal of Polymer Science, Part A: Polymer Chemistry*, 2007, 45, 1677; Chu, K., Soares, J. B. P., Penlidis, A., *Journal of Polymer Science, Part A: Polymer Chemistry*, 2000, 38, 1803
7. Koppl, A., Alt, H. G., *Chemical Reviews*, 2000, 100, 1205; Kou, B., McAuley, K. B., Hsu, C. C., Bacon, D. W., Yoa, K. Z., *Industrial Engineering and Chemical Research*, 2005, 44, 2443; Shaffer, W. K. A., Ray, W. H., *Journal of Applied Polymer Science*, 1997, 65, 1053; Koppl, A., Alt, H. G., *Journal of Molecular Catalysis, A: Chemistry*, 2001, 165, 23
8. Soares, J. B. P., Anantawaraskul, S., *Journal of Polymer Science, Part B: Polymer Physics*, 2005, 43, 1557; Simon, L. C., De Souza, R. F., Soares J. B. P., Mauler, R. S., *Polymer*, 42, 4885

4. Trimerization tandem catalysis

9. Anantawaraskul, S., Soares, J. B. P., Wood-Adams, P. M., Monrabal, B., *Polymer*, 2003, 44, 2393
10. Blom, R., Dahl, I. M., Swang, O., *Journal of Catalysis.*, 2000, 194, 352;
Johnson, L. K., Killian, C. M., Brookhart, M., *Journal of the American Chemical Society*, 1995, 117, 6414
11. Talja, M., Polamo, M., Leskel, M., *Journal of Molecular Catalysis, A: Chemistry*, 2008, 280, 102

5 Tandem ethylene-styrene co-oligomerization-copolymerization

5.1 Introduction

The use of the bis(diphenylphosphino)amine (PNP) type of ligands in combination with chromium(III) to cotrimerize ethylene and styrene has recently been reported by Bowen and Wass (see Chapter 2, Section 2.4).¹ Results from this study show that cotrimerization is possible with the ligand (*o*-OMeC₆H₄)₂PN(CH₃)P(*o*-OMeC₆H₄)₂. 1-Phenyl-1-hexene and 6-phenyl-1-hexene, were obtained as the main products. Some of these co-oligomerization products are potential comonomers for copolymerization with ethylene.

Pellecchia *et al.*² have described a procedure for the selective co-oligomerization of ethylene and styrene based on a half metallocene titanium catalyst. A new copolymer with 4-phenyl-1-butyl branches has been identified as a side product. Further *in situ* copolymerization reactions have also been described where a polymerization catalyst is added to copolymerize the co-oligomerization products, resulting in the 4-phenyl-1-butyl branched polyethylene in higher yields. These copolymers may find application in the functionalization of polyolefins when *p*-methylstyrene is co-oligomerized and the products employed as comonomers.³ *p*-Methylstyrene can be functionalized after the polymerization reaction at the activated methyl group.

Various co-oligomerization routes are possible which can result in any of the isomers described in Scheme 2.5, Chapter 2. The PNP-type ligand structure can direct styrene coordination to the catalytic centre in different manners and affect the selectivity of the reaction. The first aim of this study was to establish the influence of the ligand structure on the selectivity of the co-oligomerization products. In addition, tandem copolymerization of the co-oligomerization product mixture with a metallocene was to be investigated. A further goal was to characterize the resulting copolymers with ¹³C NMR to determine their microstructures. The extent to which the co-oligomerization products are incorporated into the ethylene copolymers during

5. Tandem ethylene-styrene co-oligomerization-copolymerization

tandem catalysis was to be determined. A styrene ethylene copolymerization reaction will serve as a reference to the co-oligomerization/copolymerization reactions.

5.2 Experimental

5.2.1 Materials

Rac-ethylenebis(indenyl)zirconiumdichloride ($\text{EtIn}_2\text{ZrCl}_2$) was obtained from Boulder Scientific, $\text{Cr}(\text{acac})_3$ from Aldrich, MAO from Crompton and the bis(diphenylphosphino)amine (PNP) type ligands from Cytec or Sasol Technology Organic Synthesis Group. All reagents were used as received. Pure ethylene was obtained from Afrox. Methylcyclohexane (Aldrich) was used as solvent and was purified by passing it through an aluminum oxide column and was stored on molecular sieves (4 Å). *p*-Methylstyrene (96 %) and styrene (≥ 99 %) were obtained from Sigma-Aldrich and were purified by passing it through an aluminum oxide column under nitrogen.

5.2.2 Co-oligomerization and polymerization procedures

Reactions were conducted under inert conditions in a 1L Parr reactor equipped with mechanical stirring and temperature control. Solvent, styrene and 50 % of the MAO were first added to the reactor followed by the MAO activated catalysts. Solutions of the catalysts were prepared under nitrogen atmosphere in a glove box using dry methylcyclohexane or toluene as solvent. Chromium/PNP-type catalysts were activated with 50 % of the MAO before transferring it to the reactor by syringe. Reactions were initiated by starting the ethylene flow to the reactor. Reactor pressures of 30 bar were used unless otherwise stated. Reactions were terminated by venting the ethylene. The polymers were washed with acetone and dried under vacuum at 60 °C for 12 h.

5.2.3 Quantitative ^{13}C NMR analysis

The polymer (60 mg) was dissolved in 0.6 mL deuterated 1,1,2,2-tetrachloroethane (6 wt%) stabilized with 2,6,-di-*tert*-butyl-4-methylphenol. The sample was placed in a ventilated oven to homogenize at 130 °C for approximately 2 hours. Quantitative ^{13}C NMR experiments were performed at 150 MHz on a 5 mm PFG switchable/broadband probe (^1H - ^{19}F , ^{15}N - ^{31}P) on a Varian ^{UNITY}INOVA 600 MHz spectrometer at 120 °C. 90° pulse widths of approximately 6 μs and delay times

5. Tandem ethylene-styrene co-oligomerization-copolymerization

between pulses of 15 s were used with an acquisition time of 1.8 s. The number of scans was set to 5040, but a signal-to-noise parameter was set to 2000. Therefore either 5040 scans were acquired or the acquisition was stopped after the required signal-to-noise was reached. Consequently the analysis time ranged from 3 -10 hours.

Chemical shifts were referenced internally to the main backbone methylene carbon resonance (30 ppm). Chemical shifts from the literature were used for identification of peaks resulting from styrene, 1-hexene and 1-octene incorporation.⁴ Peaks resulting from the incorporation of the ethylene-styrene co-oligomerization products were identified by calculating the chemical shifts according to the Grant and Paul⁵ additivity rules as described in the text.

5.2.4 GC analysis

GC-FID and GC-MS analysis of the liquid product were performed using a CP Sil PONA column (100 m x 250 μm x 0.50 μm) with hydrogen as carrier gas at a flow rate of 5 mL.min⁻¹. The oven temperature program comprised a 5 minutes isothermal step at 35 °C followed by a ramp to 260 °C at a rate of 5°C.min⁻¹. The co-oligomerization selectivity and styrene conversion were estimated from the GC data.

5.2.5 Hydrogenation of co-oligomerization reaction mixture

The co-oligomerization reaction mixtures were hydrogenated in order to help with the identification of the products. The hydrogenation was done using a Pt/C (0.5 %) hydrogenation catalyst in the presence of hydrogen.

5.2.6 CRYSTAF analysis

CRYSTAF analyses were performed on a Polymer Char combination CRYSTAF-TREF apparatus fitted with an IR detector using 1,2,4-trichlorobenzene as solvent. Samples (20 mg) were first dissolved in 30 mL solvent at 160 °C after which the temperature was decrease to 100 °C and stabilized for 30 minutes. The temperature was then decreased from 100 °C to 30 °C at a controlled rate of 0.2 °C.min⁻¹ while the change in polymer concentration was recorded.

5.2.7 Thermal analysis

Differential Scanning Calorimetry (DSC) analyses were performed on a TA Q200 instrument. The instrument was calibrated using indium as standard. Samples were first melted at 180 °C to remove the thermal history followed by crystallization and melting at 10 °C.min⁻¹. Melting temperatures obtained from the latter heating run are reported.

5.2.8 High Temperature GPC analysis

High temperature GPC analyses were conducted on a PL-GPC 220 high-temperature chromatograph equipped with a differential refractive index detector and four PL gel MIXED-B columns (Polymer Laboratories). The concentration of the samples was 2 mg.mL⁻¹ in 1,2,4-trichlorobenzene, stabilized with 0.0125 % 2,6-di-*tert*-butyl-4-methylphenol. A flow rate of 1 mL.min⁻¹ and temperature of 140 °C were maintained for all experiments. The molecular weight calibration was done with monodisperse polystyrene standards (EasiCal from Polymer Laboratories).

5.3 Results and discussion

5.3.1 Co-oligomerization

5.3.1.1 The effect of ethylene pressure and styrene concentration on ethylene-styrene co-oligomerization

Results from Bowen and Wass¹ showed that cotrimerization with up to 96 % selectivity to the cotrimer products (4% homotrimerization products) at 1 bar ethylene pressure is possible with the ligand (*o*-OMeC₄H₆)₂PN(CH₃)P(*o*-OMeC₄H₆)₂ in combination with CrCl₃(THF)₃, but the activity was low (8000 g.(g_{Cr})⁻¹). In an initial co-oligomerization investigation the work reported by Bowen Wass was repeated using the same ligand *in situ* with Cr(acac)₃ at 1 bar ethylene pressure (Table 5.1). Additionally, the effects of a higher ethylene pressure and styrene concentration were investigated.

5.3.1.1.1 Reaction conditions

Reactions were performed in a 1 L Parr reactor at 50 °C in methylcyclohexane (200 mL). Cr(acac)₃ (3.5x10⁻⁵ mol), (*o*-OMeC₄H₆)₂PN(CH₃)P(*o*-OMeC₄H₆)₂ (4.2x10⁻⁵ mol)

5. Tandem ethylene-styrene co-oligomerization-copolymerization

and MAO (21×10^{-3} mol) were used. Reaction time was 30 minutes. The ethylene pressures and styrene concentrations used in the experiments are displayed in Table 5.1.

5.3.1.1.2 Results

The results indicating the effects of the changing parameters, ethylene pressure and styrene concentration, are displayed in Table 5.1. The concentration of the monomers influences both the activity and selectivity of the reactions.

Table 5.1: Effect of ethylene pressure and styrene concentration on ethylene-styrene co-oligomerization

Styrene mol.dm ⁻³	Ethylene bar	Activity g.(g _C ,h) ⁻¹	Co-oligo %	1-Hexene %
2.3	1	2 930	84	16
2.3	30	39 775	36	64
0.3	30	113 625	6	94
5.6	30	13 426	56	44

The productivity of the reaction increases at higher ethylene pressure. The productivity decreases with an increase in the styrene concentration. Selectivity to 1-hexene increases when the ethylene pressure was increased to 30 bar, but decreases when the styrene concentration is increased at this pressure.

5.3.1.2 The effect of ligand structure on co-oligomerization

The effect of different PNP-type ligand structures on the activity and selectivity of ethylene-styrene co-oligomerization reactions was explored. Structures and numbering of the PNP-type ligands used in the screening reactions are given in Figure 5.1.

5. Tandem ethylene-styrene co-oligomerization-copolymerization

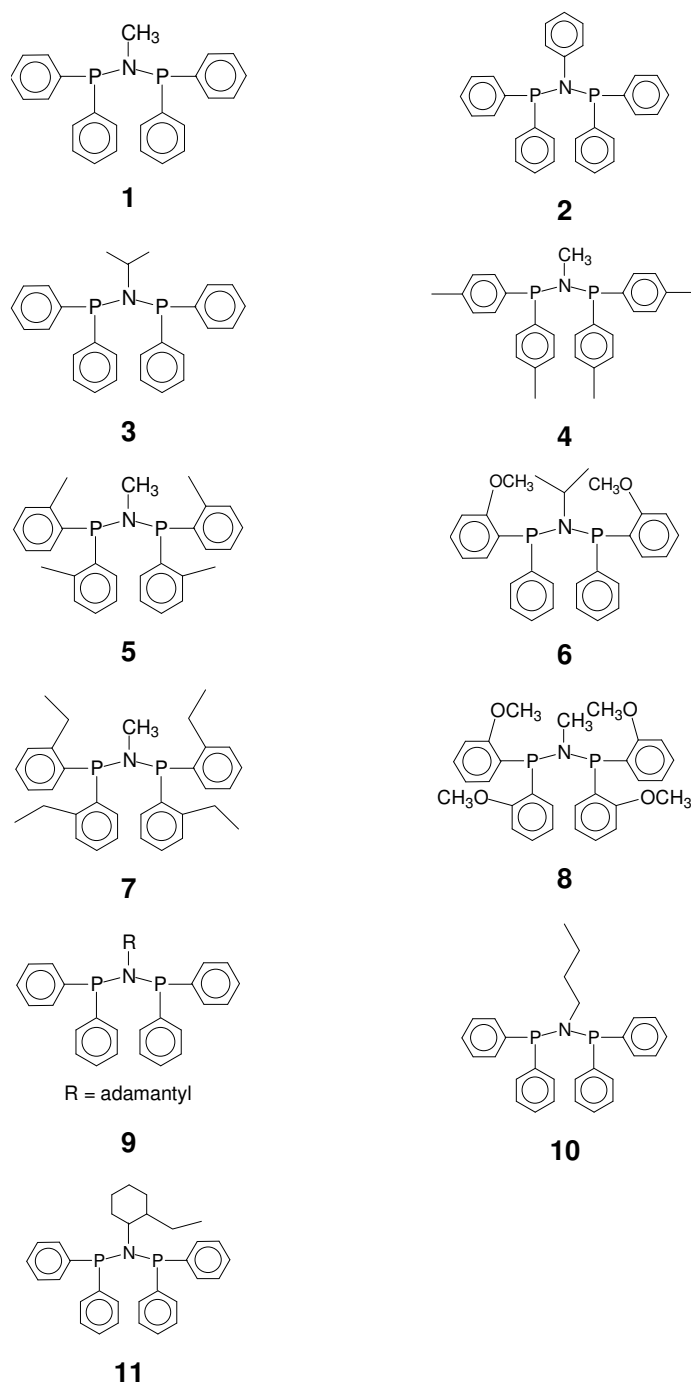


Figure 5.1: PNP-type ligands employed in ethylene-styrene co-oligomerization screening experiments

5. Tandem ethylene-styrene co-oligomerization-copolymerization

5.3.1.2.1 Reaction conditions

Reactions were performed in a 1 L Parr reactor at 50 °C in methylcyclohexane (200 mL). Cr(acac)₃ (3.5x10⁻⁵ mol), PNP-type ligand (4.2x10⁻⁵ mol) and MAO (21x10⁻³ mol) were used. The ethylene pressure was 30 bar and the styrene concentration 2.1 mol.L⁻¹.

5.3.1.2.2 Results

The styrene conversion and the selectivity to ethylene-styrene co-oligomerization products are displayed in Table 5.2. The ligand structure has a significant effect on the styrene conversion and product distribution. The results in Table 5.2 are arranged in order of decreasing selectivity to co-oligomerization.

Table 5.2: The effect of ligand on ethylene-styrene co-oligomerization

Ligand	Selectivity co-oligo %	Selectivity 1-hexene %	Selectivity 1-octene %	Styrene conversion %
1	96	1	3	94
4	96	1	3	83
2	94	1.5	4.5	44
10	93	1.5	5.5	90
3	77	7	25	74
9	60	8	32	60
11	53	9	38	32
6	51	45	4	71
5	42	39	19	27
8	36	64	0	26
7	2	95	3	6

From the results in Table 5.2 it is clear that ligand 7 favors ethylene homo-oligomerization. This might be due to the steric influence of the *ortho* substituent on the phenyl ring of this ligand. The low co-oligomerization selectivity (< 51%) displayed by ligands 5, 6 and 8 with *ortho* substituents, supports this observation. Ligand 1, without this *ortho* substituent favors co-oligomerization. Comparison of the co-oligomerization behaviour of ligands 1 and 4 indicates that the presence of *para* methyl substituents does not have any effect on the selectivity. Steric hinderance near the catalyst centre explains the lower selectivity to co-oligomerization products

5. Tandem ethylene-styrene co-oligomerization-copolymerization

when *ortho* substituents are present which block the coordination of the bulky styrene molecules. Similarly, could be important when the substituent on the nitrogen atom becoming increasingly bulky. The co-oligomerization selectivity decrease to below 90 % when isopropyl (ligand 3), adamantyl (ligand 9) or 2-ethyl-cyclohexyl (ligand 11) groups are present on the nitrogen atom. Ligand 1 with a methyl group on the nitrogen atom, results in the highest co-oligomerization selectivity (96 %) and styrene conversion (94 %).

5.3.1.3 Selectivity in the co-oligomerization fraction

The product distribution in the co-oligomerization fractions was determined by GC-FID. A typical gas chromatogram in Figure 5.2 shows the distribution of the ethylene-styrene co-oligomerization products obtained when using ligand 3. Five main components are present, while several byproducts are also detected.

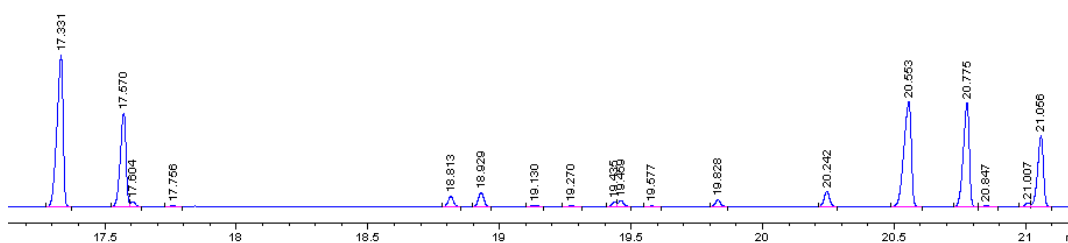


Figure 5.2: A typical gas chromatogram showing the distribution of co-oligomerization products (ligand 3) in the ethylene-styrene co-oligomerization reaction

The main co-oligomerization products were identified from the literature¹ and by interpretation of their mass spectra. The results were also confirmed by hydrogenation of the reaction mixture and identification of the resulting products by mass spectroscopy.

Several product peaks in the product distribution resulting from co-oligomerization while using ligand 8 at 1 bar ethylene pressure, could be identified when it was compared with the distribution described by Bowen and Wass at similar reaction conditions (Table 5.1).¹ These were the cotrimerization products: 1-phenyl-1-hexene, 3-phenyl-1-hexene, 4-phenyl-1-hexene and 6-phenyl-1-hexene. Additionally, cotetramerization products were observed in the GC-MS analysis of ligand 3 with the molecular ion at 188 g.mol⁻¹. Table 5.3 displays a summary of the GC-MS analysis.

5. Tandem ethylene-styrene co-oligomerization-copolymerization

Table 5.3: Identification of peaks from GC-MS analysis for the co-oligomerization products (ligand 3)

Retention time min	Molecular ion	Main fragments	Assignment
17.33	160	91, 119	4-phenyl-1-hexene
17.57	160	91, 117	3-phenyl-1-hexene
17.76	160	91	unknown x1
18.81	160	91, 104, 117	6-phenyl-1-hexene
18.93	160	91, 104, 117	unknown x2
19.27	160	91	unknown x3
19.43	160	91	unknown x4
19.45	160	91, 104, 117, 131	unknown x5
19.83	158	80, 91, 104, 115, 129, 143	unknown x6 (diene)
20.24	160	91, 104, 117	1-phenyl-1-hexene
20.55	188	91, 147	4-phenyl-1-octene
20.76	188	91, 159	6-phenyl-1-octene
21.06	188	91, 117	3-phenyl-1-octene

Hydrogenation of the reaction mixture prepared using ligand 3, was executed using a Pt/C heterogenous catalyst. The main fractions present after the hydrogenation of the reaction mixture were 3-phenyl-hexane, 4-phenyl-octane and 3-phenyl-octane. This is consistent with the assignments of the main products: 3-phenyl-1-hexene and 4-phenyl-1-hexene result in 3-phenyl-hexane, 4-phenyl-1-octene results in 4-phenyl-1-octane (possibly also 5-phenyl-1-octene) and 3-phenyl-1-octene and 6-phenyl-1-octene yield 3-phenyl-octane after hydrogenation.

Results from the ligand screening reactions are displayed in Table 5.4 and show the effect of the ligand structure on the selectivity in the co-oligomer fraction.

5. Tandem ethylene-styrene co-oligomerization-copolymerization

Table 5.4: Selectivity in the co-oligomerization fraction (x = unknown)

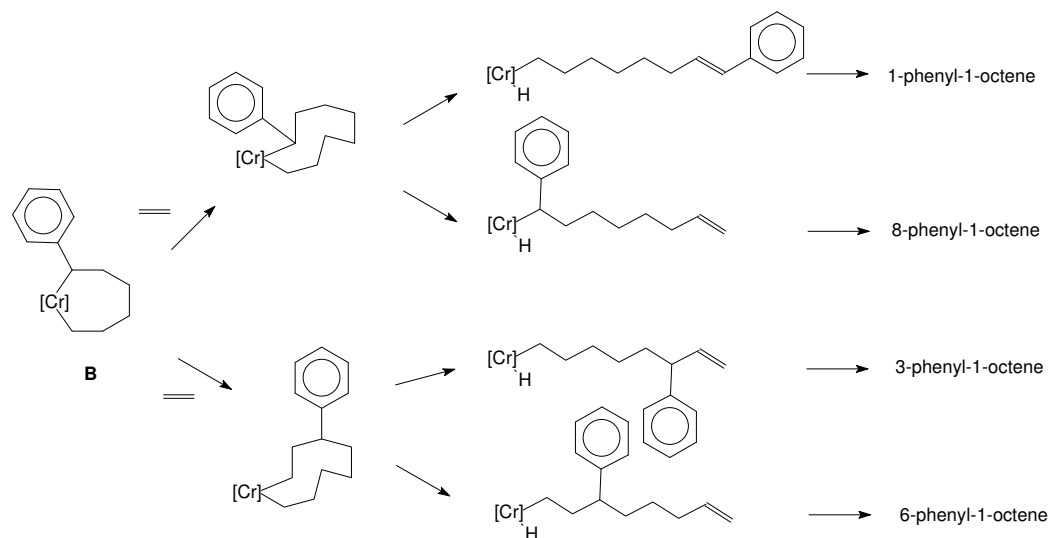
Ligand	1	2	3	4	5	6	7	8	9	10	11
product											
4-phenyl-1-hexene %	9	11	26	10	25	23	21	10	26	15	28
3-phenyl-1-hexene %	6	11	15	7	20	20	14	8	14	9	16
x1 %							9				
6-phenyl-1-hexene %		1	1		9	4	33	23	2	1	2
x2 %	9	5	2	8	3				3	6	1
1-phenyl-1-hexene %						5		10	1		1
x3 %	1	1		1		1				1	
x4 %	2	1	1	2	2				1	2	
x5 %	4	3	1	4		3				4	1
x6 %	6	3	1	5	2					4	1
1-phenyl-1-octene %		1	2		4	41	20	49	6	1	7
4-phenyl-1-octene %	30	29	22	31	17		4		20	28	17
6-phenyl-1-octene %	19	21	17	19	10				16	19	15
3-phenyl-1-octene %	12	13	11	12	7				10	12	9

Ligands 8 and 7, with methoxy or ethyl groups in the *ortho* position of the phenyl ring (Figure 5.1), are known ligands for ethylene trimerization while the ligands without bulky *ortho* substituents on the phenyl rings are known to have selectivity for both 1-octene and 1-hexene.⁶ It is evident from GC-MS analysis that this behaviour also holds true for co-oligomerization; cotrimerization is observed when ligands with bulky *ortho* substituents are employed, while cotrimer as well as cotetramer products are observed when ligands without bulky *ortho* substituents are used.

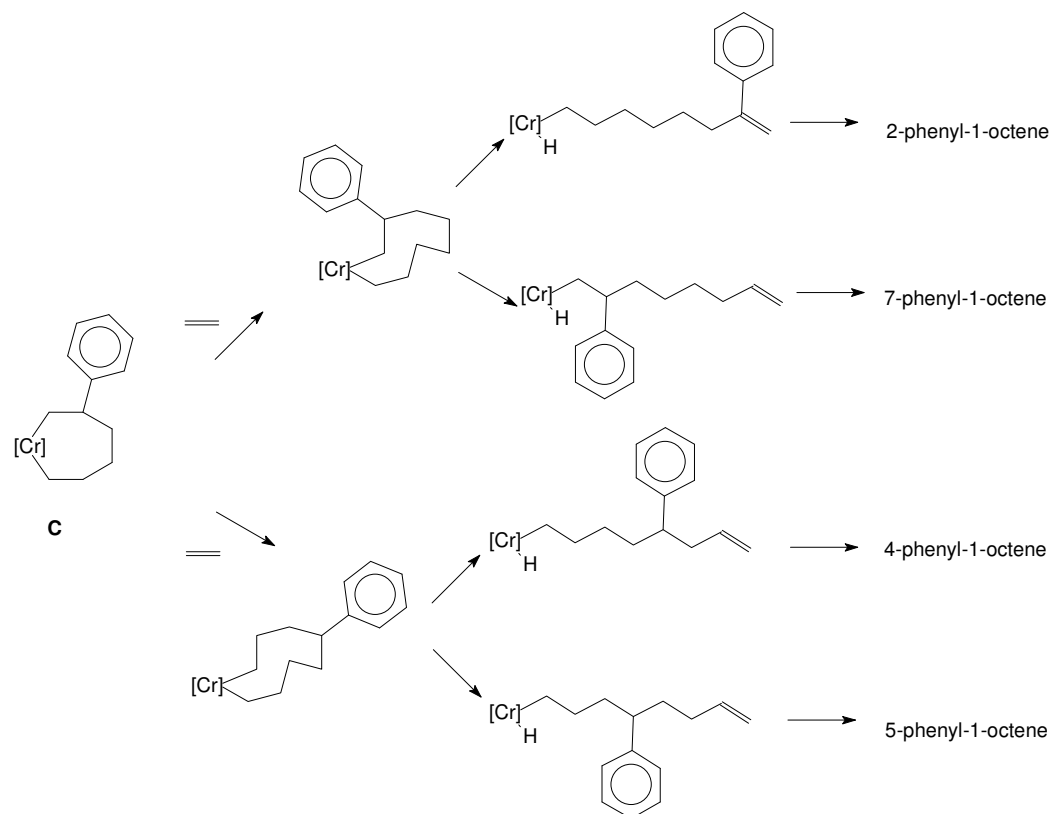
Based on this observation it is expected that a mechanism similar to that occurring in ethylene tetramerization is again valid for ethylene-styrene cotetramerization reactions. Cotrimerization is believed to occur via the metallacyclic mechanism described in Chapter 2, Scheme 2.5. Ethylene tetramerization involves the incorporation of a further ethylene into the metallacycloheptane intermediate to yield a metallacyclononane.⁷ Scheme 5.1 illustrates the proposed routes to explaining the

5. Tandem ethylene-styrene co-oligomerization-copolymerization

formation of the different phenyl-1-octene isomers obtained during ethylene-styrene cotetramerization based on such metallacyclic intermediates.



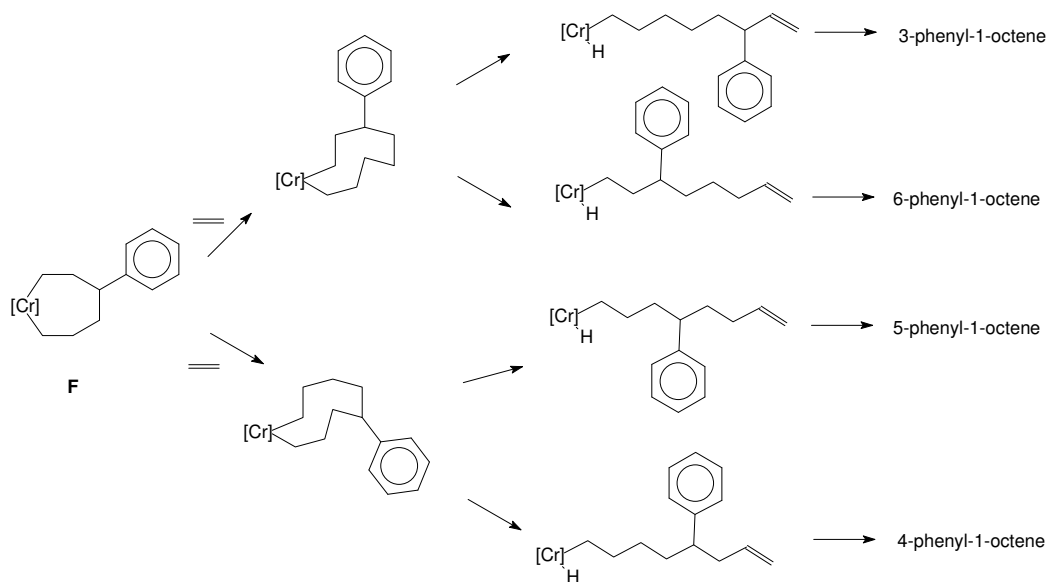
Route 1



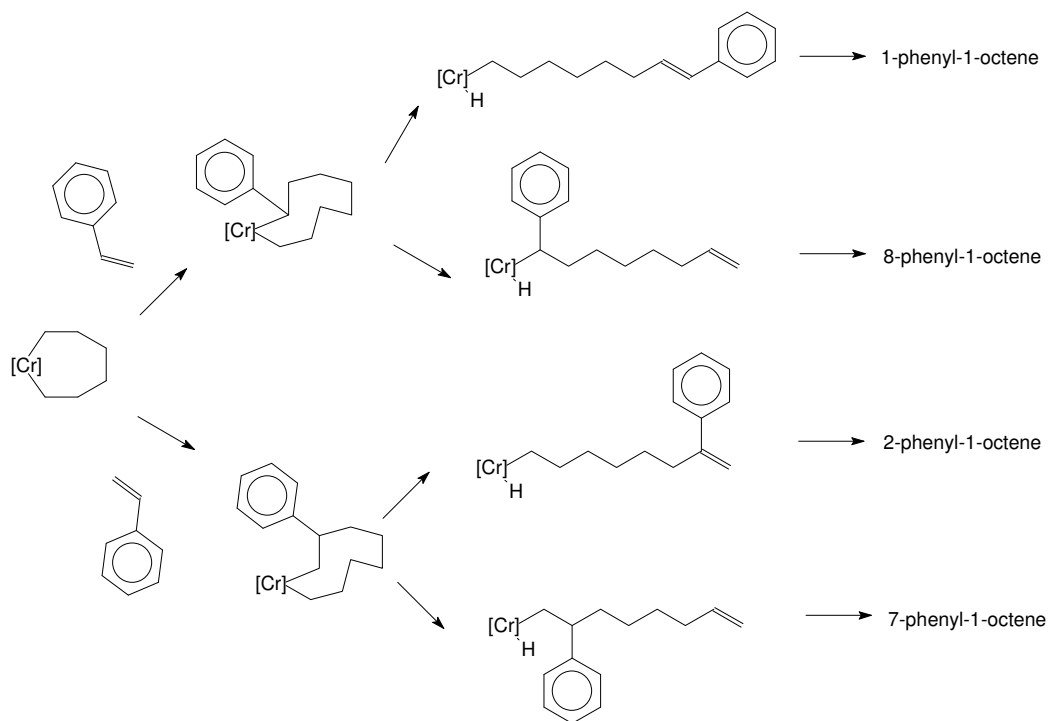
Route 2

Scheme 5.1: Possible routes to ethylene-styrene cotetramerization products (continued on next page)

5. Tandem ethylene-styrene co-oligomerization-copolymerization



Route 3



Route 4

Scheme 5.1: Possible routes to ethylene-styrene cotetramerization products (continued from previous page)

5. Tandem ethylene-styrene co-oligomerization-copolymerization

Four metallacycloheptane intermediates are possible. The routes to intermediates B, C and F were described in Chapter 2, Scheme 2.5 and involve the coordination of the monomers (ethylene/ethylene or ethylene/styrene) at the catalyst centre to form a five membered metallocycle. Coordination and insertion of another monomer (ethylene or styrene) result in the metallacycloheptane intermediates. These seven-membered metallacyclic intermediates each contains one styrene unit. An additional metallacycloheptane intermediate, composed of only ethylene monomers, is also possible (Route 4, Scheme 5.1). Insertion of a styrene molecule into this intermediate, in either 1,2- or 2,1-fashion leads to the formation of a metallacyclononane which after elimination yields 1-phenyl-1-octene, 2-phenyl-1-octene, 7-phenyl-1-octene or 8-phenyl-1-octene. Similarly, the formation of cotetramer isomers can be explained via Routes 1 to 3 and involve ethylene insertion into intermediates B, C, and F. The insertion of the ethylene molecule and β -hydride elimination of the product can occur at either side of the metallocycles, thus resulting in four isomers each.

The steric effect of the ligand in directing styrene coordination in these co-oligomerization routes is not clear when studying the results in Table 5.4. A clear differentiation in the distribution of the main co-oligomerization products is observed between the trimerization and tetramerization ligands, but no further conclusions can be drawn. The product distribution in the cotrimerization reaction was explained by Bowen and Wass to be due to the preferred 2,1-styrene insertion above 1,2-insertion (see Section 2.4).¹ It can then be reasoned that intermediates B and F should be the most probable, which will cause the formation of 1-phenyl-1-octene, 3-phenyl-1-octene, 4-phenyl-1-octene, 5-phenyl-1-octene and 8-phenyl-1-octene. Of these, only 3-phenyl-1-octene and 4-phenyl-1-octene were identified without doubt.

5.3.1.4 Ethylene-*p*-methylstyrene co-oligomerization

p-Methylstyrene copolymers can be applied in polyolefin functionalization as pointed out in Chapter 2 and the ultimate aim of this study was to introduce ethylene-*p*-methylstyrene co-oligomerization products into polyethylene chains. Therefore, ethylene-*p*-methylstyrene co-oligomerization was investigated in a subsequent reaction using Ligand 8. The distribution of the main type of products in the co-oligomerization fraction does not seem to change significantly when compared with the product distribution obtained in an ethylene-styrene co-oligomerization reaction using the same ligand (Table 5.5). The *para* substituent of the comonomer does not

5. Tandem ethylene-styrene co-oligomerization-copolymerization

affect the co-oligomerization product selectivity. This is to be expected, because the substituent is not directed towards the catalyst centre.

Table 5.5: Comparison of the selectivity in the co-oligomerization fraction of ethylene-styrene and ethylene-*p*-methylstyrene co-oligomerization reactions

Co-oligomerization product	Styrene	<i>p</i> -Methylstyrene
4-Phenyl-1-hexene %	11	13
3-Phenyl-1-hexene %	9	11
6-Phenyl-1-hexene %	24	25
1-Phenyl-1-hexene %	55	51

5.3.1.5 The effect of temperature on ethylene-styrene co-oligomerization

In a subsequent reaction the co-oligomerization reaction was performed at a higher temperature. Ligand **3**, a known ethylene tetramerization ligand at low temperatures, was employed in this reaction. It was found that the effect of temperature on the selectivity behaviour is similar to that in an ethylene homo-oligomerization.⁸ The ratio of the cotrimerization products relative to the cotetramerization products increases with an increase in the reaction temperature (Table 5.6). The styrene conversion decreases in this reaction, but the selectivity of co-oligomerization relative to homo-oligomerization is not affected by the change in reaction temperature.

Table 5.6: Effect of the reaction temperature on the ethylene-styrene co-oligomerization

	50°C	80°C
Styrene conversion %	75	50
Co-oligomerization selectivity %	77	75
Selectivity in co-oligomerization fraction %		
4-Phenyl-1-hexene	28	37
3-Phenyl-1-hexene	16	22
6-Phenyl-1-hexene	1	2
1-Phenyl-1-hexene	2	3
4-Phenyl-1-octene	22	16
6-Phenyl-1-octene	18	12
3-Phenyl-1-octene	12	8

5.3.2 Copolymerization

Tandem reactions of chromium/PNP-type ethylene-styrene co-oligomerization catalysts combined with a metallocene polymerization catalyst were performed to establish to what extent the co-oligomerization products and the unreacted styrene insert into the polyethylene chain. Conventional ethylene-styrene copolymers were also prepared for comparative purposes.

The ligand $\text{Ph}_2\text{PN}(\text{CH}_3)\text{PPh}_2$ (ligand 1) was employed in these tandem reactions due to its high co-oligomerization selectivity and styrene conversion (Table 5.2). The co-oligomerization selectivity is 96 %. The styrene concentration was chosen to obtain a balance between the selectivity and activity of the oligomerization reaction based on the results in Table 5.1. *Rac*-ethylenebis(indenyl)zirconiumdichloride ($\text{EtIn}_2\text{ZrCl}_2$) (Figure 5.3) was used as the polymerization catalyst in the copolymerization study. This metallocene is reported to produce a crystalline alternating ethylene styrene copolymer at 0 °C, but at room temperature a polymer with low styrene content is obtained.⁹ It was therefore expected that the polymerization catalyst would not be able to significantly incorporate unreacted styrene into the copolymer chain at the polymerization temperature of 50 °C.

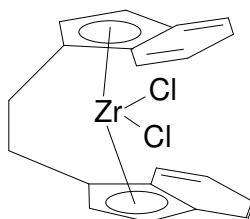


Figure 5.3: *Rac*-ethylenebis(indenyl)zirconiumdichloride ($\text{EtIn}_2\text{ZrCl}_2$)

5.3.2.1 Reaction conditions

Reactions were performed in a 1L Parr reactor at 50 °C in methylcyclohexane (200 mL). $\text{Cr}(\text{acac})_3$ (3.5×10^{-5} mol), $\text{Ph}_2\text{PN}(\text{CH}_3)\text{PPh}_2$ (4.2×10^{-5} mol), $\text{EtIn}_2\text{ZrCl}_2$ (4.0×10^{-7} mol) and MAO (2.1×10^{-2} mol) were used with a styrene concentration of $2.1 \text{ mol} \cdot \text{L}^{-1}$. The ethylene pressure was 30 bar. Tandem reactions were executed simultaneously or sequentially as described in the text. A conventional styrene copolymerization

5. Tandem ethylene-styrene co-oligomerization-copolymerization

reaction were performed using the same catalyst concentrations, but without the addition of the oligomerization catalyst.

5.3.2.2 Results

Table 5.7 displays the polymer yields and the molecular weights of the copolymers obtained from the tandem, sequential and conventional copolymerization reactions. The co-oligomerization of ethylene and styrene in the presence of $\text{EtIn}_2\text{ZrCl}_2$ yielded Polymer 1. A conventional styrene copolymerization reaction under the same reaction conditions yielded Polymer 2. Polymer 3 was obtained under similar reaction condition as Polymer 1, but *p*-methylstyrene was used instead of styrene. This copolymer from the simultaneous co-oligomerization-copolymerization is also compared to a sequential co-oligomerization-copolymerization product (Polymer 4). The polymerization catalyst was added after 30 minutes were allowed for the co-oligomerization reaction. Polymer 5 was obtained from a conventional *p*-methylstyrene copolymerization reaction. Polymer 6 was produced in a reaction under similar conditions, but with only the oligomerization catalyst present.

Table 5.7: Copolymers from tandem and sequential co-oligomerization-copolymerization reactions

Copolymer	Polymer yield g	DSC mp °C	$\langle M_n \rangle$	$\langle M_w \rangle$
Polymer 1	100	117	67	147
Polymer 2	20	128	108	215
Polymer 3	128	114	43	102
Polymer 4	91	102	71	151
Polymer 5	24	127	94	211
Polymer 6	0.5	(92) broad	not available	not available

Polymer yields are significantly higher in the tandem reactions in comparison to the conventional copolymerization reactions. Melting peak maximum temperatures and molecular weights of the tandem copolymers are constantly lower than the conventional copolymers.

In Figure 5.4 the CRYSTAF analysis shows the chemical composition distribution of Polymer 1 produced in a tandem manner. It is compared to the CRYSTAF trace of the conventional ethylene-styrene copolymer (Polymer 2). A very low incorporation

5. Tandem ethylene-styrene co-oligomerization-copolymerization

of styrene occurred in the conventional styrene copolymerization (Polymer **2**) consistent with results reported in the literature.⁹ It is clear that the tandem reaction yields a copolymer (Polymer **1**) with a lower crystallization temperature than the product from the conventional ethylene-styrene copolymerization (Polymer **2**). In addition, the chemical composition distribution of the co-oligomerization-copolymerization reaction is much broader and some uncrystallized material is present at 30 °C in the CRYSTAF trace. This soluble fraction is absent in the conventional copolymerization product. All of these factors point to a fairly complex mixture of products in the case of the co-oligomerization-copolymerization reaction.

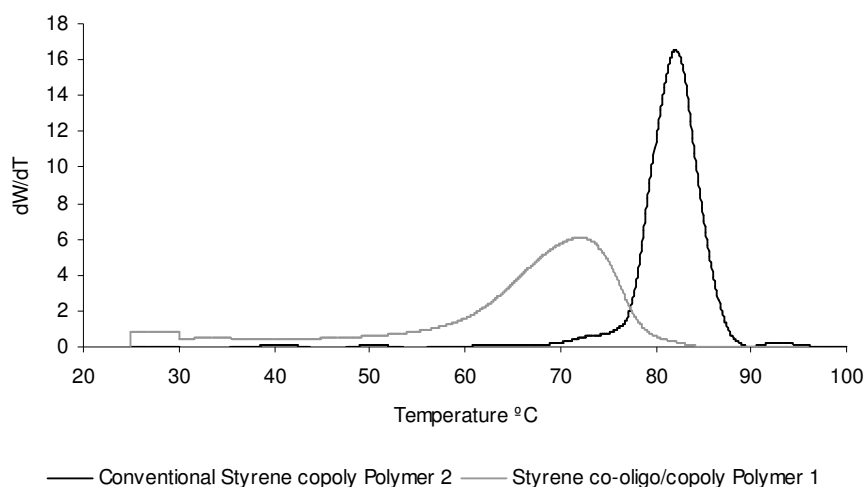


Figure 5.4: Comparison of CRYSTAF traces of Polymers 1 and 2

Figure 5.5 displays a comparison of the chemical composition distribution of the copolymers obtained when *p*-methylstyrene was used. In this case the simultaneous co-oligomerization-copolymerization (Polymer **3**) is also compared to the sequential co-oligomerization-copolymerization product (Polymer **4**). The CRYSTAF trace of Polymer **5** (conventional ethylene-*p*-methylstyrene copolymerization) is also shown.

5. Tandem ethylene-styrene co-oligomerization-copolymerization

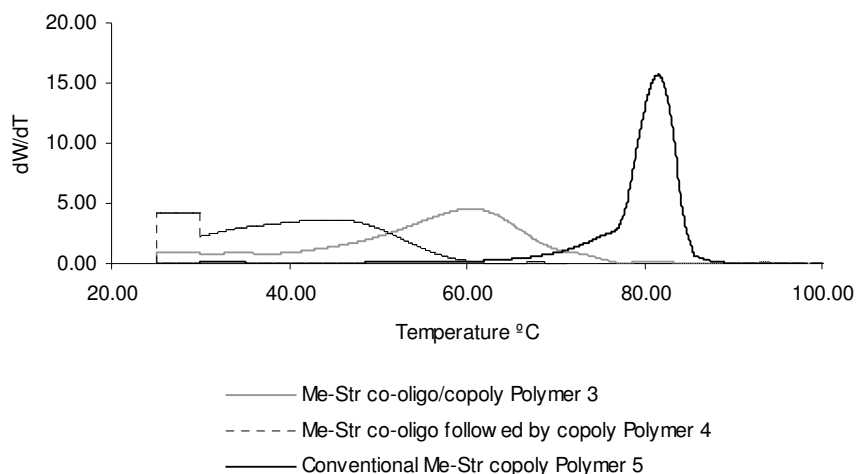


Figure 5.5: CRYSTAF traces of Polymers **3**, **4** and **5**

From the CRYSTAF traces of Polymers **3** and **4** (Figure 5.5) it is apparent that the crystallization temperature decreases substantially with a sizeable soluble fraction remaining at 30°C. This result indicates significant incorporation of a comonomer additional to *p*-methylstyrene (possibly also 1-octene and 1-hexene which are formed in smaller quantities). Significant here is not only the larger differences in products obtained by conventional ethylene-*p*-methylstyrene copolymerization reaction compared to the tandem co-oligomerization-copolymerization reaction (which were expected in the light of the results shown in Figure 5.4), but also the difference between the latter product and that obtained by the sequential co-oligomerization and copolymerization reaction. The product obtained by the sequential reaction has a very low crystallization temperature, a very broad chemical composition distribution and a significant amount of uncrystallized material. The final product can thus be tailored by the timing of the initiation of the copolymerization reaction, in other words, at what stage the metallocene catalyst is added. ¹³C NMR analysis gave some insight into the final product composition.

Figure 5.6 and Figure 5.7 show the aromatic and aliphatic regions in the ¹³C NMR spectrum of the simultaneous ethylene-*p*-methylstyrene co-oligomerization-copolymerization product (Polymer **3**). It is evident from the spectrum that the lower crystallization temperatures observed in the CRYSTAF traces are not only a result of 1-octene and 1-hexene incorporation. The aromatic region of the NMR spectrum (Figure 5.6) shows the incorporation of different aromatic molecules. A complex spectrum in the aliphatic region (Figure 5.7) is apparent indicating significant incorporation of the co-oligomerization products.

5. Tandem ethylene-styrene co-oligomerization-copolymerization

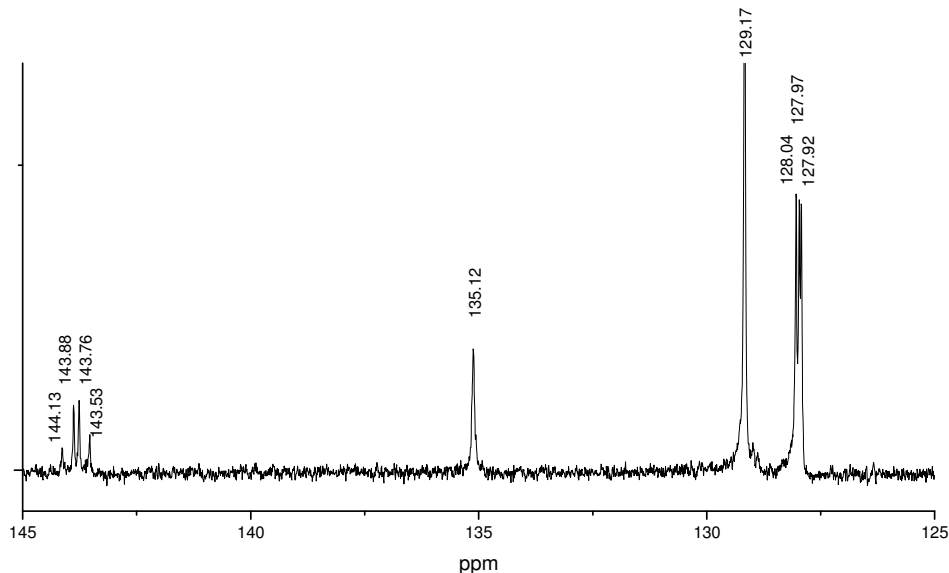


Figure 5.6: The aromatic region in the ^{13}C NMR spectrum of Polymer 3

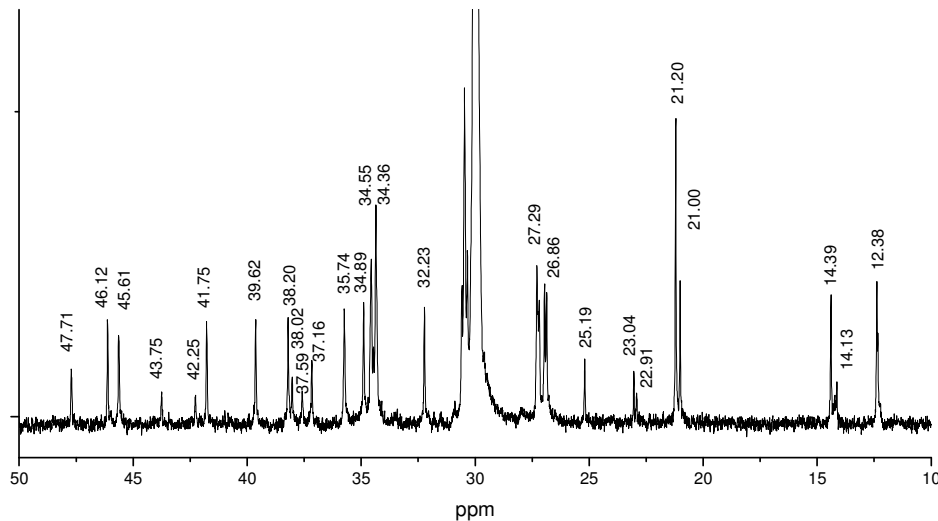


Figure 5.7: The aliphatic region in the ^{13}C NMR spectrum of Polymer 3

5.3.2.2.1 Incorporation of *p*-methylstyrene/styrene

Peaks resulting from conventional ethylene-*p*-methylstyrene or ethylene-styrene copolymerization were identified by measuring the ^{13}C NMR spectra of Polymers 2

5. Tandem ethylene-styrene co-oligomerization-copolymerization

and **5** and from the literature values for ethylene-styrene copolymers. The spectra of Polymers **2** and **5** were of poor quality, possibly because of poor solubility due to their high molecular weights and high melting temperatures (Table 5.7). Consequently, not all expected resonances were observed. An ethylene-*p*-methylstyrene copolymer was also prepared at a higher reaction temperature to decrease the molecular weight and increase the solubility. The ^{13}C NMR spectrum of the product is displayed in Figure 5.8. Table 5.8 lists the assignment of the resonances resulting from styrene or *p*-methylstyrene incorporation. The numbering scheme of the carbons is displayed in Scheme 5.2.

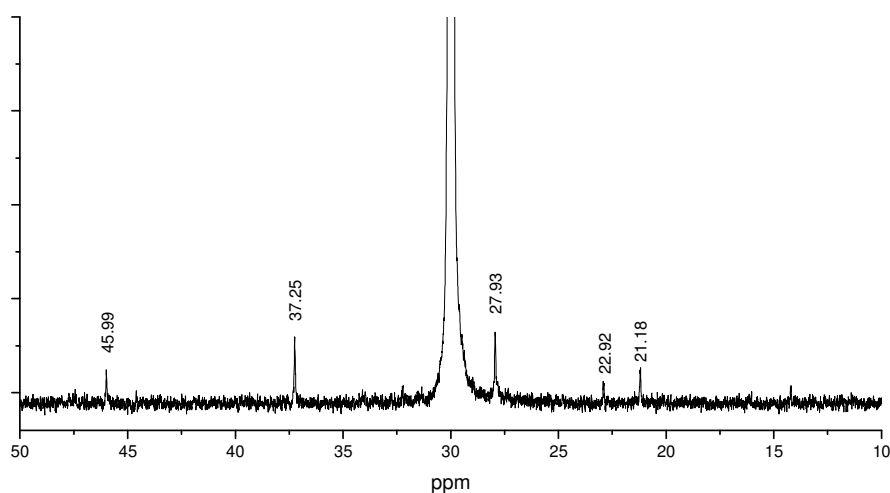
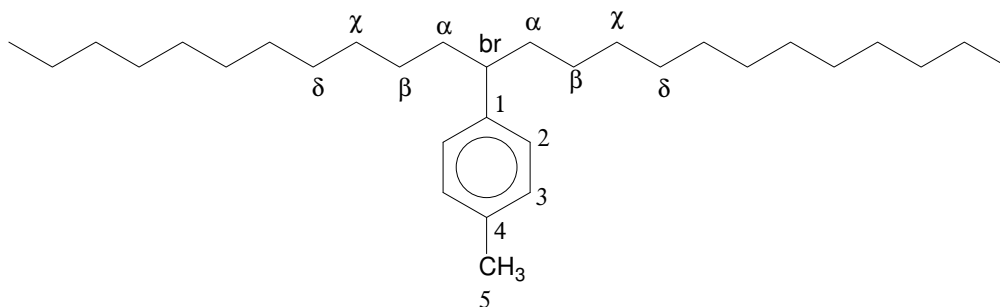


Figure 5.8: Aliphatic region in the ^{13}C NMR spectrum of an ethylene-*p*-methylstyrene copolymer prepared at higher temperature than Polymer **5**



Scheme 5.2: Numbering scheme for carbons in an ethylene-*p*-methylstyrene-copolymer

5. Tandem ethylene-styrene co-oligomerization-copolymerization

Table 5.8: Assignment of the ^{13}C NMR resonances in ethylene-styrene-copolymers

Literature ⁴ ppm	Styrene ppm	<i>p</i> -Methylstyrene ppm	Assignment (Scheme 5.2)
37.0-36.0	37.3	37.3	α
28.0-27.4	27.9	27.9	β
29.7	(30)	(30)	χ
48-46	46.5	46.0	br
146.7	not observed	144.0	1
133.9-133.4	128.1-128.5	129.3-127.9	2, 3
125.8	126.0	not observed	4
-	-	21.2	5

The *p*-methyl group on the phenyl ring shows practically no effect on the chemical shift of the branching carbon and the peak shifts from 46.5 ppm in a styrene copolymer to 46.0 ppm in a *p*-methylstyrene copolymer. The resonances resulting from the polyethylene backbone are not affected at all by the *p*-methyl substituent. The ^{13}C NMR spectra confirm that the copolymers obtained by the copolymerization of styrene or *p*-methylstyrene and ethylene using $\text{EtIn}_2\text{ZrCl}_2$ as catalyst have very low levels of these comonomers incorporated.

5.3.2.2.2 Incorporation of co-oligomerization products

It is evident from the CRYSTAF trace (Figure 5.5) that a substantial soluble fraction is present in Polymer **3**. A Soxhlet extraction was performed using hexane as solvent to remove the soluble, highly branched and/or low molecular weight material. The CRYSTAF trace of the resulting product is displayed in Figure 5.9 with that of Polymer **3**.

5. Tandem ethylene-styrene co-oligomerization-copolymerization

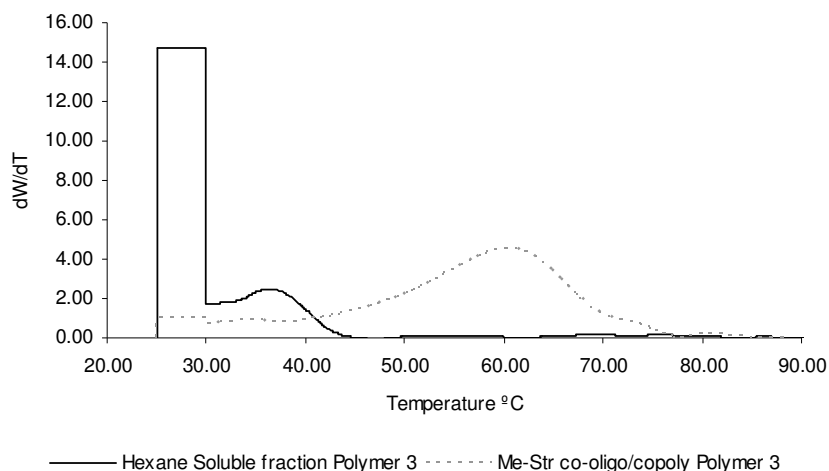


Figure 5.9: CRYSTAF trace of hexane soluble fraction from Polymer **3** compared to Polymer **3**

^{13}C NMR analysis of the extracted product yielded a spectrum similar to that of the complete copolymer mixture (Figure 5.6), but of much improved resolution. Peaks at 46.0 ppm and 27.9 ppm, assigned to an ethylene-styrene copolymer in Table 5.8, are not present, thus it seems as if styrene was not incorporated into the polymer. An Attached Proton Test (APT) was performed on the extracted fraction to assist in the identification of the peaks by differentiating between the resonances resulting from CH and CH_2 groups. The APT spectrum (Figure 5.10) indicates the presence of four CH groups at lower field than 43 ppm, directed downwards in the spectrum. These are expected to represent CH groups adjacent to a phenyl ring. Distinct resonances are expected for these groups due to the electronic influence of the aromatic ring. Other CH-groups are present in the region 38 - 35 ppm, which are probably branching carbons. The downward directed peak at 21.2 ppm is assigned to the *p*-methyl group on the benzene ring.

5. Tandem ethylene-styrene co-oligomerization-copolymerization

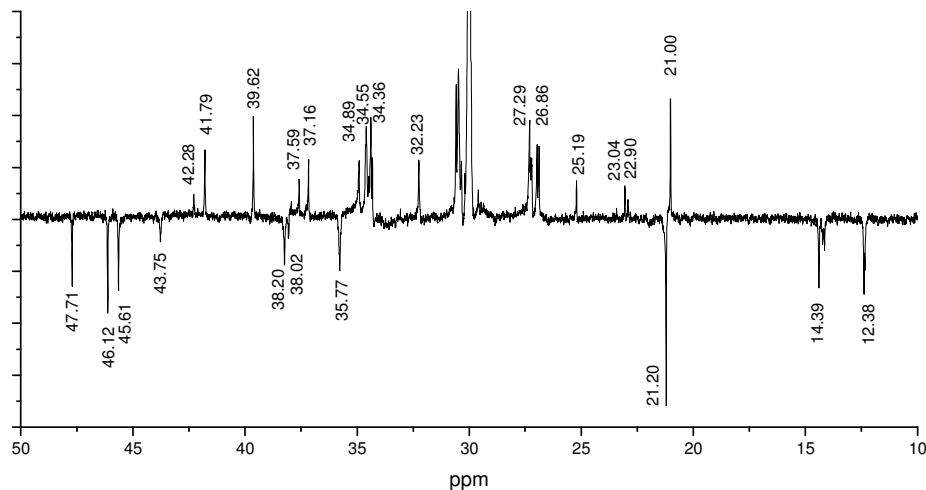


Figure 5.10: ^{13}C APT NMR spectrum of the hexane extracted fraction from Polymer 3

Figure 5.11 shows the aromatic region of the APT spectrum. Sets of chemical shifts are here present at ~ 144 ppm and ~ 135 ppm showing upwards; while chemical shifts at ~ 129 and ~ 128 ppm are downwards directing. These resonances are assigned to the carbons of the phenyl groups in the co-oligomerization products which are incorporated into the polyethylene chains. When comparing these chemical shifts to the assignments in Table 5.8 it is believed that the resonances at ~ 144 ppm are due to carbons attached to the phenyl ring, similar to 1C in Scheme 5.3. Likewise, the resonances at ~ 129 and ~ 128 ppm are assigned to carbons similar to 2C and 3C in Scheme 5.3. The resonance at ~ 135 ppm is probably the 4C resonance (adjacent to the methyl group on the phenyl ring) which was not detected in the spectrum of the conventional ethylene-*p*-methylstyrene copolymer.

5. Tandem ethylene-styrene co-oligomerization-copolymerization

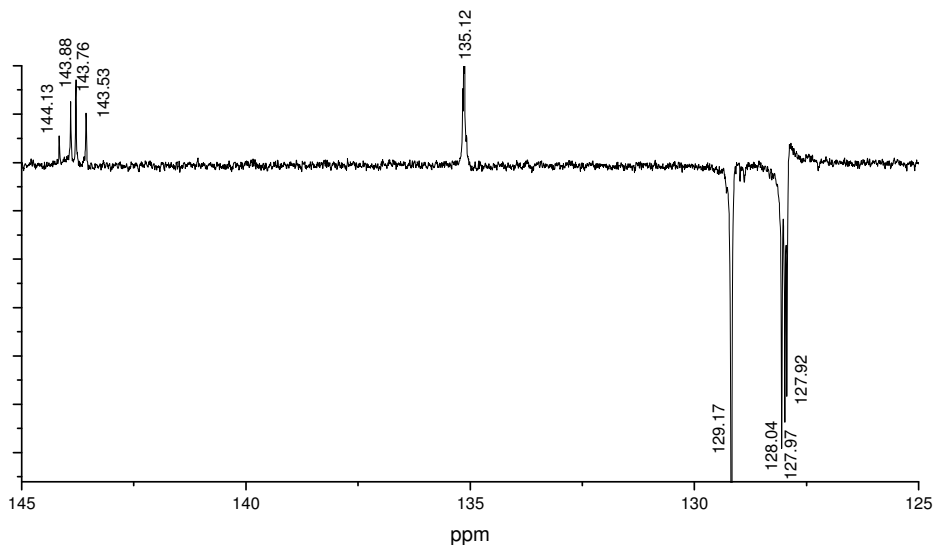


Figure 5.11: ^{13}C APT NMR spectrum of the hexane soluble fraction from Polymer 3

5.3.2.2.3 Assignment of NMR resonances

The Grant and Paul additivity rules were used to predict the chemical shifts of copolymers containing isolated branches of the co-oligomerization products.¹⁰ Table 5.9 indicates the different terms used in the calculations. Grant and Paul have demonstrated that ^{13}C NMR chemical shifts for alkanes could be described by a linear equation incorporating empirically determined additivity coefficients. Additive coefficients (α to ξ in Table 5.9) are considered for carbons up to five atoms removed from the specific carbon. The equation predicts that the chemical shift of a specific carbon is equal to a constant (-1.87 in Table 5.9) plus the sum of the additivity coefficients multiplied by the number carbons present in position α (one carbon away) to position ξ (five carbons away). Correction terms are required to account for steric effects e.g. a secondary carbon adjacent to a tertiary carbon [2(3) in Table 5.9] or a phenyl substituent adjacent to the specific carbon [a(Ph) in Table 5.9].

Table 5.9: Values of the terms used in the calculation of the chemical shifts

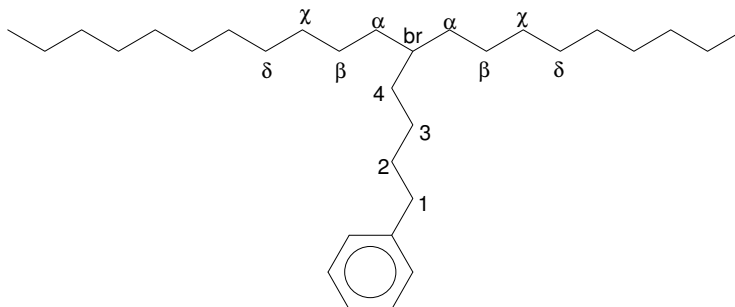
α	β	γ	δ	ξ	3(2)	2(3)	1(3)	a(Ph)	b(Ph)	c(Ph)	constant
8.61	9.78	-2.88	0.37	0.06	-2.65	-2.45	-1.4	22.1	9.3	-2.6	-1.87

5. Tandem ethylene-styrene co-oligomerization-copolymerization

The incorporation of 6-phenyl-1-hexene into a polyethylene chain has been described by Pellecchia *et al.* and 4-phenylbutyl branches are identified in the ^{13}C NMR spectrum of the copolymer.² Table 5.10 displays the assignments of the observed carbon resonances according to Pellecchia in comparison with the calculated chemical shifts according to the terms in Table 5.9. The numbering scheme of Scheme 5.3 was used.

Table 5.10: Peak assignments for carbons in a 4-phenylbutyl branched polyethylene

Experimental Chemical shift ppm	Assignment (Scheme 5.3)	Calculated Chemical shift ppm
34.6	α	34.9
27.3	β	27.6
30.5	χ	30.4
(30)	δ	30.1
38.1	br	37.9
36.3	1	36.2
31.0	2	32.4
27.0	3	27.4
34.3	4	34.5

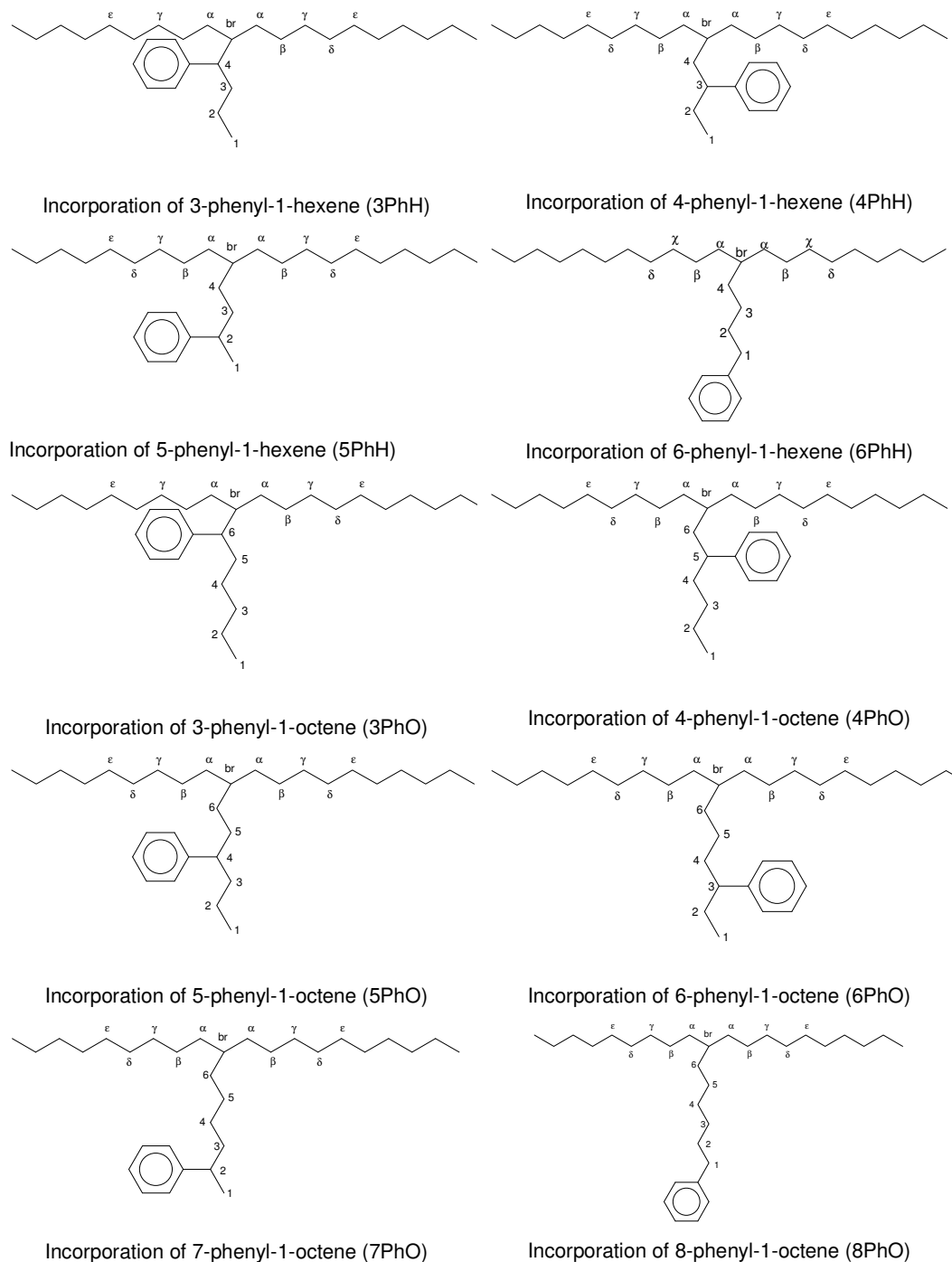


Scheme 5.3: Numbering scheme for 6-phenyl-1-hexene carbons in copolymer framework

The calculated and experimentally observed chemical shift values for incorporated 6-phenyl-1-hexene in the polyethylene chain (Table 5.10) are similar, except for the resonance of 2C which differs with 1.4 ppm. The chemical shifts for resonances resulting from the incorporation of all potential isomers obtainable from styrene-ethylene co-oligomerization were subsequently calculated using the Grant and Paul additivity rules and the values assigned to the terms in Table 5.9. Scheme 5.4

5. Tandem ethylene-styrene co-oligomerization-copolymerization

displays the numbering schemes for the different carbons in the copolymer structures. The calculated chemical shift values for the carbons in the various possible copolymer structures are given in Table 5.11 and Table 5.12.



Scheme 5.4: Numbering scheme for carbons in the copolymer frameworks resulting from the incorporation of the co-oligomerization products

5. Tandem ethylene-styrene co-oligomerization-copolymerization

Table 5.11: Calculated chemical shifts for ethylene copolymers containing phenyl-hexene isomers (blue for CH₃ and red for CH)

	1	2	3	4	Br	α	β	γ	δ
	ppm	ppm	ppm	ppm	ppm	ppm	ppm	ppm	ppm
3PhH	14.1	20.5	36.9	56.4	49.9	32.3	27.6	30.4	30.1
4PhH	11.5	30.0	46.8	41.3	35.3	34.9	27.6	30.4	30.1
5PhH	22.0	42.6	36.9	31.9	37.9	34.9	27.6	30.4	30.1
6PhH	36.2	32.4	27.4	34.5	37.9	34.9	27.6	30.4	30.1

Table 5.12: Calculated chemical shifts for ethylene copolymers containing phenyl-octene isomers (blue for CH₃ and red for CH)

	1	2	3	4	5	6	Br	α
	ppm	ppm	ppm	ppm	ppm	ppm	ppm	ppm
3PhO	14.1	22.7	32.5	27.4	34.4	56.8	50.0	32.3
4PhO	14.1	22.7	29.9	36.9	44.4	41.7	35.4	34.9
5PhO	14.1	20.1	39.4	46.8	34.4	32.3	38.0	34.9
6PhO	11.5	29.5	49.3	36.9	24.9	34.9	38.0	34.9
7PhO	22.0	42.1	39.4	22.4	27.5	34.9	38.0	34.9
8PhO	36.2	32.0	29.9	30.0	27.5	34.9	38.0	34.9

The chemical shifts predicted for carbons in the polyethylene backbone close to isolated branches, i.e. α , β , χ , δ and ϵ , do not differ between the different copolymer structures. It is expected that the peaks resulting from these carbons will overlap in the ¹³C NMR spectrum, and individual assignments will not be possible. Only the distinctly different resonances were used for the chemical shift assignments and to elucidate the microstructure of the copolymer. It was assumed that 1-phenyl-1-hexene and 2-phenyl-1-hexene as well as 1-phenyl-1-octene and 2-phenyl-1-octene would not incorporate owing to the steric bulk next to the double bond and consequently, these isomers are not included in the calculations.

Peaks at ~56 ppm were not observed in Figure 5.10, thus it is clear that 3-phenyl-1-hexene and 3-phenyl-1-octene did not incorporate. It is also concluded that 7-phenyl-1-octene and 5-phenyl-1-hexene are not present in the copolymer framework, because CH₃ peaks (downward directing) at ~22.0 ppm in the NMR spectrum were not seen. The only CH₃ resonance observed in the APT spectrum in this region is a

5. Tandem ethylene-styrene co-oligomerization-copolymerization

peak at 21.2 ppm. This peak is not present in the ^{13}C NMR spectrum of Polymer 1 (styrene/ethylene co-oligomerization copolymerization product) and can thus be assigned to the *p*-methyl group on the benzene ring.

Resonances at ~36 ppm and ~38 ppm directed downwards in the APT spectrum are seen, which indicates the presence of CH groups. Although these resonances may be those of the branching carbon (br) or the carbon adjacent to the phenyl group of a copolymer containing 8-phenyl-1-octene or 6-phenyl-1-hexene it is rather assigned to a copolymer containing 4-phenyl-1-hexene, 4-phenyl-1-octene and 6-phenyl-1-octene. The assignment is based on the fact that GC analysis did not detect 8-phenyl-1-octene and 6-phenyl-1-hexene in the co-oligomerization product mixture. A resonance for a CH_2 group occurring at 32.2 ppm could indicate the presence of any of these two isomers, but this peak is rather assigned to the carbon 6C, resulting from the incorporation of 5-phenyl-1-octene. 5-Phenyl-1-octene was not identified in the GC analysis of the co-oligomerization reaction mixture, but may co-elute with 4-phenyl-1-octene. 5-Phenyl-1-octene results in 4-phenyloctane when hydrogenated similarly to 4-phenyl-1-octene and this may explain why it was not identified previously. Upward directing peaks at 39.6 ppm and 21.0 ppm in the APT spectrum confirm this assignment. These peaks belong to the CH_2 groups, 3C and 2C, in the framework of a 5-phenyl-1-octene copolymer. CH peaks at ~47 ppm and at ~38.0 ppm are predicted to occur in the spectrum due to the carbon adjacent to the phenyl group (4C) and the branching carbon (br), respectively. Several CH resonances in the 44 – 48 ppm and 35 – 39 ppm regions are observed.

Additional to those resonances expected for 5-phenyl-1-octene in the mentioned field strength regions, the CH resonances can be assigned to 4-phenyl-1-hexene, 4-phenyl-1-octene and 6-phenyl-1-octene. These isomers were identified in the co-oligomerization reaction mixture (Table 5.4, Ligand 1) and are the isomers more likely to incorporate into the copolymer structure. The remaining peaks in the ^{13}C NMR spectrum match the predicted chemical shifts for such copolymer frameworks. CH groups adjacent to the phenyl rings are expected to occur at ~44 ppm (4PhO), ~47 ppm (4PhH) and ~49 ppm (6PhO), while the CH branching groups are predicted to occur at ~35 ppm (4PhH and 4PhO) and ~38 ppm (6PhO). The four CH resonances observed in the region 44 – 48 ppm are thus assigned to 4PhO (43.8 ppm), 5PhO or 4PhH (45.6 ppm or 46.1 ppm) and 6PhO (47.7 ppm). Similarly, the CH branching carbons (br) are observed at 35.8 ppm and 38.0 ppm, although

5. Tandem ethylene-styrene co-oligomerization-copolymerization

overlapping of the resonances in this region occurs and four distinct peaks are not seen. The peak at 38.2 ppm can be understood in terms of the incorporation of 1-octene and 1-hexene which are also formed in the oligomerization reaction. Other distinct CH₂ resonances confirming the assignments for the incorporation of the isomers 4-phenyl-1-hexene, 4-phenyl-1-octene and 6-phenyl-1-octene are observed as upwards directing peaks. These occur at 42.2 ppm (6C in 4PhO), 41.8 ppm (4C in 4PhH), 37.6 ppm and 37.2 ppm (4C in 6PhO or 4PhO) and were predicted at 41.7 ppm, 41.3 ppm and 36.9 ppm, respectively.

Table 5.13 summarizes the final assignments made for the chemical shifts in the ¹³C NMR spectra of Polymer **1** and Polymer **3** which are ethylene copolymers of the co-oligomerization products of ethylene-styrene and ethylene-*p*-methylstyrene, respectively. The chemical shifts of the resonances of these two copolymers are similar and differ only at the carbons directly adjacent to the styrene or *p*-methylstyrene group.

The integration of the various resonances is also listed in Table 5.13. These values are consistent with the proposed assignments. For example, peak assignments made for carbons belonging to a 6-phenyl-1-octene copolymer integrate for 1 carbon (3C, 4C and 5C). Carbon resonances assigned to incorporated 4-phenyl-1-hexene have integrals ~2 (3C and 4C), while those assigned to 4-phenyl-1-octene have values less than 0.5 (5C, 6C, 4C and 2C). The peaks assigned to 5-phenyl-1-octene incorporation have integrals of ~2 (4C, 3C, 6C and 2C).

The co-oligomerization products are formed in a ratio of 6PhO:4PhH:(4PhO+5PhO) of 2:1:3 if assuming that 4-phenyl-1-octene and 5-phenyl-1-octene co-elute in the GC analysis (Table 5.4, Ligand 1). The ratio in which these co-oligomerization products are incorporated is thus 1:2:(2.5) for 6PhO:4PhH:(4PhO+5PhO). It seems that 4-phenyl-1-hexene incorporates easier than the phenyl-octene isomers, which can be attributed to the relative sizes of the molecules.

5. Tandem ethylene-styrene co-oligomerization-copolymerization

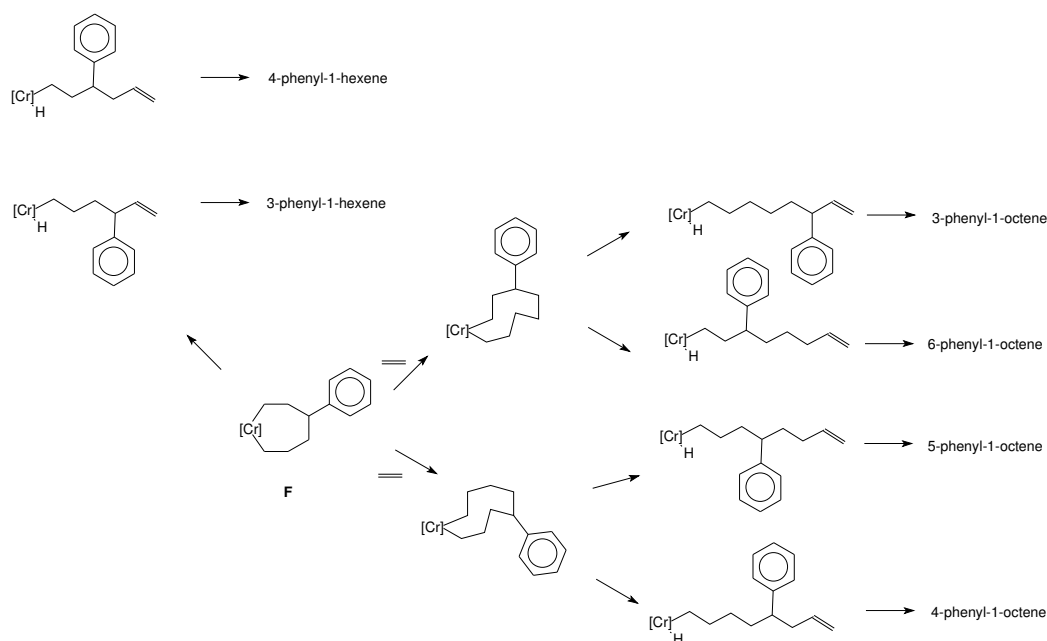
Table 5.13: Proposed assignments of the ^{13}C NMR resonances in the (*p*-methyl)styrene co-oligomerization-co-polymerization products (Polymer **1** and **3**)

Experimental Shift ppm Styrene	Experimental Shift ppm MeStyrene	Odd/Even from APT MeStyrene	Integral Measured MeStyrene	Assignment	Predicted shift ppm
48.2	47.7	odd	1	C_3 6PhO	49.3
46.6	46.1	odd	1.9	C_3 4PhH/C₄ 5PhO	46.8
46.1	45.6	odd	2.1	C_3 4PhH/C₄ 5PhO	46.8
44.3	43.8	odd	0.3	C_5 4PhO	44.3
42.3	42.3	even	0.3	C_6 4PhO	41.7
41.8	41.8	even	1.8	C_4 4PhH	41.3
39.6	39.6	even	1.8	C_3 5PhO	39.4
38.3 to 38.1	38.2 to 38.0	odd odd	3.1	br O br 6PhO br 5PhO	38.0 38.0 38.0
37.6	37.6	even	0.5	C_4 4PhO	36.9
37.2	37.2	even	1.1	C_4 6PhO	36.9
35.9 36.3	35.8	odd	2.7	br 4PhH br 4PhO	35.3 35.4
35.0 to 34.4	35.0 to 34.4	even		α all C_5 5PhO C_6 6PhO	34.9 34.4 34.9
32.2	32.2	even	1.9	C_6 5PhO	32.3
30.6 to 29.6	30.6 to 29.6	even		γ all δ all C_2 6PhO C_2 4PhH C_3 4PhO	30.4 30.1 29.5 29.9 29.9
27.0 to 28.0	27.0 to 28.0	even		β all	27.6
25.2	25.2	even	0.8	C_5 6PhO	25.0
23.4	23.0	even	0.6	C_2 4PhO	22.7
22.9	22.9			C_2 O	
absent	21.2	odd	6.1	<i>p</i> CH_3	
21.0	21.0	even	2.5	C_2 5PhO	20.1
14.4 to 14.14	14.4 to 14.14	odd	3.1	C_1 O C_1 5PhO C_1 4PhO	14.1 14.1
12.4 to 12.3	12.4 to 12.3	odd	4.2	C_1 6PhO C_1 4PhH	11.5 11.5

5. Tandem ethylene-styrene co-oligomerization-copolymerization

In summary, according to the calculated chemical shifts (Table 5.11 and Table 5.12) and taking the product distribution of co-oligomerization products (Table 5.4, Ligand 1) into account it was thus determined that the co-oligomerization products incorporated into polyethylene chain are possibly 4-phenyl-1-hexene, 4-phenyl-1-octene, 5-phenyl-1-octene and 6-phenyl-1-octene. 5-Phenyl-1-octene was not identified by GC analysis of the reaction mixture, but could be co-eluting with any of the other phenyl-octene isomers, possibly 4-phenyl-octene.

The co-oligomerization of styrene and ethylene using this ligand in combination with $\text{Cr}(\text{acac})_3$ thus yielded 3-phenyl-1-hexene, 4-phenyl-1-hexene, 3-phenyl-1-octene, 4-phenyl-1-octene, 5-phenyl-1-octene and 6-phenyl-1-octene as main products. The occurrence of these specific co-oligomerization products indicates that the co-oligomerization route (employing ligand **1**) preferentially occurs through the intermediate F (Scheme 5.5). Elimination from intermediate F would result in 3-phenyl-1-hexene and 4-phenyl-1-hexene, while further insertion of an ethylene molecule will produce either 3-phenyl-1-octene, 4-phenyl-1-octene, 5-phenyl-1-octene or 6-phenyl-1-octene after elimination.



Scheme 5.5: Possible routes to the observed co-oligomerization products

5.4 Conclusions

GC results from the styrene-ethylene co-oligomerization study indicated that various phenyl-hexene and phenyl-octene isomers are produced either through cotrimerization or cotetramerization and possibly by a metallacyclic mechanism such as the one proposed for selective ethylene oligomerization. Previously known ethylene trimerization catalysts also display cotrimerization behaviour, while chromium catalysts that contain ligands with known selectivity for ethylene tetramerization also yield cotetramerization products. The ligands with more bulk in the *ortho* position of the phenyl rings, display lower selectivity towards co-oligomerization and greater preference for ethylene homotrimerization.

Simultaneous and sequential tandem copolymerization of the oligomerization reaction mixture using a metallocene catalyst, resulted in copolymers with branched structures as indicated by CRYSTAF and ^{13}C NMR analyses. Assignments for the ^{13}C NMR resonances of these compounds were made based on an Attached Proton NMR experiment and calculated chemical shifts using Grant and Paul additivity rules for NMR predictions.

An indication of the tendency shown by the different co-oligomerization products to incorporate into the polyethylene chain could be established from these assignments. Unreacted styrene and the more bulky isomers, 3-phenyl-1-hexene and 3-phenyl-1-octene, are not incorporated readily, while branches resulting from the other isomers present in the co-oligomerization product mixture are detected in the NMR spectrum.

5.5 References

1. Bowen, L. E., Wass, D. F., *Organometallics*, 2006, 25, 555
2. Pellecchia, C., Pappalardo, D., Oliva, L., Mazzeo, M., Gruter, G., *Macromolecules*, 2000, 33, 2807; Pellecchia, C., Mazzeo, M., Gruter, G., *Macromolecular Rapid Communication*, 1999, 20, 337
3. Chung, T. C. in *Functionalization of Polyolefins*, Academic Press, San Diego, CA, 2002, p.43
4. De Pooter, M., Smith, P. B., Dohrer, K. K., Bennett, K. F., Meadows, M. D., Smith, C. G., Schouwenaars, H. P., Geerards, R. A., *Journal of Applied Polymer Science*, 1991, 42, 399; Liu, W., Rinaldi, P. L., *Macromolecules*, 2001, 34, 4757; Ren, J., Hatfield, G. R., *Macromolecules*, 1995, 28, 2588; Longo, P., Grassi, A., Oliva, L., *Macromolecular Chemistry*, 1990, 191, 2387; Sernetz, F. G., Mülhaupt, R., Fokken, S., Okuda, J., *Macromolecules*, 1997, 30, 1562
5. Grant, D. M, Paul, G., *Journal of the American Chemical Society*, 1964, 86, 2984; Breitmaier, E., Bauer, G in *¹³C NMR spectroscopy*, Harwood Academic Publishers, 1984, 52
6. Bollmann, A., Blann, K., Dixon, J. T., Hess, F. M., Killian, E., Maumela, H., McGuinness, D. S., Morgan, D. H., Neveling, A., Otto, S., Overett, M., Slawin, A., Wasserscheid, P., Kuhlmann, S, *Journal of the American Chemical Society*, 2004, 126, 14712; Bollmann, A., Blann, K., Dixon, J. T., Hess, F. M., Killian, E., Maumela, H., Morgan, D.H., Neveling, A., Otto, S., Overett, M. J., *Chemical Communications*, 2005, 620
7. Overett, M., Blann, K., Bollmann, A., Dixon, J. T., Haasbroek, D., Killian, E., Maumela, H., McGuinness, D. S., Morgan, D. H., *Journal of the American Chemical Society*, 2005, 127, 10723
8. Walsh, R., Morgan, D. H., Bolmann, A., Dixon, J. T., *Applied Catalysis, A*, 2006, 306, 184
9. Oliva, L., Longo, P., Izzo, L., Di Serio, M., *Macromolecules*, 1997, 30, 5616

5. Tandem ethylene-styrene co-oligomerization-copolymerization

-
10. Grant, D. M, Paul, G., Journal of the American Chemical Society, 1964, 86, 2984; Breitmaier, E., Bauer, G in ^{13}C NMR spectroscopy, Harwood Academic Publishers, 1984, 52; Carman, C.J., Tarpley, A.R., Goldstein, J.H., Macromolecules, 1973, 6, 719

6 Summary and general conclusion

The main objective of this dissertation was to investigate the possibility of utilizing the chromium/PNP-type catalysts in homogeneous catalysed ethylene polymerization processes. These processes include the production of linear low density polyethylene (LLDPE), the synthesis of special comonomers for ethylene copolymerization and the production of polyethylene waxes.

Previous studies have shown that the production of LLDPE is highly possible by combination of an oligomerization and a polymerization catalyst in one reactor, but the two catalysts need to be compatible under the same reaction conditions. The first objective was to use the chromium/ $\text{Ph}_2\text{PN}\{\text{CH}(\text{CH}_3)_2\}\text{PPh}_2$ ethylene tetramerization system in combination with a ethylene polymerization catalyst to afford ethylene copolymers with controlled branching. The aim was to understand the factors of importance when using the combination of catalysts in one reactor to produce LLDPE with ethylene as only monomer. The effects of reaction variables on the type and amount of product produced were investigated. Copolymers with bimodal chemical composition distributions were obtained in these tandem reactions. It has been found that the chromium/PNP-type tetramerization catalyst and metallocene polymerization catalyst are not completely compatible in a tandem catalysis system due to different optimum temperatures for effective functioning. Successful tandem catalysis is possible when the reactions are performed in a sequential way and ethylene copolymers of 1-hexene and 1-octene are obtained from an ethylene only feed. The oligomerization to polymerization catalyst ratios, the catalyst to cocatalyst ratios and the temperature profile are all factors influencing the amount of α -olefins formed and therefore the type of copolymer produced. Additionally it was found that the two catalysts interfere chemically. The activity of the polymerization catalyst decreases in the presence of the oligomerization catalyst, possibly because of a competitive mechanism between the oligomerization catalyst components and the monomers at the active polymerization catalyst centre.

6. Summary and general conclusion

A part of the study was directed to the determination and comparison of the properties and microstructures of the resulting tandem copolymers with copolymers obtained from the conventional process of adding a comonomer to the reactor. The main difference between tandem and conventional copolymers is the presence of a small amount of low molecular weight material produced by the oligomerization catalyst and a highly crystalline component. The latter component results from the oligomerization catalyst and also the initial low concentration of α -olefins.

The low molecular weight material present in the tandem copolymers resulted in the higher melt flow of the copolymers which will be an advantage during injection moulding processes. A significant difference in the tensile properties was not observed, indicating that the polymer may be used in the same applications than the conventional LLDPE. Based on the copolymer properties obtained it seems that the chromium/ $\text{Ph}_2\text{PN}\{\text{CH}(\text{CH}_3)_2\}\text{PPh}_2$ tetramerization system is suitable to produce copolymers to replace the studied commercial LLDPE. A drawback of this system is that a cascade reaction sequence is necessary, requiring two reactors operating at two different temperatures. The second reactor will increase capital cost. At first sight it seems that capital cost is eliminated in the tandem process for separation, purification and storage of the produced α -olefins. However, these costs will still be applicable since excess α -olefins are present after the copolymerization step which will require separation and work-up. Although MAO is used to activate both the oligomerization and polymerization catalysts simultaneously, it does not result in less MAO consumption in the tandem process. Increased catalyst and co-catalyst consumption is a consequence of the decrease in the activity of the polymerization catalyst in the presence of the oligomerization catalyst.

LLDPE with butyl branches was obtained when a selective trimerization catalyst was used in combination with a polymerization catalyst. The chromium/ $(o\text{-OMeC}_6\text{H}_4)_2\text{PN}(\text{CH}_3)\text{P}(o\text{-OMeC}_6\text{H}_4)_2$ trimerization system is more suitable for use in tandem reactions with polymerization catalysts than the chromium/ $\text{Ph}_2\text{PN}\{\text{CH}(\text{CH}_3)_2\}\text{PPh}_2$ tetramerization system due to its high activity and selectivity to 1-hexene at higher temperatures. The performed tandem copolymerization reactions illustrate the effect of increasing reaction time on the chemical composition distribution due to the increasing amount of 1-hexene produced. Comparison of CRYSTAF traces of tandem copolymers with conventional copolymers showed that the tandem copolymers have a broader chemical

6. Summary and general conclusion

composition distribution. Addition of 1-hexene during the course of a conventional copolymerization reaction produces copolymers with similar chemical composition distributions to that of the tandem copolymers. Later addition of the polymerization catalyst to the oligomerization reaction resulted in copolymers with higher comonomer content, similar to conventional copolymers.

An advantage of the chromium/ $(o\text{-OMeC}_6\text{H}_4)_2\text{PN}(\text{CH}_3)\text{P}(o\text{-OMeC}_6\text{H}_4)_2$ trimerization system over the chromium/ $\text{Ph}_2\text{PN}\{\text{CH}(\text{CH}_3)_2\}\text{PPh}_2$ tetramerization system is that a simultaneous ethylene oligomerization/copolymerization reaction occur because of the same operating temperatures for the two processes. One reactor operating at a constant temperature is thus required in this process while the tetramerization tandem process entails a cascade reactor system, operating at different temperatures. Although the trimerization tandem catalyst system will be capable of manufacturing a range of LLDPE grades it should be noted that highly reproducible functioning of the oligomerization catalyst is crucial to ensure that the same grade of LLDPE is produced at every conversion. The LLDPE composition, and thus properties, will correspond to minute variations in the oligomerization catalyst kinetics because of poisons or MAO quality.

It was found that chromium/ $(o\text{-EtC}_6\text{H}_4)_2\text{PN}(\text{CH}_3)\text{P}(o\text{-EtC}_6\text{H}_4)_2$ is not suitable to yield LLDPE in tandem reactions, since it is selective to higher oligomers or polyethylene waxes at the higher temperatures employed. Syntheses of such polyethylene waxes were, however, investigated at different MAO and hydrogen concentrations using this temperature-switchable chromium/PNP-type catalyst. The extent to which these variables influence the viscosity, crystallization behaviour and yields was determined. Low MAO concentrations resulted in multiple melting peaks, while higher concentrations display single melting peaks and lower viscosity values. An increase in poorly crystallisable material was apparent from CRYSTAF at high hydrogen concentrations and NMR data indicate increased methyl branching pointing to a chain isomerisation mechanism.

Although the chromium/PNP-type systems are suitable to produce a range of PE waxes under different reaction conditions, the occurrence of chain isomerisation affect the tuning of the application based properties, e.g. viscosity and hardness. For instance, the hardness is affected negatively when the wax viscosity is lowered by adding hydrogen as a chain transfer agent to reduce the molecular weight. Increased isomerisation under these conditions resulted in an increase in the methyl

6. Summary and general conclusion

branching which affected the crystallizability of the wax and thus the wax hardness. PNP-type ligands with more rigid structures may be investigated in future to reduce the possibility of fluxional behaviour of the catalyst to limit different possible catalyst conformations and thus the chemical composition distribution obtained with such a catalyst.

A further objective of the investigation was to utilize the chromium/PNP-type oligomerization technology in ethylene co-oligomerization reactions with styrene as additional substrate. The first aim of this part of the study was to establish the influence of the ligand structure on the selectivity of the co-oligomerization products. Results showed that various phenyl-hexene and phenyl-octene isomers are produced either through cotrimerization or cotetramerization; possibly through the metallacyclic mechanism proposed for selective ethylene oligomerization. The known ethylene trimerization ligands display cotrimerization behaviour, while the ligands with known selectivity for ethylene tetramerization also yield cotetramerization products. The more bulky ligands display lower selectivity towards co-oligomerization and greater preference for ethylene homotrimerization.

The possibility of adding these co-oligomerization products to a polyethylene chain by copolymerization in a tandem or sequential manner was investigated. The combined co-oligomerization-polymerization reactions yielded copolymers with lower crystallinity than obtained from the conventional ethylene-styrene copolymerization. The polymer yields were higher in the co-oligomerization-copolymerization reactions. Both the simultaneous and sequential tandem copolymerization of the oligomerization reaction mixture using a metallocene catalyst resulted in copolymers with branched structures as indicated by CRYSTAF and ^{13}C NMR analyses. Assignments of the ^{13}C NMR resonances were proposed on the basis of an Attached Proton NMR experiment and calculated chemical shifts using Grant and Paul additivity rules for NMR predictions. An indication of the ability of the different co-oligomerization products to incorporate into the polyethylene chain was established from these assignments: unreacted styrene and the more bulky isomers, 3-phenyl-1-hexene and 3-phenyl-1-octene, are not incorporated readily while branches resulting from 4-phenyl-1-hexene, 4-phenyl-1-octene, 5-phenyl-1-octene and 6-phenyl-1-octene are clearly detected in the NMR spectrum.

Ethylene/*p*-methylstyrene co-oligomerization resulted in comonomers that are more polymerizable than *p*-methylstyrene, because the phenyl ring is spaced further away

6. Summary and general conclusion

from the active catalytic site. Therefore steric bulk is reduced in the vicinity of the double bond as well as causing less interacting of the phenyl ring with the metal centre. The higher copolymer yield and higher comonomer incorporation of the ethylene/*p*-methylstyrene co-oligomerization/copolymerization reaction in comparison to the *p*-methylstyrene copolymerization reaction are a consequence thereof. Co-oligomerization with other bulky, functionalizable monomers may be investigated in further studies to increase their polymerizability. Such monomers include *p*-divinylbenzene, 5-ethylidene-2-norbornene, 4-vinyl-1-cyclohexene, dicyclopentadiene or 2,5-norbornadiene.